DESIGN AND ASSESSMENT OF A NEW DEVICE FOR GAS-LIQUID SEPARATION

by

Samina Noor

A Thesis submitted to the Faculty of Graduate Studies
The University of Manitoba
In Partial Fulfillment of the Requirements for the Degree of

Master of Science

Department of Mechanical Engineering
University of Manitoba
Winnipeg, Manitoba

ABSTRACT

An experimental investigation was conducted with a novel system of combined impacting tee junction in order to study the phase-separation capability of the system for air-water two-phase flows. The system consisted of one horizontal and two vertical equal-sided impacting tee junctions of internal diameter 13.5 mm, having one inlet and two vertical (top and bottom) outlets. Two groups of experiments were conducted to generate partial- and full-phase-separation curves at ambient temperature and at a nominal pressure of 200 kPa (abs) in the center of the combined junction.

Full-phase-separation experiments were conducted within inlet gas superficial velocity, J_{G1} = 0.2 - 20 m/s and inlet liquid superficial velocity, J_{L1} = 0.001 - 0.34 m/s, which fell in the annular, wavy, slug and plug flow regimes. Results show that compared to a system with a single vertical impacting tee junction, the combined design nearly doubled the J_{L1}, at a fixed J_{G1} and J_{G1} at a fixed J_{L1}, under which full separation of phases takes place, in the wavy and annular flow regimes. In the slug and plug flow regimes, limiting conditions of J_{G1} and J_{L1} for full phase separation also increased with the system of combined junction, based on a proposed criterion of 99% F_{L3} (liquid mass extraction ratio in the bottom outlet).

Beyond the range of full phase separation, partial-phase-separation experiments were performed for six sets of inlet conditions in the annular flow regime, with gas mass extraction ratio in the bottom outlet, F_{G3} ranging from 0 to 1. Three sets of these experiments were performed at fixed J_{G1} of 40 m/s, with J_{L1} of 0.01, 0.04 and 0.18 m/s. The value of J_{L1} was fixed at 0.04 m/s for the other three sets of experiments, with J_{G1} of 20, 25 and 30 m/s. Results show that at a fixed J_{L1}, as J_{G1} was decreased, tendency of liquid to enter outlet-3 (bottom outlet) increased. As a result,

partial-phase-separation curves moved in anti-clockwise direction in the F_{G3} versus F_{L3} plot. Partial-phase-separation curves did not follow any consistent trend as J_{L1} was changed, keeping J_{G1} fixed. Compared to a system of a single vertical impacting tee junction, the combined system showed increased proportion of liquid entering the bottom outlet, with proportionally less amount of gas (i.e., better phase separation).

In order to quantify the effectiveness of the combined system as a phase separator, a 'phase-separation parameter, η' has been defined. Results show that η increases with decreasing J_{G1} or J_{L1}. In addition, all partial-phase-separation experiments yielded higher values of η for the present system, in comparison with a system of a single vertical impacting tee junction, proving the increased effectiveness of the combined system as a two-phase flow separator. Better phase-separation effectiveness was found for the present system when results were compared to other combined junctions reported in the literature with the same number of dividing tees.

ACKNOWLEDGEMENTS

TABLE OF CONTENTS

.

LIST OF FIGURES

LIST OF TABLES

NOMENCLATURE

Symbol	Description	Units
D	Pipe diameter	m
F_G	Fraction of inlet gas exiting through an outlet	-
F_L	Fraction of inlet liquid exiting through an outlet	-
J_G	Superficial gas velocity	m/s
J_L	Superficial liquid velocity	m/s
P	Pressure	kPa
P_{TS}	Pressure at the center of the combined junction	kPa
T_G	Temperature of gas	K
T_L	Temperature of liquid	K
V_G	Gas volume flowrate	SLPM
V_L	Liquid volume flowrate	cc/min
W	Total mass flowrate	kg/s
W_G	Gas mas flowrate	kg/s
W_L	Liquid mas flowrate	kg/s
ρ_G	Density of gas	kg/m^3
ρ_L	Density of liquid	kg/m^3
ρ_{STD}	Standard density	kg/m^3

Subscripts: 1-Inlet

2- Outlet 2

3-Outlet-3

CHAPTER 1

INTRODUCTION

1.1   Overview

Industrial operations ranging from mining of hydrocarbons to power generation in nuclear reactors use piping networks for transportation of single- or multi-phase fluids. Very often, these piping networks contain tee junctions, which can be of different types depending on their functions and orientations of their inlets and outlets. Tee junctions, which combine two inlet flows to produce a single outlet flow, is a combining type tee junction. Again, dividing type tee junctions divide an inlet flow into two outlet flows. Both combining and dividing type tee junctions can be of impacting or branching type, based on the configuration of their inlets and outlets. Combining tee junctions are called branching type, when one of the inlets and the outlet are co-axial to each other or impacting type, when the two inlets are co-axial to each other. Dividing tee junctions are called branching type, when the inlet and one of the outlets are co-axial to each other or impacting type, when the two outlets are co-axial to each other. These four kinds of tee junctions are illustrated in Figure 1.1. It should be noted that the junctions illustrated in Figure 1.1 have the co-axial inlet(s)/outlet(s) at right angles to the other inlet/outlet, but the angles between them can vary, such as the case in wye junctions.

Two-phase flows, particularly gas-liquid two-phase flows passing through tee junctions are very commonly found in different industries. Work in this thesis is focused on air-water two-phase flows passing through a system of combined dividing impacting type tee junction. It is well established in the literature of two-phase flows flowing through dividing junctions that the phases are not equally divided between the two outlets, which often creates undesirable working conditions for devices downstream of these junctions. A considerable amount of research has been

done in search of reasons for this phenomenon and researchers reported that factors like inlet liquid and gas superficial velocities, operating pressure, angle of inclination of the outlets, geometry of the junctions, inlet flow regime, inlet quality etc. can be the reasons for this. Most of these works presented phase-redistribution data showing that equal phase-split occurs only at specific conditions. A limited amount of work focused on achieving total/partial phase separation using a single impacting dividing tee junction can also be found in literature. The inspiration for these works come from the fact that at extreme conditions of phase redistribution, total phase-separation can be achieved, where the two outlets of the dividing junction will each have a single-phase flow. Detailed review of notable works in this area are included in the next chapter.

(a) Combining branching   (b) Combining Impacting

(c) Dividing branching   (d) Dividing impacting
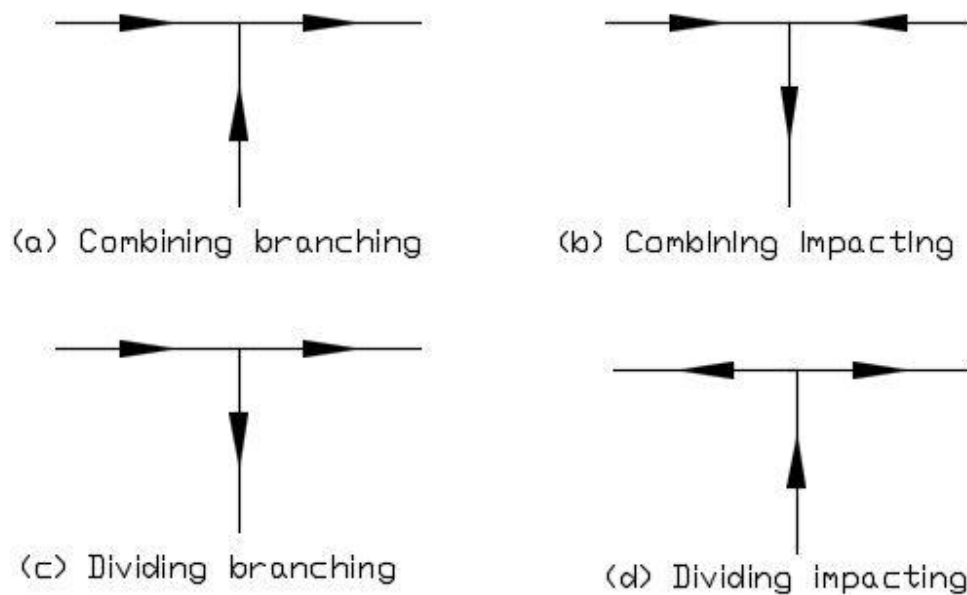
Figure 1.1   Different types of tee junctions

Recently, some research has been reported where multiple branching tee junctions were used to enhance phase separation. To the best of author's knowledge, till date, no evidence of work on multiple impacting tees for phase-separation can be found in the open literature. The present

investigation exclusively focuses on enhancing phase-separation effectiveness using multiple or combined impacting tee junctions.

1.2   Engineering Significance of the Present Study

Phase separation of a two-phase flow is a desirable or necessary process in many industries, like offshore mining of oil and gas, chemical processes, power generation in nuclear reactors etc. Traditionally, gravity-based separators are used in these industries, which are expensive to operate and maintain, large in size and often pose danger to the environment if containing hazardous chemicals. Compared to such separators, tee junctions are cheap, compact, easy to maintain and install and have lower depreciation, due to the absence of moving parts. As a result, if separators capable of total phase separation of two-phase flows can be developed out of a combination of tee junctions, a very simple and efficient alternative to gravity-based separators will be available. Such tee-junction based separators could also be installed in refrigeration or air-condition cycles, multi-channel heat exchangers etc. where single-phase flow can increase the efficiency of the system by facilitating condensation or evaporation processes. The major objective of this study is to experimentally investigate the limiting conditions up to which a system of combined impacting tee junction can totally separate phases. This thesis, thus, explores the idea of developing separators with only tee junctions and provides experimental data to support the viability of such separators.

1.3   Problem Definition

In this research, a system of combined impacting tee junction (one horizontal and two vertical junctions) has been designed, which has a horizontal inlet (represented by 1) and two vertical outlets (top and bottom outlets represented by 2 and 3, respectively). An air-water two-

phase mixture having air mass flow rate, W_{G1} and water mass flow-rate, W_{L1} enters the inlet of the combined system. The total inlet mass flow rate is therefore,

$$W_1 = W_{G1} + W_{L1} \qquad (1.1)$$

This inlet mass flowrate is divided in the two outlets, each having mass flowrates of W_2 and W_3, in a way that,

$$W_1 = W_2 + W_3 \qquad (1.2)$$

Again, each of the outlets may have both gas and liquid flowing in them, the gas and liquid mass flowrates in outlets 2 and 3 being represented by W_{G2}, W_{L2} and W_{G3}, W_{L3}, respectively. Hence, the total mass flowrates in outlets 2 and 3 can be denoted by,

$$W_2 = W_{G2} + W_{L2} \qquad (1.3)$$

$$W_3 = W_{G3} + W_{L3} \qquad (1.4)$$

Some more parameters, which will be used in the analysis of the experimental data, are:

Overall mass-split ratio, $\qquad\qquad W_R = W_3 / W_1 \qquad\qquad (1.5)$

Mass fraction of gas in outlet-2, $\qquad F_{G2} = W_{G2} / W_{G1} \qquad (1.6)$

Mass fraction of liquid in outlet-2, $\qquad F_{L2} = W_{L2} / W_{L1} \qquad (1.7)$

Mass fraction of gas in outlet-3, $\qquad F_{G3} = W_{G3} / W_{G1} \qquad (1.8)$

Mass fraction of liquid in outlet-3, $\qquad F_{L3} = W_{L3} / W_{L1} \qquad (1.9)$

Superficial gas velocity, $\qquad\qquad J_G = W_G / (\rho_G \times \pi \times D^2 / 4) \qquad (1.10)$

Superficial liquid velocity, $\qquad\qquad J_L = W_L / (\rho_L \times \pi \times D^2 / 4) \qquad (1.11)$

For any inlet condition, $F_{G2} + F_{G3} = 1$ and $F_{L2} + F_{L3} = 1$. The present experimental investigation aims at generating 'partial-phase-separation' or 'phase-redistribution' and 'full-phase-separation' data for air-water two-phase flows using the system of a combined junction for

different inlet conditions. These two terms have been amply used in the literature of two-phase

flows and will be defined in this thesis, in line with previous researchers.

<u>Partial Phase Separation or Phase Redistribution</u>

Partial phase separation or phase redistribution refers to the cases where there is gas and

liquid in both outlet branches and the fraction of inlet flow of one phase in one outlet is not equal

to the fraction of inlet flow of the second phase in the same outlet. In other words, partial phase

separation takes place when, $F_{G2} \neq F_{L2} \neq 0.5$ or $F_{G3} \neq F_{L3} \neq 0.5$. To demonstrate this term, the

following graph from Mohamed (2012) can be used:
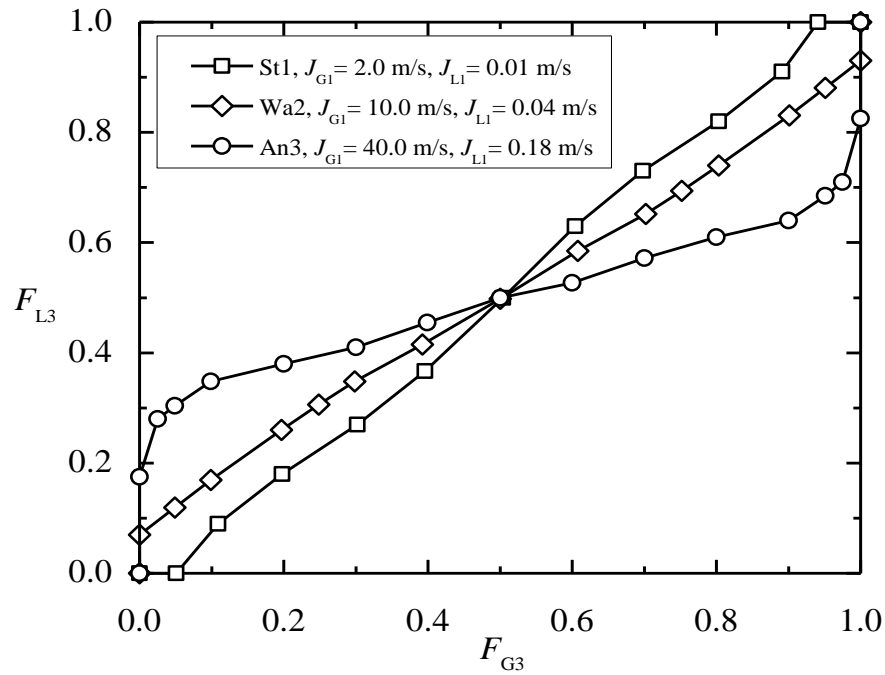
Figure 1.2   Partial-phase-separation plot for single horizontal tee junction, from
Mohamed (2012)

Figure 1.2 is an F_{G3} versus F_{L3} plot, or partial phase-separation plot for air-water two-phase

flow through a single horizontal tee junction, for three different sets of inlet conditions. It can be

observed from the figure that, except for the point of equal phase-split at $F_{G3} = F_{L3} = 0.5$, phases

are not divided equally in the two outlets, i.e., $F_{G3} \neq F_{L3} \neq 0.5$ or partial phase separation is taking place. For example, in the curve of inlet conditions St1, at $F_{G3} = 0.4$, F_{L3} has a value of 0.3, which means 40% of the inlet gas is entering outlet 3, with only 30% of inlet liquid. Thus, phases are being redistributed or partially separated. A straight line in this graph, joining the points (0, 0) and (1, 1) will have $F_{G3} = F_{L3}$, at all points and such a line is called 'equal-phase-split' line.

Full Phase-Separation

Full phase separation can be defined as the process when all of the inlet gas enters one outlet (in our case, top outlet or outlet 2) and all of the inlet liquid enters the other outlet (in our case, bottom outlet or outlet 3), for a set of operating conditions. In other words, full phase-separation takes place when $F_{G2} = 1$ and $F_{L2} = 0$ or $F_{G3} = 0$ and $F_{L3} = 1$.

1.4 Objectives

The objectives of the present investigation are listed below:

i. To find the limiting conditions of inlet gas and liquid superficial velocities, J_{G1} and J_{L1} for which full separation of phases can be achieved for the system of a combined impacting tee junction.

ii. Beyond the range of full phase separation, to generate partial-phase-separation data for inlet conditions in the annular flow regime using the system of a combined junction.

iii. To define a term to quantify phase-separation effectiveness of the present system and to apply it on the obtained experimental results.

iv. To compare the present full- and partial-phase-separation results with results from a system of a single vertical impacting tee junction.

v. To compare the present results with previous research on combined branching junctions.

CHAPTER 2

LITERATURE REVIEW

2.1 Overview

When a gas-liquid two-phase flow encounters a dividing tee junction, redistribution of phases takes place in the two outlets almost inevitably (Azzopardi and Whalley, 1982). As a result, liquid-rich and gas-rich streams are produced. Often times, this phenomenon creates undesirable working conditions for devices downstream of the dividing junction, due to change in quality of the inlet mixture. However, recent studies have shown that this phenomenon of redistribution of phases can be utilized to achieve partial to full phase separation (Azzopardi et al., 2002). Full phase separation is a desirable phenomenon in many practical applications where single-phase flow can enhance heat transfer or decrease power consumption for condensation or evaporation (e.g., multi-channel heat exchangers, refrigeration and air-conditioning cycles, etc.). In addition, tee junctions can serve as smaller, cheaper and less cumbersome substitutes of traditional gravity-based separators. Consequently, this provides researchers with an important area of research. So far, very limited amount of experimental/theoretical work has been done on phase separation using tee junctions. Notable among these are works by Wren and Azzopardi (2004), Yang et al. (2010), Mohamed et al. (2012), Tuo and Hrnjak (2012).

In the literature of two-phase flows, branching and impacting tees are treated independently. While there is a wealth of literature on two-phase flows passing through branching tees, limited research has been done on impacting tees. Again, almost all of the available works on impacting tees are focused on the use of a single junction. Recently, some researchers have focused on the use of multiple branching tee junctions to enhance phase separation. To the best of the

7

author's knowledge, till date, no evidence of work on multiple impacting tees for phase separation can be found in the literature. The work in this thesis exclusively focuses on enhancing phase-separation capability using multiple impacting tee junctions. Hence, the present work is expected to contribute significantly in the field phase separation of two-phase flows.

In this review, attempt has been made to examine the progression of knowledge in the field of two-phase flows flowing through dividing junctions from two perspectives:

1. Studies on Single impacting Tee Junctions

2. Studies on Multiple Tee Junctions

2.2 Studies on Single Impacting Tee Junctions

Two-phase flow through a single impacting tee junction has been studied under various conditions or inlet/outlet parameters. Researches have been conducted on the effects of inlet flow regime, geometry of the junction, inlet quality, inlet liquid and gas superficial velocities, pressure fluctuations and angle of inclination of inlet/outlets. Most of these works presented phase-redistribution data showing that equal-phase split occurs only at equal mass split in the two outlets. A limited amount of work focused on achieving phase-separation. This review will examine available literature on single impacting tee junctions in two parts:

1. Studies on Phase Redistribution with Single Impacting Tee junction
2. Studies on Phase Separation with Single Impacting Tee Junction

2.2.1 Studies on Phase Redistribution with Single Impacting Tee Junctions

Phase redistribution in impacting tee junctions has been studied for various operational conditions, flow regimes and structure of the junction, mostly with air-water two-phase flows. Some works can also be found with wet steam, air-nitrogen and various refrigerants. Owing to the large number of variables and complexity of mechanisms of a two-phase flow through dividing junctions, it is very difficult to produce an exact simulation environment for this kind of study. Therefore, the majority of the work in this field is experimental. However, a few analytical models have also been reported.

A considerable amount of work can be found in literature on phase redistribution using a single impacting tee. Table 2.1 gives a summary of some of the previous works in this area.

Hong (1978) was one of the first to conduct experiments on impacting tees with air-water two-phase flow. His experimental set-up consisted of a horizontal impacting tee junction with equal diameters of 9.525-mm for both inlet and outlets. In this paper, the author presented phase-redistribution data and commented on effect of inlet liquid flow rate, inlet superficial gas velocity (J_{G1}), inlet flow regime, test liquid viscosity and gravity on phase redistribution. Data were obtained for inlet superficial liquid velocity, J_{L1}, of 0.02 m/s and inlet superficial gas velocity, J_{G1}, of 27.4 m/s. These conditions fell in the annular flow regime in Mandhane et al. (1974) map. The viscosity of liquid used was one cP. The phase-redistribution data showed that when 15 to 85 percent of gas enters one of the outlet branches, liquid splits in the same proportion as the gas. Thus, he obtained equal phase split for F_{G3} of 0.15 to 0.85. These results deviated with those of other researchers who suspected that Hong's data were affected by strong surface tension influence due to the small tube diameter used.

Table 2.1.   References on phase redistribution using a single impacting tee junction

Author(s)	Inlet Dia. (mm)	Test Fluids	Tee Junction Orientation	System Pressure (bar)	J_{G1} (m/s)	J_{L1} (m/s)	Inlet Flow-Regime
Hong (1978)	9.525	Air-water	Horizontal	1.22 (abs)	27.4	0.02	An
Azzopardi et al. (1986a)	31.8	Air-water	Vertical inlet and horizontal outlets	1.7 (abs)	9.8 - 21.6	0.03 - 0.08	An
Azzopardi et al. (1986b)	31.8	Air-water	Vertical inlet and horizontal outlets	1.7 (abs)	1.6 - 3.7	0.08 - 0.8	Ch
Hwang et al. (1989)	38	Air-water	Horizontal	1.3-1.9 (abs)	1.4 - 5.7	1.3 - 2.7	B, B-St
Chien and Rubel (1992)	50.8	Steam-water	Horizontal	27.6-41.4 (gauge)	12.2 - 39.6	0.04 - 1.5	An, An-Mt
Hong and Griston (1995)	19.05, 50.8, 101.6	Air-water	Horizontal	-	4.6 - 22.9	-	-
Fujii et al. (1995)	10	Nitrogen-water	Horizontal	-	0.03 - 12	0.05 - 0.5	St, W, Sl, Pl, An
El-Shaboury et al. (2007)	37.8	Air-water	Horizontal	1.5 (abs)	0.5 - 40	0.01 - 0.18	St, W, An
Elazhary and Soliman (2012)	1.87 × 20 [rectan--gular]	Air-water	Horizontal	2 (abs)	0.04 - 10	0.02 – 0.7	B, Ch, Pl, An
Mohamed et al. (2011)	13.5	Air-water	Horizontal inlets and inclined outlets	2 (abs)	2 - 40	0.01 - 0.18	St, W, An
Mohamed et al. (2014)	13.5, 37.8	Air-water	Horizontal	1.5, 2 (abs)	2 - 40	0.01 - 0.18	St, W, An
Chen et al. (2014)	0.5 × 0.5 [square]	Nitrogen-Water	Horizontal	1.2 (abs)	13 - 30	0.018 - 0.08	An
Chen et al. (2015)	0.5 × 0.5 [square]	Nitrogen-Water	Horizontal	1.06 - 1.15 (abs)	0.36 - 2.4	0.1 - 0.9	Sl
Sun et al. (2018)	1 × 0.5 [rectan--gular]	Nitrogen-Water	Horizontal	1.2 (abs)	0.47 - 15.1	0.01 -0.41	An, Sl, Sl-An

* St - Stratified, W - Wavy, An - Annular, Sl- Slug, Pl - Plug, B - Bubbly, Mt - Mist, Ch – Churn
B-St – Bubbly-Stratified, An-Mt – Annular-Mist, St-An – Stratified-Annular

Azzopardi et al. (1986a) presented phase-redistribution data for air-water two-phase flows in an impacting tee junction with vertical inlet and horizontal outlets. His set-up consisted of equal diameter pipes of 31.8-mm for both inlet and outlet and the operating pressure was 1.7 bar. Liquid flow rate ranged from 0.0252 - 0.0630 kg/s and gas flow rate ranged from 0.0157 - 0.0346 kg/s. Inlet quality ranged from 0.21 - 0.58 and the corresponding inlet flow regime was annular. Phase-redistribution data showed that, gas flow splits 50/50 in the two outlets only when liquid splits equally. Otherwise, data points lied above the equal phase split line for $F_{G3} < 0.5$, in F_{G3} vs. F_{L3} graph. Beyond the point (0.5, 0.5) in the graph, data points were inverted mirror images for $F_{G3} > 0.5$. In this work, authors also proposed a model to predict phase redistribution when an annular flow enters an impacting junction with horizontal or vertical inlet.

Azzopardi et al. (1986b) used an identical set-up as Azzopardi (1986a). Here, the inlet liquid flow rate was varied from 0.06 - 0.620 kg/s and the inlet gas flow rate was varied from 0.0025 - 0.006 kg/s; the operating pressure was 1.7 bar. The corresponding inlet flow regime of the air-water two-phase flow was churn flow. The trend of phase-redistribution data obtained in this work was similar to that of Azzopardi (1986a). Equal phase split was reported only at equal mass split. However, phase redistribution under the test conditions mentioned above was found to be insensitive to inlet liquid and gas flow rates.

Hwang et al. (1989) performed experimental and analytical studies of two-phase air-water flows through horizontal equal-sided tee and wye with 38 mm I.D. tubes. The experimental data were taken at operating pressures of 0.13 - 0.19 MPa. Low, medium and high inlet mass fluxes of 1350 kg/m²s, 2050 kg/m²s and 2700 kg/m²s were used and inlet qualities of 0.002, 0.003 and 0.004 were tested for each mass flux. The inlet flow regimes corresponded to bubbly and bubbly-stratified flows. The experimental results for the impacting tee junction showed that equal phase

split took place only when the mass split ratio in both the outlet branches was equal ($W_2/W_1 = W_3/W_1 = 0.5$). This conclusion is in agreement with Azzopardi (1986a, 1986b) and thus it can be said that, it holds for both horizontal and vertical impacting tees. Data were presented in terms of quality ratio (x_3/x_1) versus mass split ratio (W_3/W_1) graphs. It was observed that very little gas entered the branch for $W_3/W_1 < 0.4$. From $W_3/W_1 = 0.4$ to 0.6, both gas and liquid were present in the branch. For $W_3/W_1 > 0.6$, all the gas entered outlet 3 ($W_1/W_3 = x_3/x_1$). Thus, it can be said that, tee junction could be used as a fluidic switch for the given conditions. In this work, an analytical model was also proposed based on the "dividing streamline concept" and this model was capable of predicting 95% of the presented data within $\pm$ 25% accuracy.

Chien and Rubel (1992) presented phase-redistribution data of wet steam passing through a horizontal equal-sided impacting tee with a diameter of 50.8-mm. In this study, the inlet pressure ranged from 27.6 - 41.4 bars, the inlet quality (x_1) ranged from 0.2 - 0.8, vapor extraction ratio (F_{G3}) ranged from 0.2 - 0.5 and inlet vapor superficial velocity (J_{G1}) ranged from 12.2 - 39.6 m/s. The corresponding flow regimes were annular and annular-mist. From the experimental data, the relative importance of x_1, F_{G3}, inlet mass fluxes and inlet pressure on phase redistribution was determined. The authors came to the conclusion that the phases split equally only at F_{G3} of 0.5, which is in agreement with previous work by Hwang et al. (1989) and Azzopardi et al. (1986a, 1986b). It was also observed that phase splitting or difference between outlet and inlet steam qualities reduces as F_{G3} increases from 0 to 0.5, under the tested conditions. In addition, at constant F_{G3}, x_3/x_1 became closer to 1 as x_1 was increased. Keeping other parameters constant, when J_{G1} was changed (12.2, 18.3, 24.4 and 33.5 m/s) only a slight change in outlet steam quality (x_3) was noticed for a particular x_1. Changing inlet pressure also did not produce any significant change in

data. The authors thus concluded that, among the parameters that effect phase redistribution in an impacting tee, F_{G3} and x_1 are major, whereas inlet pressure and J_{G1} are minor.

Hong and Griston (1995) studied phase redistribution of air-water two-phase flow passing through a horizontal equal-sided impacting tee of 19.05-mm diameter, with the aim of developing a method to predict qualities of split streams and to find insert devices which can increase the range of F_{G3} for equal phase split. Experiments were conducted over F_{G3} of 0.05 to 0.95 and upstream liquid volume fraction of 0.005 to 0.06. Inlet gas superficial velocity, J_{G1} was varied from 4.6 m/s to 22.9 m/s. Experimental results with varying input liquid volume fraction and J_{G1}, concluded that except for equal vapor phase split ratio (1:1) in the two outlets, liquid stream does not divide equally, resulting in unequal phase redistribution. This is in agreement with previous existing works on two-phase flow through tee junctions. It was also observed that for the lowest J_{G1} (4.6 m/s) used and low upstream liquid volume fraction (0.01) almost equal phase split occurs throughout the entire range of F_{G3}. Increasing J_{G1} increased the extent of phase redistribution, for low input liquid volume fraction (up to 0.02 in this case). As the input liquid fraction was increased further, phase-redistribution data became insensitive to J_{G1}, which is in line with work of Chien and Rubel (1992). The phase-redistribution data rotated in clockwise direction from equal phase split line as the input liquid volume fraction was increased. In fact, for input liquid fraction of 0.04 and above, the phase-redistribution data for the entire inlet superficial gas velocity range, became a horizontal line passing through (0.5, 0.5) point in the F_{L3} versus F_{G3} graph.

Hong and Griston (1995) also conducted experiments with field steam flows to ascertain their phase-redistribution characteristics when passed through tee junctions of diameter 50.8-mm and 101.6-mm. Eighteen tests were run by varying inlet liquid fraction from 0.01 to 0.1 and J_{G1} from 1.5 m/s to 21.3 m/s. The results showed that for the 101.6-mm diameter, almost equal phase

split occurred throughout the entire range, if J_{G1} was kept below 6 m/s. For the 50.8-mm diameter, equal phase split only happened at equal mass extraction ratio in both outlets. Their work was extended by placing tee insert devices downstream of the junction to increase the range of mass extraction ratio that will give equal phase split. Among the various devices tested, the greatest improvements were obtained for pre-separator vane, downstream nozzles and vane/nozzle combinations. Some of the devices tested did not provide any improvement at all or even narrowed the range.

Fujii et al. (1995) presented phase-redistribution data of nitrogen-water passing through a horizontal impacting equal-sided tee junction of 10-mm diameter. The authors aimed at developing a technique using tee junction in which only one phase will flow in an outlet at a specific mass extraction ratio, to be used under micro gravity. Two-phase flows in various flow regimes were tested and the effect of flow regime on phase split was studied. The range of J_{L1} and J_{G1} used in the experiments were 0.05 - 0.5 m/s and 0.03 - 12 m/s, respectively and they corresponded to stratified, wavy, slug, plug and annular flow regimes. Whole range of extraction ratio (W_3/W_1), from 0 to 1 was tested. In the plug flow regime, J_{L1} of 0.5 and 0.2 m/s were tested. For each J_{L1}, J_{G1} was varied from 0.03 - 0.46 m/s. It was observed that for both J_{L1}, gas take-off did not take place until $W_3/W_1 = 0.3$, which implied that there was pure water flow through outlet 3. After that for a wide range of extraction ratio, there was gas and liquid flow in that outlet. On further increasing the extraction ratio beyond $W_3/W_1 = 0.6$ for $J_{L1} = 0.5$ m/s and $W_3/W_1 = 0.7$ for $J_{L1} = 0.2$ m/s, only gas started to flow in outlet 3. For J_{L1} of 0.5 m/s, J_{G1} did not have much effect on phase redistribution, but for J_{L1} of 0.2 m/s, the gas take-off point decreased with increasing J_{G1}. In addition, the effect of J_{L1} on phase redistribution increased with increasing J_{G1}. Phase redistribution was strongly influenced by J_{L1} in the annular flow regime and effect of J_{G1} was found

to be small. Thus, the authors concluded that the flow regime and J_{L1} influenced phase-redistribution data. As J_{G1} increased, the influence of J_{L1} also increased. The observations in this paper agreed with Hong and Griston (1995) and Hwang et al. (1989).

El-Shaboury et al. (2007) experimented with air-water two-phase flow through a horizontal equal-sided tee junction with a diameter of 37.8-mm. The effects of flow regime and inlet quality on the phase redistribution was studied in this work. Pressure-drop data were also generated and a model was proposed that could predict the pressure drop and phase redistribution. The range of J_{G1} and J_{L1} tested in this work was 0.5 - 40 m/s and 0.01 - 0.18 m/s, respectively, which covered stratified, wavy, stratified-wavy and annular flow regimes. Data for whole range of mass extraction ratio (from 0 to 1) were presented, assuming symmetry and the inlet quality ranged from 0.02 to 0.96. Like previous works, it was observed that equal phase split only occurs at equal mass extraction ratio in both outlets. It was also observed from the experimental data that, within a particular flow regime, as J_{G1} increases, at fixed J_{L1}, phase-redistribution curves rotate in counter-clockwise direction around the point (0.5, 0.5) in an F_{L3} versus F_{G3} graph. Opposite effect was observed for increasing J_{L1}, at fixed J_{G1}. These observations are consistent with the works of Azzopardi (1986a, 1986b) and Hong and Griston (1995). When the effect of inlet quality x_1 was tested for each flow regime, it was found that as x_1 was increased, the phase-redistribution curve moved in counter-clockwise direction around equal phase split point. The influence of x_1, J_{G1} and J_{L1} were found to be continuous in the boundary of stratified and wavy flow regime, but not in the boundary between wavy and annular flow regime.

Mohamed et al. (2011) generated phase-redistribution data for two-phase air-water flow through an equal-sided impacting tee junction with horizontal inlet and inclined outlets of 13.5-mm diameter. The angle of inclination of the outlet branches, θ, was varied from 0^0 to 90^0. The

ranges of J_{G1} and J_{L1} tested were 2 - 40 m/s and 0.01 - 0.18 m/s, respectively. That corresponded to stratified, wavy and annular flow regimes. The operating pressure was 200 kPa (abs), x_1 ranged from 0.1 to 0.9 and the whole range of mass extraction ratio (0 to 1) was tested. The effects of inlet flow regime, mass extraction ratio at the junction, and angle of inclination, θ, on the phase redistribution were examined and the possibility of full phase separation was considered.

The authors reported full separation of phases at $\theta = 0.7^0$ and $\theta = 7.5^0$, for stratified flows with conditions, $J_{G1} = 2$m/s, $J_{L1} = 0.01$ m/s and $J_{G1} = 2$m/s, $J_{L1} = 0.04$ m/s, respectively. At $\theta = 0^0$, almost equal phase split occurred throughout the entire range of F_{G3} for $J_{G1} = 2$m/s and $J_{L1} = 0.01$ m/s. The observations for stratified flow held good for wavy flows also. Two sets of wavy flow data were taken at various angles of inclination, with inlet conditions of $J_{G1}=10$ m/s, $J_{L1}=0.01$ m/s and $J_{G1}=10$ m/s, $J_{L1}=0.04$ m/s, with inlet qualities 0.7 and 0.37, respectively. As the inlet quality was decreased from 0.7 to 0.37, phase-redistribution data lines rotated in clockwise direction around equal phase split point, which is consistent with observations of El-Shaboury et al. (2007). For $J_{G1}=10$ m/s, $J_{L1}=0.01$ m/s, full separation of phases took place at $\theta = 87.5^0$ and for $J_{G1}=10$ m/s, $J_{L1}=0.04$ m/s, full separation was not achieved even at $\theta = 90^0$. Similar trend was observed for annular flow also. In the annular flow regime, changing angle of inclination did not produce much difference in phase redistribution. Changing J_{L1}, keeping J_{G1} and θ fixed did not produce any fixed trend, for any inlet condition. However, with increased θ and decreased J_{G1}, tendency of liquid to exit through the lower branch increased.

Elazhary and Soliman (2012) studied phase redistribution of air-water two-phase flows through a mini-sized horizontal impacting tee junction, having rectangular cross-section of 1.87 mm × 20 mm. Experimental data were collected at 200 kPa (abs) nominal pressure and at room temperature with J_{G1} and J_{L1} ranging from 0.04 – 10 m/s and 0.02 - 0.7 m/s, respectively. The

collected experimental results fell in the bubbly, plug, churn and annular flow-regimes. Experimental results showed that phase-redistribution data depended on the inlet flow regimes, as well as on the values of J_{L1}, within the same flow regime. The trend of phase-redistribution curves obtained in their experiments were consistent with those reported by El-Shaboury et al. (2007), who used macro-sized horizontal impacting junctions with circular cross-section of 37.8-mm diameter. However, comparison with the data of El-Shaboury et al. (2007) showed that effects of J_{L1} on the values of F_L for the present mini-sized junctions are significantly smaller compared to macro junctions, under similar inlet conditions. The authors also proposed a model, by slightly modifying the model proposed by Hwang et al. (1989) for predicting phase redistribution of two-phase flows. This modified model was able to predict the experimental results reported in this paper within a deviation range of - 15% to + 20%.

Mohamed et al. (2014) investigated the effect of pipe diameter and system pressure on phase redistribution of air-water two-phase flow in a horizontal impacting junction. In this work, J_{G1} and J_{L1} were varied from 2 - 40 m/s and from 0.01 - 0.18 m/s, respectively, which corresponded to stratified, wavy and annular flow regimes. The operating pressures tested were 150 and 200 kPa (abs). The authors compared their data ($D = 13.5$ mm) with data by El-Shaboury et al. (2007) with $D = 37.8$ mm, under 150 kPa operating pressure (abs) and found no significant effect of diameter on phase redistribution, irrespective of flow regimes. However, effect of system pressure was evident from the experiments, particularly at the low velocities of stratified and wavy flows. As the velocities (both J_{G1} and J_{L1}) were increased, the magnitude of the effect of pressure on phase redistribution decreased.

Chen et al. (2014) conducted experiments to find if phase-redistribution behavior in an impacting tee junction differs in micro-channels compared to mini and macro channels. In this

work, a horizontal tee junction with a square cross-section of 0.5 mm $\times$ 0.5 mm and nitrogen-water two-phase mixture as working fluid were used. The ranges of J_{G1} and J_{L1} tested were 13 - 30 m/s and 0.018 - 0.08 m/s, respectively. Data for the entire range of mass split ratio (0 to 1) were presented by assuming symmetry. They corresponded to annular flow regime with x_1 varying from 0.23 to 0.58. It was observed that unlike mini and macro channels, J_{G1} and J_{L1} has little effect on phase-redistribution characteristics for micro-channels for the entire range of tested conditions. Data were presented in F_{G3} versus F_{L3} graph. Consistent with all previous studies, equal phase split was obtained only at equal mass extraction. It was observed that the branch with lower gas flow ($F_{G3} < 0.5$) had proportionately more liquid and the data points were inverted mirror image around the point (0.5, 0.5). From $F_{G3} = 0$ to 0.15, the phase-redistribution curve is steeper than from F_{G3} = 0.15 to 0.5, which implies that phase redistribution reaches a peak at $F_{G3} = 0.15$. The authors also concluded from the experiments that phase redistribution increases significantly with decrease of surface tension, especially when gas extraction ratio deviates from 0.5. Viscous forces did not seem to influence phase-redistribution under all tested conditions. Experiments with slug and slug-annular flows showed that phase redistribution was less severe for annular flow compared to slug flow. Obtained phase-redistribution data for micro-channel were compared with the data of Azzopardi et al. (1986a) having hydraulic diameter 31.8 mm (macro-channel) and Elazhary and Soliman (2012) having hydraulic diameter of 3.4 mm (mini-channel) and it was found that phase redistribution is less severe for the present test-section of 0.5 mm $\times$ 0.5 mm micro-channel.

Chen et al. (2015) experimented with nitrogen-water slug flow through a horizontal micro impacting tee junction and concluded that at small pipe dimensions (0.5 $\times$ 0.5 mm square cross-section), surface tension plays a vital role in lengths of inlet gas slugs (L_{GS}) and also increases phase-redistribution capability of the tee junction. They reported that compared to macro and mini

tee junctions, which show 5% and 15% of liquid take-off through one outlet, micro impacting tee junctions show 35% liquid take-off, when all the gas is taken off from the other outlet. The test conditions in this work were varied from 0.36 - 2.4 m/s and 0.1 - 0.9 m/s for gas and liquid inlet superficial velocities, respectively, at 18^0 C and 0.106 - 0.115 MPa (abs) test pressure. Owing to the symmetry of the test section, data points obtained were inverted mirror images of one another around (0.5, 0.5) point in F_{G3} vs. F_{L3} graph. The authors showed that as J_{G1} is increased at constant J_{L1}, L_{GS} increases, while L_{GS} decreases with increase of J_{L1} at constant J_{G1}. The effect of J_{G1} on phase redistribution was more potent than that of J_{L1}. Experimental evidence showed that the effect of surface tension on phase redistribution is linked with L_{GS}. For small L_{GS} ($< 5D_h$), with decreasing surface tension, phase redistribution decreased and for large L_{GS} ($> 5D_h$), phase redistribution increased with a decrease in surface tension. A correlation for predicting phase split of slug flow in micro impacting tee junctions was also proposed in this work.

Sun et al. (2018) conducted experiments to analyze the effect of cross-sectional diameters of the outlets on phase redistribution of a horizontal micro-impacting tee junction, with nitrogen-water two-phase flow as working liquid. The ranges of J_{G1} and J_{L1} studied in this work were 0.47 - 15.1 m/s and 0.0130 - 0.4102 m/s, respectively, at 120 kPa (abs) system pressure, which covered slug, annular and slug-annular flow regimes. The dimensions of the inlet were fixed at 1000 μm × 500 μm and the cross-section of the outlets were varied (400 μm × 500 μm, 600 μm × 500 μm and 800 μm × 500 μm). A definition of separation efficiency, $\eta = |F_{G3} - F_{L3}|$, was used in this work and the authors commented that a decreased η is conducive to uniform phase redistribution in the two outlets. In order to quantify the effect of branch channel diameter on phase redistribution, the authors used a parameter, influencing degree, I, which was defined as:

$$I = (\Delta F_{L, max} / F_{L, 800 \, \mu m}) \times 100\% \tag{2.1}$$

$$\Delta F_{L, \text{max}} = \text{maximum difference in } F_L \text{ at fixed } F_G = [F_{L, 400\ \mu m} - F_{L, 800\ \mu m}]_{\text{max}} \qquad (2.2)$$

$F_{L, 400\ \mu m}$, $F_{L, 600\ \mu m}$, $F_{L, 800\ \mu m} = F_{L3}$ at branch diameter 400 μm, 600 μm and 800 μm respectively.

In general, the results of this work were consistent with Chen et al. (2015) and other previous researchers, in the manner that, branch with lower gas flow ($F_{G3} < 0.5$) had proportionately more liquid and data points were inverted mirror image around the point (0.5, 0.5) in F_{L3} versus F_{G3} graph. Experimental results showed that data points for annular flows were closer to the equal phase-redistribution line in F_{L3} versus F_{G3} graph, followed by slug flows and slug-annular flows. In addition, as the outlets cress-sections were reduced, phase-redistribution improved, for all flow regimes. However, the influencing degree, I was highest for slug-annular flow (37.15%) compared to slug (13.13%) and annular (13.08%) flows, which means phase-redistribution is most sensitive to change in cross-section for slug-annular flows. In slug flow, as superficial velocities increased, the effect of outlet size became smaller and consequently, I decreased. For all flow regimes, η decreased with F_{G3} increasing from 0 to 0.5 and followed opposite trend after F_{G3} of 0.5. However, η was higher for slug-annular flow, followed by slug flow and annular flow, which implies that annular flow provided more uniform phase redistribution, compared to the other two flow regimes.

2.2.2 Studies on Phase Separation with Single Impacting Tee Junctions

There are very few studies on full phase separation of two-phase flows using a single impacting tee junction in the literature. As discussed in the previous section, most works on two-phase flow through a single tee junction presents phase-redistribution data and focuses on finding a range of mass extraction ratio for which even phase redistribution can be achieved, for specific operating conditions. Hwang et al. (1989) and Fujii et al. (1995), although focused on phase-

redistribution data, presented range of mass extraction ratio for which phase separation could be achieved within the operating range of their experiments. However, their work cannot be cited as works on full phase separation, according to the definition provided in this thesis (phases are considered fully separated, if the two outlets get a single-phase flow for a particular working condition, at all mass extraction ratio). These works have been reviewed in detail in the previous section. Table 2.2 gives a summary of available previous works on phase separation using a single impacting tee junction.

Mohamed et al. (2012) attempted to obtain full separation of phases using a single equal-sided impacting tee of 13.5-mm diameter at 200-kPa (abs) pressure. In this experimental study, limiting conditions of J_{G1} and J_{L1} that gives full phase-separation were found for different angles of inclination of the outlet branches, θ (2.5^0, 7.5^0, 15^0, 30^0, 60^0, 75^0 and 90^0), keeping the inlet horizontal. The authors reported that the limiting values of J_{G1} and J_{L1} for full phase separation increases as θ increases. The largest range of J_{G1} and J_{L1} for full phase separation was reported for $\theta = 90^0$ (vertical outlets). For $\theta \leq 30^0$, full phase separation took place only in the stratified flow regime. For $60^0 \leq \theta \leq 90^0$ and $J_{L1} \leq 0.08$ m/s, full phase separation took place in the stratified and stratified-wavy flow regime, at $J_{G1} > 3$ m/s. For $60^0 \leq \theta \leq 90^0$ and $J_{G1} \leq 3$ m/s, full phase separation took place in the stratified flow regime, at $J_{L1} < 0.08$ m/s. It was further observed that the value of J_{L1} for full phase separation becomes insensitive to change in J_{G1} as J_{G1} decreases, for all values θ. In addition, the value of J_{G1} for full phase separation becomes insensitive to change in J_{L1} as J_{L1} decreases. A model was proposed based on the observed flow phenomena near limiting conditions of phase separation to predict the values J_{G1} and J_{L1} for full phase separation at different θ, which agreed with experimental results within $\pm 20\%$.

Table 2.2.　　References on phase separation using a single impacting tee junction

Author(s)	Inlet Dia. (mm)	Test Fluids	Tee Junction Orientation	System Pressure (bar)	J_{G1} (m/s)	J_{L1} (m/s)	Inlet Flow-Regime
Mohamed et al. (2012)	13.5	Air-water	Horizontal inlet and inclined outlets	2 (abs)	2 - 40	0.01 - 0.18	St, W, An
Tuo and Hrnjak (2012)	8.7	R134A	Horizontal inlet and vertical outlets	-	-	-	St-W, St, An, Ch, D
Zheng et al. (2016a)	8	R134a/R245a	Horizontal inlet and vertical outlets	-	-	-	-
Zheng et. al (2016b)	8	R134a	Horizontal inlet and vertical outlets	-	2.2 - 5.8	0.02 - 0.43	Sl, St-W, An, Int

* St - Stratified, W - Wavy, An - Annular, Sl- Slug, Ch – Churn, Int – Intermittent
D – Droplet, St-W – Stratified-Wavy

Tuo and Hrnjak (2012) studied the effects of inlet mass flux, inlet quality, tube diameter and angle of inclination of the inlet tube on phase-separation capability of a vertical impacting tee junction (horizontal inlet and vertical outlets), when two-phase refrigerant R134a is passed through it. Various tests were conducted by varying inlet flow rate and quality from 10 g/s to 35 g/s and 10 to 30%, respectively. Observed inlet flow regimes were stratified-wavy, stratified, churn, annular and droplet. The inlet angle was varied from 0^0 to 45^0. The authors defined separation efficiency of liquid and vapor (η_l and η_v) as:

$$\eta_l = W_{l, b} / W_{l, i} \qquad\qquad (2.3)$$

$$\eta_v = W_{v, t} / W_{v, i} \qquad\qquad (2.4)$$

Here, the subscripts i, b and t represented the inlet and bottom and top outlets, respectively. Experimental results showed that separation efficiency decreases with increase in inlet mass flow rate and x_1 owing to the increase in J_{G1} and J_{L1}, which are proportional to vapor drag force and liquid inertial force and makes more liquid to be dragged to upper outlet. Up to a flow-rate of 20 g/s, η_1 was very close to 100% (within x_1 of 0 to 0.26) and it decreased drastically to 76% at flow rate of 35 g/s. Increasing angle of inclination of the inlet (or inclining the inlet in the downward direction) gave increased η_1. As the diameter of outlets was decreased from 18.3 mm to 13.4 mm, at 30 g/s flow rate, η_1 dropped to 62% from 80%. The authors mentioned that using a pre-separator or dual tee junction could improve separation efficiency. In another work by Tuo and Hrnjak (2014a), with similar experimental set-up, it was reported that η_1 deteriorates dramatically as the inlet flow regime changed from mist flow to churn, with increasing inlet flow rate or quality.

Zheng et al. (2016a) experimentally investigated constituent distribution capabilities of a vertical impacting tee junction (horizontal inlet and vertical outlets) when binary zeotropic mixtures, R134a/R245a (densities 511.9 kg/m^3 and 516.08 kg/m^3, respectively) were passed through it. Experiments were performed with four different mixture compositions with $x_{R134a, inlet}$ of 0.7075, 0.5146, 0.3215 and 0.7094 (represented by R1, R2, R3 and R4, respectively); qualities of each mixture ranged from 0.1 to 0.5 and inlet mass fluxes of 200, 400 and 600 kg/m^{2}s were used. Effects of these inlet parameters, along with outlet parameters like outlet to inlet flow ratio and outlet tube diameter (D_{in} / D_{out} = 0.457, 0.167) on constituent separation performance were studied in this paper. Authors designated the bottom and top outlets as outlet 2 and 3, respectively. It was observed that for all mass fluxes, $F_{R134a, 2}$ decreases with increase in inlet quality of R134a for W_2/W_1 = 0.1 and 0.3. For W_2/W_1 = 0.5 with fully opened control valves in both outlets, $F_{R134a,2}$ follow similar trend for mass flux of 200 kg/m^{2}s, but it decreases up to a certain value of inlet

quality of R134a and then start to increase for mass fluxes of 400 and 600 kg/m^{2}s. The authors defined separation efficiency as:

$$\eta_{i,j} = F_{i,j} \times 100\% \qquad (2.5)$$

where, i referred to the constituents R134a and R245a and j referred to outlet 2 or 3, respectively.

Constituent separation performance (difference between separation efficiencies of the two constituents in outlet 2, $\eta_{134a,2}$ - $\eta_{R245a,2}$) was defined and the best performance under that definition was reported to be -14.6%, with mixture R1, at 0.49 vapor quality, mass flux of 200 kg/m^{2}s and inlet to outlet mass flux ratio of 0.5. Separation efficiency difference or constituent separation performance were reported to be smaller for diameter ratio 0.457 than for diameter ratio 0.167. It is evident from this study that both inlet and outlet parameters played vital role on constituent separation efficiency of binary zeotropic mixture, when passed through a vertical (horizontal inlet and vertical outlets) impacting tee junction.

Zheng et al. (2016b) experimentally studied how a vertical impacting tee junction (horizontal inlet and vertical outlets) can act as a phase separator for two-phase flow of R134a refrigerant. The internal diameter of inlet and outlets in their experimental set-up were 8 mm and 17.5 mm, respectively. Separation efficiency of vapor and liquid was defined as:

$$\eta_{liq} = F_{L2} \times 100\% \qquad (2.6)$$

$$\eta_{vap} = F_{G3} \times 100\% \qquad (2.7)$$

The lower and upper outlets were represented as outlet 2 and outlet 3, respectively. Separation efficiency of liquid, η_{liq} was determined for inlet mass flux and inlet quality range of 100 kg/m^{2}s to 600 kg/m^{2}s and 0.1 to 0.6, respectively. These conditions correspond to slug, stratified-wavy, annular and intermittent flow regimes in the inlet. Results of the experiments with fully open valves

in both outlets showed that η_{liq} decreases with the increase of inlet mass flux and/or quality and it remains above 95%, for mass fluxes less than 200 kg/m^{2}s, but decreases slightly as quality is increased. For x_1 of 0.1, η_{liq} decreases by 2.5% as inlet mass flux is increased from 100 to 400 kg/m^{2}s and it reduces by a drastic 20% for an increase of mass flux to 600 kg/m^{2}s. These results were consistent for all tested flow regimes. It was also observed that η_{liq} decreased with increase of J_{G1} or J_{L1}. The range of change of J_{G1} and J_{L1} tested were 2.2 - 5.8 m/s and 0.02 - 0.43 m/s, respectively. Experimental results showed that when J_{G1} was kept at about 2.2 m/s, 97.5% separation efficiency could be achieved

The authors also showed that as the mass extraction ratio in the bottom outlet (W_2/W_1) increases, η_{liq} increases for the entire range of x_1. It was concluded that η_{liq} could be kept within 90%, if the mass flux remained less than 200 kg/m^{2}s or if 75% of the inlet mass flows through the lower outlet. Some analysis was done with vapor phase Froude number (Fr) in the upper outlet, which showed that as this Froude number increases, η_{liq} decreases very quickly. The authors proposed a model capable of predicting phase-separation of annular and stratified-wavy two phase-flows in vertical impacting tee junction (horizontal inlet and vertical outlets), based on a correlation between the fraction of liquid falling in the upward branch and Fr. This model was capable of predicting phase separation of annular and stratified-wavy flows within 6.4% and 6.9% deviation, respectively.

2.3 Studies on Multiple Tee Junctions

As the concept of using tee junctions as phase separator is gaining popularity, researchers are adapting various techniques to incorporate tee junctions in a system in order to separate phases. One technique that has been recently adapted to increase separation efficiency is using multiple tee junctions in a system. Studies on the use of multiple tee junctions have mostly been limited to placing multiple branching-type tee junctions in series. Some studies can also be found where a tee junction has been placed as a means of pre-separation, before entering the main separator. In some other studies, multiple vertically upward/downward branch arms have been used. However, to the best of the author's knowledge, there is no evidence of work in the literature on the use of multiple impacting tee junctions to enhance phase-separation capability or to obtain complete phase separation. It was pointed out by Mohamed et al. (2012) that multi-junction separators may be necessary to achieve full phase separation for high inlet flow rates beyond the limiting conditions that were found in their work using a single impacting tee junction. Table 2.3 gives an overview of studies present in the literature on two-phase flows through multiple tee junctions.

Wren and Azzopardi (2004) studied how two branching tee junctions of large diameter (127 mm) placed in series affect phase-separation capabilities for air-water two-phase flows. In their experimental set-up, the branch arm of the first and second tee junctions were oriented in vertically upward and downward directions, respectively. The run arm of the first tee acted as inlet to the second tee. Thus, the system had three outlets. A sketch of their set-up is shown in Figure 2.1. The effect of the junction geometry on the phase-separation capability has been studied in this paper by reducing the diameter of the second tee by a ratio of 0.6 ($D_3/D_1 = 0.6$) and by changing the distance between two tees (0.5 m and 1.2 m). The valve placed on each of the three outlets

could be completely closed or opened, thus allowing studying the separation capability of each junction separately as well as combinations of different outlets.

Table 2.3.   References of works on two-phase flows through multiple tee junctions

Author(s)	Inlet Dia. (mm)	Test Fluids	System Pressure (bar)	J_{G1} (m/s)	J_{L1} (m/s)	Number of Tee Junctions	Inlet Flow-Regime
Wren and Azzopardi (2004)	127	Air-water	1 - 1.05 (abs)	4 - 8	0.186 - 0.31	2	St, S-An
Baker et al. (2007)	38	Air-kerosene	-	3.3 - 9.6	0.07 - 0.51	2	St, Sl
Yang et el. (2010)	10	Air-water	-	0.28 - 0.75	0.06 - 0.680	3, 5, 7	St, Pl
Chen et al. (2012)	40	Oil-water	-	-	-	1 - 7	St, Mt
Tuo and Hrnjak (2014b)	8.7	R134a, R410A	-	-	-	3	St, W, Ch, Mt
Yang et al. (2017)	10	Air-water	-	0.275 - 0.9	0.056 - 0.551	3, 5, 7	St, Pl

* St - Stratified, W - Wavy, An - Annular, Sl- Slug, Pl - Plug
S-An –Semi-Annular, Mt - Mist, Ch – Churn

The entire range of mass extraction ratio (from 0 to 1) was studied with J_{G1} and J_{L1} ranging from 4 - 8 m/s and 0.186 - 0.31 m/s, respectively at ambient temperature and pressure, which corresponded to stratified and semi-annular flows. The results showed that the use of two tee junctions consistently out-performed the use of a single branching tee junction (with vertically downward outlet) as phase separator for all flow regimes and geometries of the test section. The authors suggested that in order to be a good separator, a system should be able to separate liquid and gas with 10% (volume/volume %) of the unwanted phase. With the designed system, it was

possible to achieve gas-rich stream in the upper and run arms and liquid-rich stream in the downward arm.
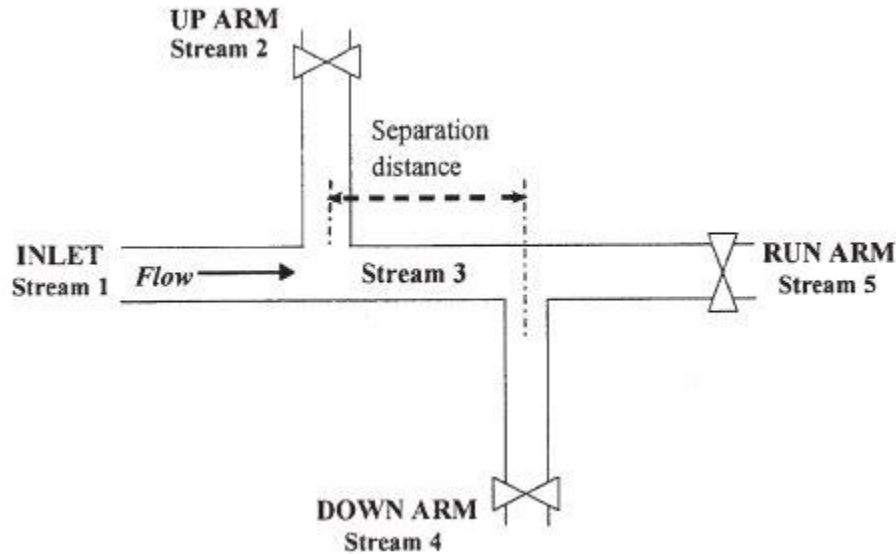
Figure 2.1   Arrangement of tee junctions in Wren and Azzopardi (2004)

When the diameter in the second tee was reduced, improved phase separation was obtained owing to lower gas entrained in the downward arm of second tee. With this arrangement, less than 10% liquid in the gas stream was obtained, which met their criteria of good separator. Changing distance between the two tee junctions did not produce any significant effect on phase-separation capability for semi-annular flow in both regular and reduced diameter set-ups. The reason for this is the presence of a downward branch arm downstream of the upward branch arm, which acted as a liquid drain, providing no condition in which liquid could climb up in the branch arm of the first tee and eliminated the problem of hydraulic jump. For stratified flow, the separation distance between the two tees did not affect phase separation in the reduced junction, but in the regular junction, as this distance was changed from 1.2 m to 0.5 m, increased gas take-off with decreased liquid entrained in the downward side arm was observed. However, the use of three outlets in the

system complicated the analysis and the authors did not present a proper definition of a phase-separation parameter in this work.

Baker et al. (2007) made efforts to improve on the work of Wren and Azzopardi (2004) using a similar set-up, with some alterations. They were able to a get gas-free liquid stream and reduce liquid intake in the gas stream by adding two control valves, one on the downward branch arm with an automatic level control system and the other on the run arm, which was operated manually across entire operating range of 0 - 100%. Two-phase flow of air and high flash point kerosene was used in this study. The pipe diameters were all equal (38 mm I.D.) and supplied air pressure was six bars. The range of J_{G1} and J_{L1} tested were 3.3 - 9.6 m/s and 0.07 - 0.51 m/s, respectively, which corresponded to stratified and slug flow regimes. A comparative study with a single branching junction showed that when a single junction gave 88% gas extraction with 8% liquid, dual junction gave 100% gas extraction with the same level of liquid for stratified flow in the vertically upward branch arm (for no valve control). For slug flow, this liquid extraction in the vertically upward branch arm could be reduced by almost 50% for low gas take-off in it, compared to a single branching tee. The vertically downward side arm of the second tee acted as a liquid drain and reduced the phenomenon of hydraulic jump and inclusion of a liquid level control in it prevented any measurable gas entrainment in the liquid stream. Thus, a pure liquid stream was achieved in the downward branch arm.

The optimum opening of the control valve in the run arm for enhanced phase separation was found out by experiments. For stratified flow, the optimum opening of the run arm valve was 20% and for slug flow, it was 54% to 60%. For stratified flow with lower J_{G1}, less than 0.05% (volume/volume %) liquid in gas-rich stream was achieved for all tested conditions in the vertically upward branch arm and only for the most intensive slug flow, liquid volume in the gas stream

exceeded 6% (volume/volume %). They were able to improve over Wren and Azzopardi's (2004) work by producing a separator system, which gives gas-free liquid stream and a gas-rich stream with less than 10% liquid by volume over a wide range of inlet conditions.

Yang et el. (2010) presented how the separation efficiency increases when 3, 5 or 7 branching tee junctions are placed in series, in comparison with a single branching tee. The main entrance pipe of the experimental set-up was mounted horizontally and the branch arms of the tees (or the risers) were oriented vertically upward, all of them connected to an upper header. The run arm of the first tee junction acted as inlet for the second tee and so on. A diagram of the arrangement of tee junctions in this paper is shown in Figure 2.2.

Figure 2.2   Arrangement of tee junctions by Yang et al. (2010)

The distance between the main inlet tube and the upper header was 60 mm and the tee junctions were 30 mm apart. All the tubes had an internal diameter of 10-mm. Air-water two-phase mixtures, with J_{G1} and J_{L1} ranging from 0.28 - 0.75 m/s and 0.06 - 0.68 m/s were used in the experiments, which corresponded to stratified and plug flow regimes. The inlet air was supplied at 0.1 MPa (g). In this work, the authors used the definition of separation efficiency by Yang et al.

(2006) in which kerosene (k)-water (w) two-phase flow was studied with the horizontal inlet, vertically upward branch arm and horizontal run arm of branching tee designated by subscripts 1, 2 and 3, respectively. The definition of separation efficiency proposed was:

$$\eta = \mid F_k - F_w \mid \qquad (2.8)$$

where, $F_k = W_{k3} / W_{k1}$ and $F_w = W_{w3} / W_{w1}$

The effect of inlet flow regime, J_{G1} and J_{L1} on the separation efficiency for multiple branching tees was studied in this work. The authors generally concluded that separation efficiency increases for increased number of tee junctions. For the inlet condition in the stratified flow regime reported in this study, η increased from 85% and 95% to 100% when 1, 3 and 5 (or more) tee junctions were used, respectively. For the inlet condition in the plug flow regime reported in this work, η increased from 42% and 81% to 100% when 1, 3 and 5 (or more) tee junctions were used, respectively. When J_{G1} or J_{L1} was increased within the same flow regime and same number of tee junctions, η was found to decrease. However, the paper does not provide any result regarding the separation efficiency of individual tee junctions. In addition, the design of the system creates additional impacting tee junctions in the header whose influence on the system performance is not described.

A numerical study on the effects of interval between two tee junctions or the effect of branch-arm height on separation efficiency of oil-water two-phase flows in a system similar to Yang et al. (2010) can be found in the work of Chen et al. (2012). A diagram of their set-up can be found in Figure 2.3.

The authors used the commercial CFD software Fluent to analyze the flow split characteristics and separation efficiency using κ-ε turbulence model and an Eulerian multi-fluid

model. The definition of separation efficiency (subscript o and w representing oil and water, respectively) used was:

$$\eta = \mid F_o - F_w \mid \qquad\qquad (2.9)$$

where, $F_o = W_{o\ (upper)} / W_{o\ (inlet)}$ and $F_w = W_{w\ (upper)} / W_{w\ (inlet)}$
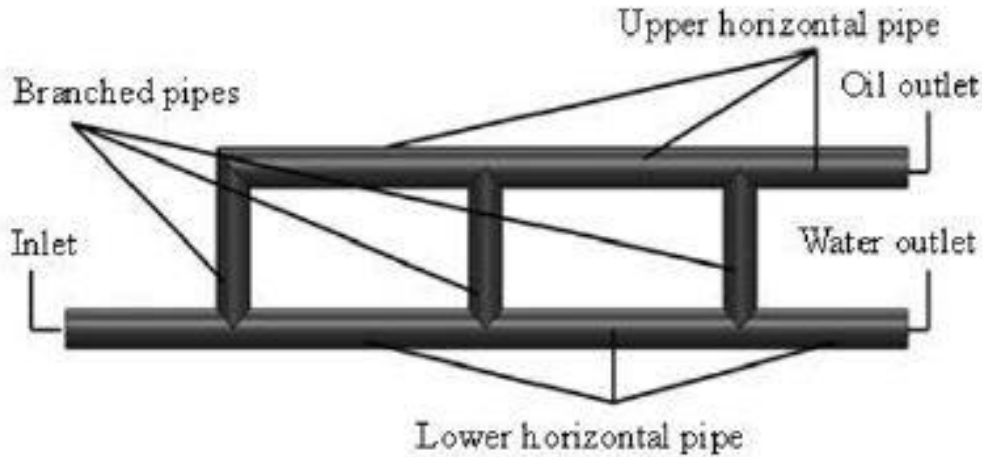
Figure 2.3   Arrangement of tee junctions by Chen et al. (2012)

In their design, 1 to 7 branching tee junctions were used in series having equal tube diameter of 40-mm. Working fluid was oil-water, where density of oil (LP-14) was lower than that of water. A mixture velocity of 0.5 m/s with oil volume fraction of 40% and split ratio of 0.4 was used in all the runs, which corresponds to stratified and mist flow regimes. The distance between two consecutive tee junctions were varied from 4D, 8D….28D and it was observed that η increases with the increase of interval between two tees, but at a lower rate with higher branch interval. Branch arm height was changed from 4D, 6D…14D and no significant change in η was noticed. Within the test condition, η was found to be close to 70% for all variations of branch arm height. However, in certain heights, reverse flow was noticed, which added further complication to the system. No evidence of experimental validation of this work was provided.

Tuo and Hrnjak (2014b) explored various design options to enhance vapor-liquid separation of both R134a and R410A refrigerants' two-phase flow through a vertical impacting tee junction, which can be used to increase the efficiency of a vapor compression cycle with flash gas bypass. The inlet flow rate and quality tested, ranged from 30 g/s to 35 g/s and 10% to 30%, respectively. In this paper, the definitions of separation efficiency, η_l and η_v, by Tuo and Hrnjak (2012) were used. The authors studied the effects of inlet inclination angle, use of dual inlets, relative diameter of inlet to outlet ($D_i / D_o = 0.465$, 0.563 and 0.656), shape of inlet tube (rectangular and round cross-sections) and location of inlet with respect to the vertical part on the separation efficiency. The experimental results showed that η_l increased with increase in inlet's downward inclination angle (from 0^0 to 45^0) and with the increase of diameter of inlet tube. The increase in the value of η_l was limited to only 5% within explored condition. Liquid separation efficiency, η_l also increased on using rectangular inlet over circular (increase of η_l was up to 8% and 6% for circular tubes with same and double cross-sectional areas, respectively) and on using tangential flat inlet configuration over centered. The authors also explored the use of a pre-separator, which was essentially a branching tee junction with horizontal inlet and vertically upward branch arm, before entering the impacting tee junction. In this arrangement, the inlet was inclined at a downward angle of 30^0 with respect to the outlets of the second (impacting) tee (Figure 2.4). Thus, there was a two-stage separation, as the mixture passes through two tee junctions in series. The pre-separator divided the flow into vapor-rich and liquid rich-streams, entering the upward branch-arm and run-arm, respectively, under the effect of gravitational forces. As the mixture quality was changed, this initial separation affects the flow pattern and it becomes closer to stratified flow, which is a favorable flow regime for separation, as indicated by Mohamed (2011). Liquid separation efficiency, η_l was enhanced significantly on using the pre-separator or

combined junction, especially at higher flow rate (35 g/s). Although this paper shows that efficiency is increased by using two tee junctions in series, the phase-redistribution data presented here is very limited.
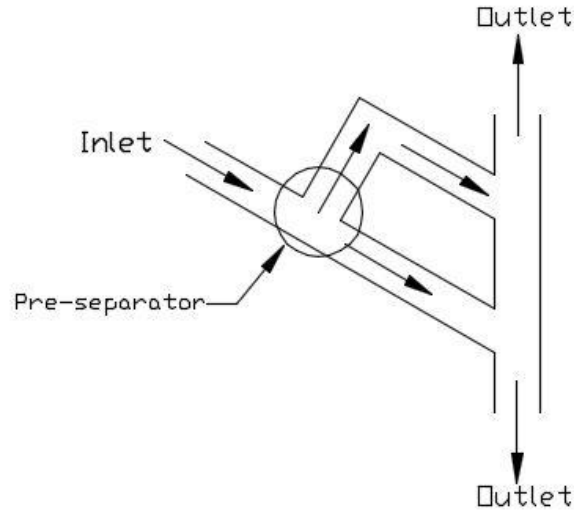
Figure 2.4   Pre-separator used in Tuo and Hrnjak (2014b)

Yang et al. (2017) proposed a novel multitube tee junction separator containing multiple branching tee junctions in two- or three-layers, which could give complete separation of gas-liquid two-phase flow. Air-water two-phase flow in stratified and plug flow regimes (J_{G1} and J_{L1} ranging from 0.275 - 0.9 m/s and 0.0560 - 0.551 m/s, respectively) was passed through these separator units with inlet quality and mixture velocity ranging from 0.00384 - 0.0114 and 0.331-1.45 m/s, respectively. The two-layer separator unit used in this paper is identical in structure to the separator described in Yang et al. (2010) which has been reviewed previously in the thesis. A schematic diagram of the three-layer unit taken from the paper is shown in Figure 2.7.
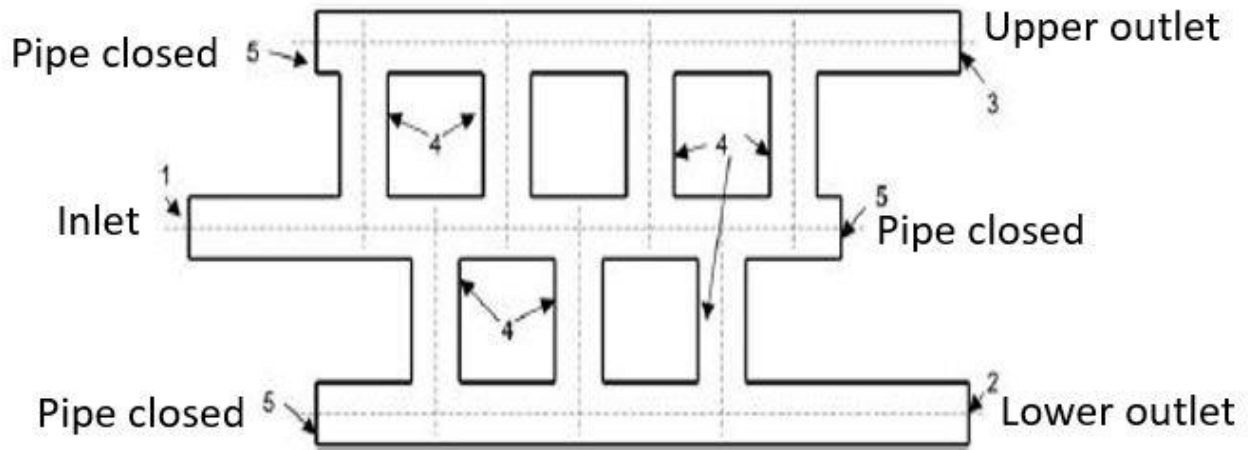
Figure 2.5   Three-layer multitube separator unit by Yang et al. (2017)

The two-layer unit was described previously in this chapter in the review of the study by Yang et al. (2010). In the three-layer unit, there were four upward and three downward connecting tubes, with sides 1, 2 and 3 (as indicated in Figure 2.5) acting as inlet, lower outlet and upper outlet, respectively. The distances between the inlet and upper/lower headers were 100 mm and 50 mm, for two-layer and three-layer units, respectively and distance between two adjacent connecting tubes were 50 mm, in all arrangements. All the tubes had internal diameter of 10 mm and supplied air pressure was 0.1 MPa (g).

The effect of flow regime, J_{G1}, J_{L1}, mixture velocity and tee junction configuration on phase separation were examined in this paper and the results were presented in extraction ratio versus separation efficiency plots. The definition of separation efficiency proposed by Yang et al. (2006) was used in this paper. The results show that the phase-redistribution data move away from the equal phase split line, or separation efficiency increases, as number of connecting tubes in the two-layer unit increases. For stratified flow, 100% separation efficiency was achieved with 5 or 7 connecting tubes in both two-layer and three-layer units, whereas a single branching tee junction

could give maximum separation efficiency of 85%. It was also reported that phase separation or separation efficiency deteriorates as the flow regime changed from stratified to plug flow. However, complete phase separation was also achieved under certain conditions of plug flow, with seven connecting tubes in the two-layer unit. It was also reported that within the same flow regime, increasing J_{G1}, J_{L1} or mixture velocity was detrimental to phase-separation efficiency.

2.4 Concluding Remark

Careful examination of the literature led to the following conclusions:

i. There has been significant research on phase redistribution of two-phase flow passing through an impacting tee junction and its use as a partial separator.

ii. Comparatively, less work has been done on the use of impacting tee junction as a complete phase separator.

iii. Using multiple tee junctions for full phase separation is a relatively new concept and most of available studies on this concept have been done using branching tee junctions, arranged in different ways.

iv. To date, and to author's best knowledge, no publication on the use of multiple impacting tee junctions for full phase separation has been found. This presents a gap in literature and this area will be explored in the present study.

CHAPTER 3

TEST RIG AND EXPERIMENTAL PROCEDURE

3.1 Overview

An existing two-phase flow loop was used in this investigation. A test section consisting of a system of combined impacting tee junctions was designed in order to fulfill the objectives of this study. Details of various components and measuring devices in the test rig are presented in this chapter. In addition, this chapter contains details of the experimental procedures and methods of data reduction that were followed in this investigation.

3.2 Experimental Test Rig

The main functions of the test-rig components used in the present study are:

i.   Measuring the amount of inlet air and water

ii.   Mixing the inlet air and water to form a homogenous mixture

iii. Dividing the inlet mixture in the system of combined junction, to form two outlet flows

iv.   Separating phases of the two outlet flows in separation tanks

v.   Measuring the outlet air and water flows

vi.   Releasing the outlet air to the atmosphere and the outlet water to a reservoir to complete the loop.

3.2.1 Air-Water Loop

Figure 3.1 contains a schematic diagram of the test rig and Figures 3.2 - 3.4 contain actual pictures of its different parts. Compressed air from the building supply line was passed through an air filter and a pressure regulator before entering one of three calibrated inlet air rotameters (of

overlapping ranges) to measure the inlet air flow rate. Temperature and pressure readings of inlet air were taken with a thermocouple and a pressure gauge, respectively. A submersible pump was used to circulate distilled water from the water reservoir to the test loop. Water temperature was maintained with a cooling coil placed in the water reservoir. After passing the water through a filter, the inlet water flow rate was measured and controlled with one of the three inlet water rotameters. The inlet water temperature and pressure were also taken with a thermocouple and a pressure gauge, respectively.

Air and water from the inlet were mixed in a mixing tee before entering the test section. A visual section made of acrylic resin was placed at 62 pipe diameters from the mixing tee to visualize the inlet flow regime. The visual section was 15 pipe diameters long. A horizontal impacting tee junction was located 32 pipe diameters further away from the visual section. It was made of acrylic resin, with inside diameter of 13.5 mm and outlet lengths were 81 pipe diameters. A pressure gauge was installed at the junction inlet to measure test-section pressure. Visual sections were placed in the outlets of the horizontal impacting tee junction at a distance 50 pipe diameters away from the junction to visualize the flow regimes. These outlets acted as inlets to the two vertical impacting tee junctions. Symmetry of the test loop ensured that inlet flow was split evenly in the horizontal impacting tee and two identical flows enter its two outlets. The outlets of the vertical impacting tee junctions were 29.5 pipe diameters long. The top outlets of both vertical impacting junctions were combined (outlet-2) and passed to a separation tank, where air and water were separated. The two bottom outlets were also combined in similar manner (outlet-3) and the flow was passed through another separation tank. Transparent tygon tubes were used to connect these outlets to the separation tanks. More details of the test section are given later.
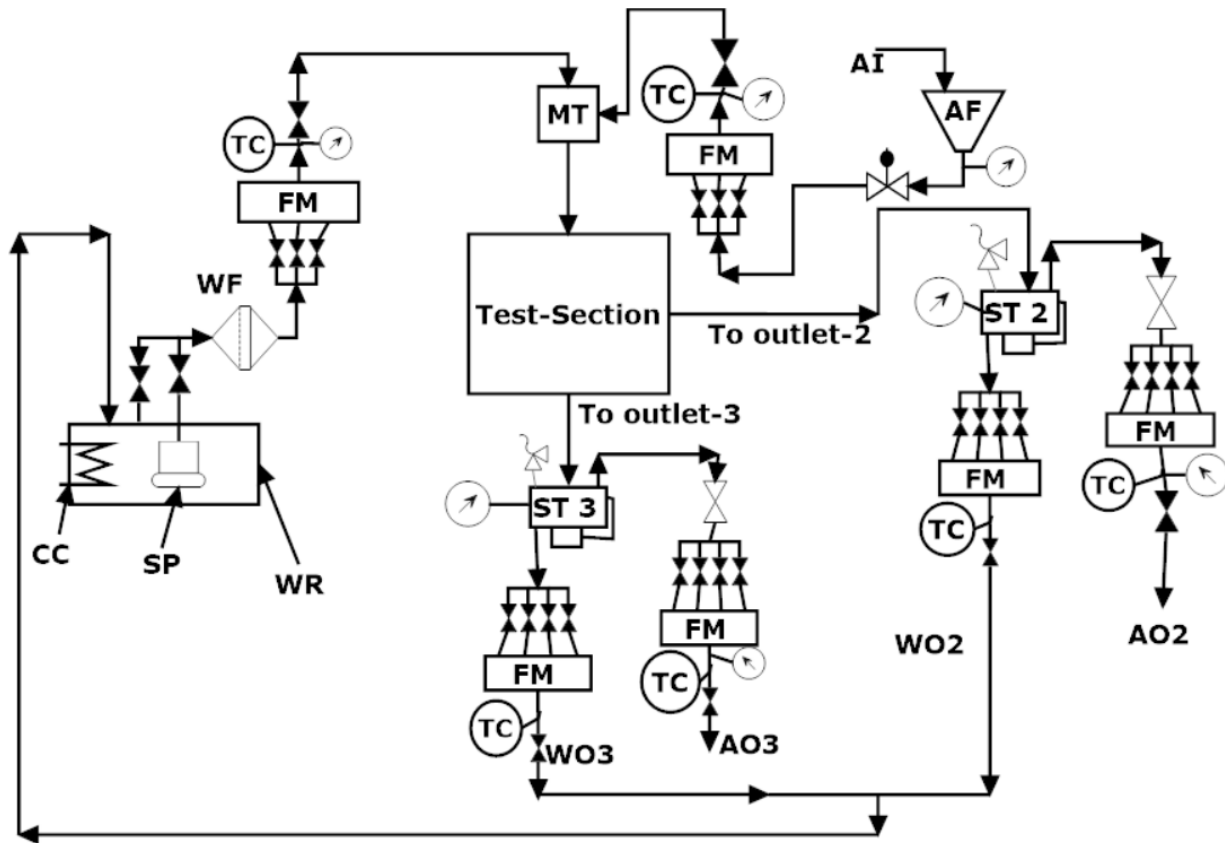
Symbol	Description	Symbol	Description
AF	Air filter	SP	Submersible pump
AI	Air inlet	ST	Separation Tank
AO	Air outlet	TJ	Tee junction
CC	Cooling Coil	WF	Water filter
FM	Flow meter	WO	Water outlet
MT	Mixing tee	WR	Water reservoir
►◄ (Control valve symbol)	Control valve	(Pressure gauge symbol)	Pressure gauge
▷◁ (Valve symbol)	Valve	(TC)	Thermocouple
(Pressure controller symbol)	Pressure controller	(Safety valve symbol)	Safety valve

Figure 3.1   Schematic diagram of the test rig
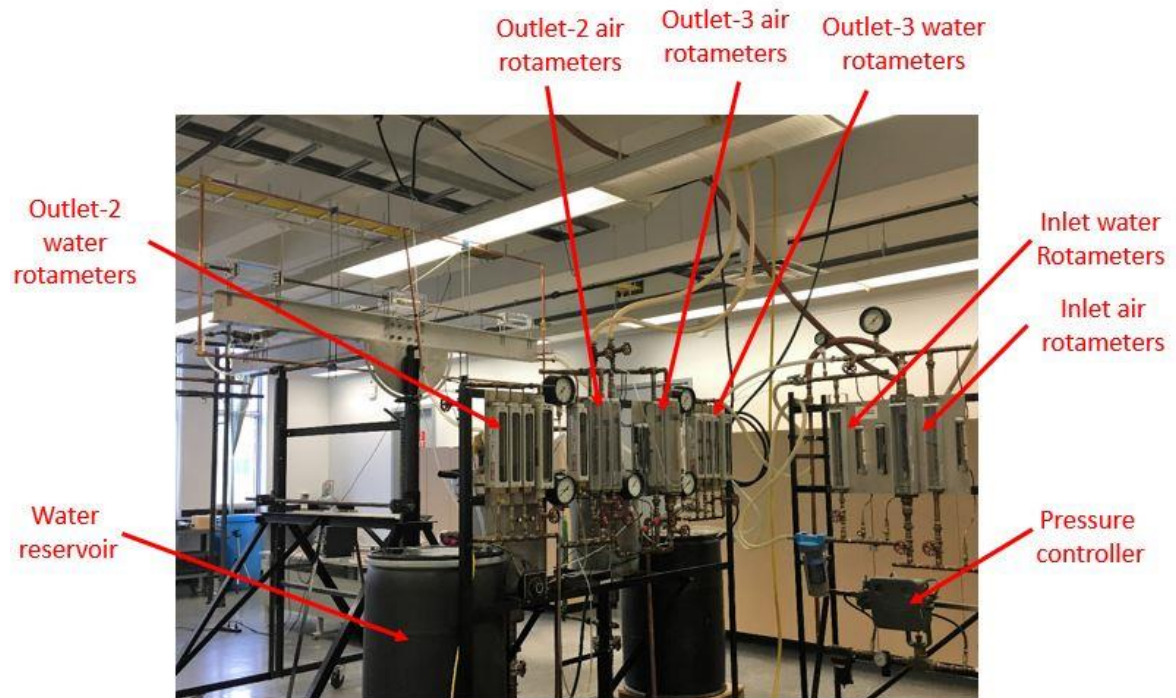
Figure 3.2   Image of inlet and outlet rotameters

Figure 3.3   Image of the mixer and inlet

Figure 3.4   Image of the separation tanks

There were banks of four air rotameters and four water rotameters, connected to each of the separation tanks. The outlet air and water mass flow rates, coming from the top and bottom outlets were measured with these outlet rotameters. Thermocouples were installed to measure temperatures of both air and water outlet rotameters. Pressure gauges were installed to monitor outlet air pressures. Air from the outlet rotameters was released to the atmosphere, after passing through a muffler and water was returned to the reservoir, thus completing the loop.

3.2.2 Test Section

Figures 3.5 and 3.6 show a schematic diagram and an image of the test section, respectively. The test-section is a combination of one horizontal and two vertical impacting type tee junctions and visual sections. The tee junctions used were all equal sided and sharp edged with

an internal diameter of 13.5 mm. The horizontal junction was machined from acrylic resin and the vertical junctions were made of brass. The inlet and outlets of all the tee junctions were made of copper tubing. Visual sections made of acrylic resin were placed in the two outlets of the horizontal tee junction. These transparent entities help to visualize the flow regimes under different inlet conditions. The horizontal impacting tee junction, along with the visual sections and the mixer were mounted on a rigid aluminum frame. To ensure horizontal alignment of the test section, a survey theodolite (AN 20, Wild Heerbrugg, Lewis International Limited) was used. In addition, an inclinometer was used to check both vertical and horizontal alignment of the different parts of the test section.
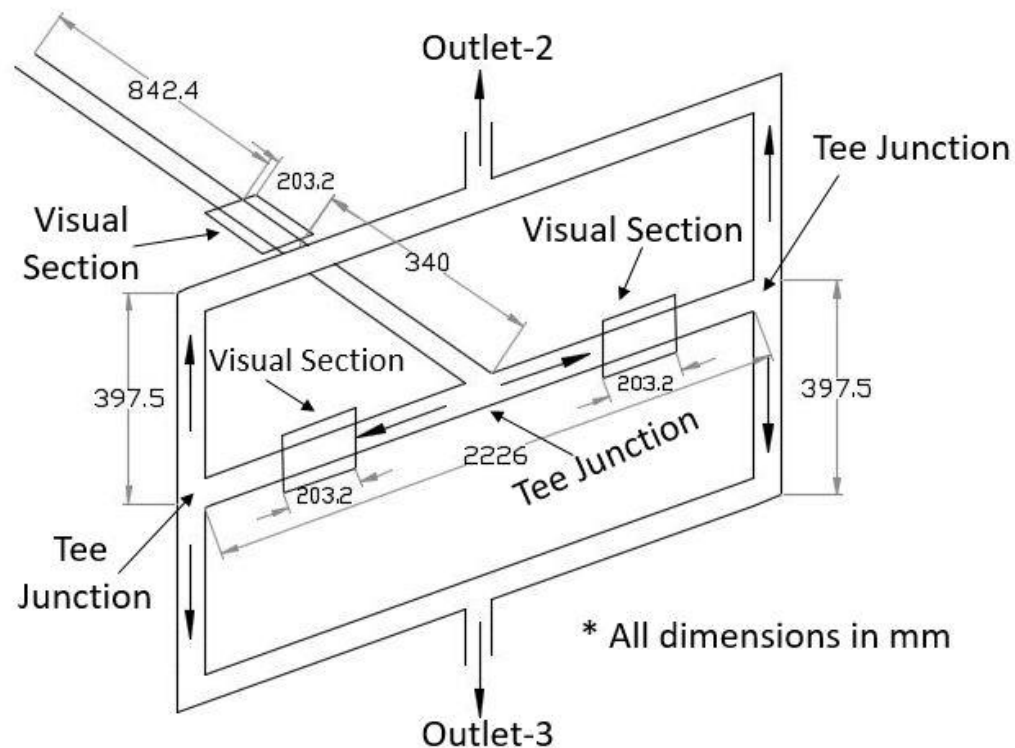
Figure 3.5   Schematic diagram of the test section

Figure 3.6   Image of the test section

3.2.2.1 Horizontal Tee Junction

The horizontal tee junction was machined out of an acrylic resin block, having dimensions of 203.2×179.0×86.2 mm. Two bores of 13.5±0.1 mm were drilled perpendicular to each other, to construct the inlet and two outlets of this tee junction. Care was taken so that the centerline of the bores were aligned with the centerline of the acrylic resin block. To eliminate radius of curvature in the experimental work, square edges were machined at the point where the two bores met. A pressure tap was attached at the inlet of this junction. There were three flanges bolted to the acrylic resin block that connected it with the copper tubes, which acted as extensions of the inlet and outlets of the tee junction. The copper tubes were soldered to the flanges. Extreme care was taken in machining so that the diameters of the bores matched with the diameter of the copper tubes perfectly.

3.2.2.2 Vertical Tee Junctions

The vertical tee junctions were made of brass, with tube O.D. of 5/8". They were picked off the shelf from Swagelok (Brass Swagelok Tube Fitting, Union Tee, 5/8 in. Tube OD, B-1010-3). The I.D. of these fittings were 12.7 mm and they were machined to match the I.D. of the copper tubes, at 13.5 mm. Figure 3.7 contains a diagram of these tees (supplied by Swagelok), highlighting their dimensions and machining details. These tees were connected to the copper tubing in the test-section by compression fitting.

To form drainage mechanism of the test rig, elbows were placed at the ends of the outlets of the vertical tee junctions. They were also picked off the shelf from Swagelok (Brass Swagelok Tube Fitting, Union Elbow, 5/8 in. Tube OD, B-1010-9). The internal diameter of these elbows (which were 12.7 mm originally) were machined to fit the copper tubes I.D. of 13.5 mm and they were connected by compression fitting. Figure 3.8 contains a diagram of these elbows with their dimensions (supplied by Swagelok). The elbows connected the two bottom outlets of the vertical junctions with horizontally placed copper tubes. Two copper tubes coming from the bottom outlets of each of the vertical junctions merged in a tee of the same type as described before. The outlet of that tee entered separation tank 3 via transparent tygon tubing. The two top outlets of the vertical junctions were combined and connected to separation tank 2 in a similar manner. Figure 3.9 contains a diagram of the front view of the test section showing the positions of the tees and elbows from Swagelok in it.

3.06[77.7]

1.53[38.9]

0.96[24.4]

5/8" Tube O.D.

ø0.50[12.7]

1.53[38.9]

1"

NOTE A

1" WRENCH PAD

Note A - Detail View

Shoulder diameter to
match the tubing ID
(13.5 mm)
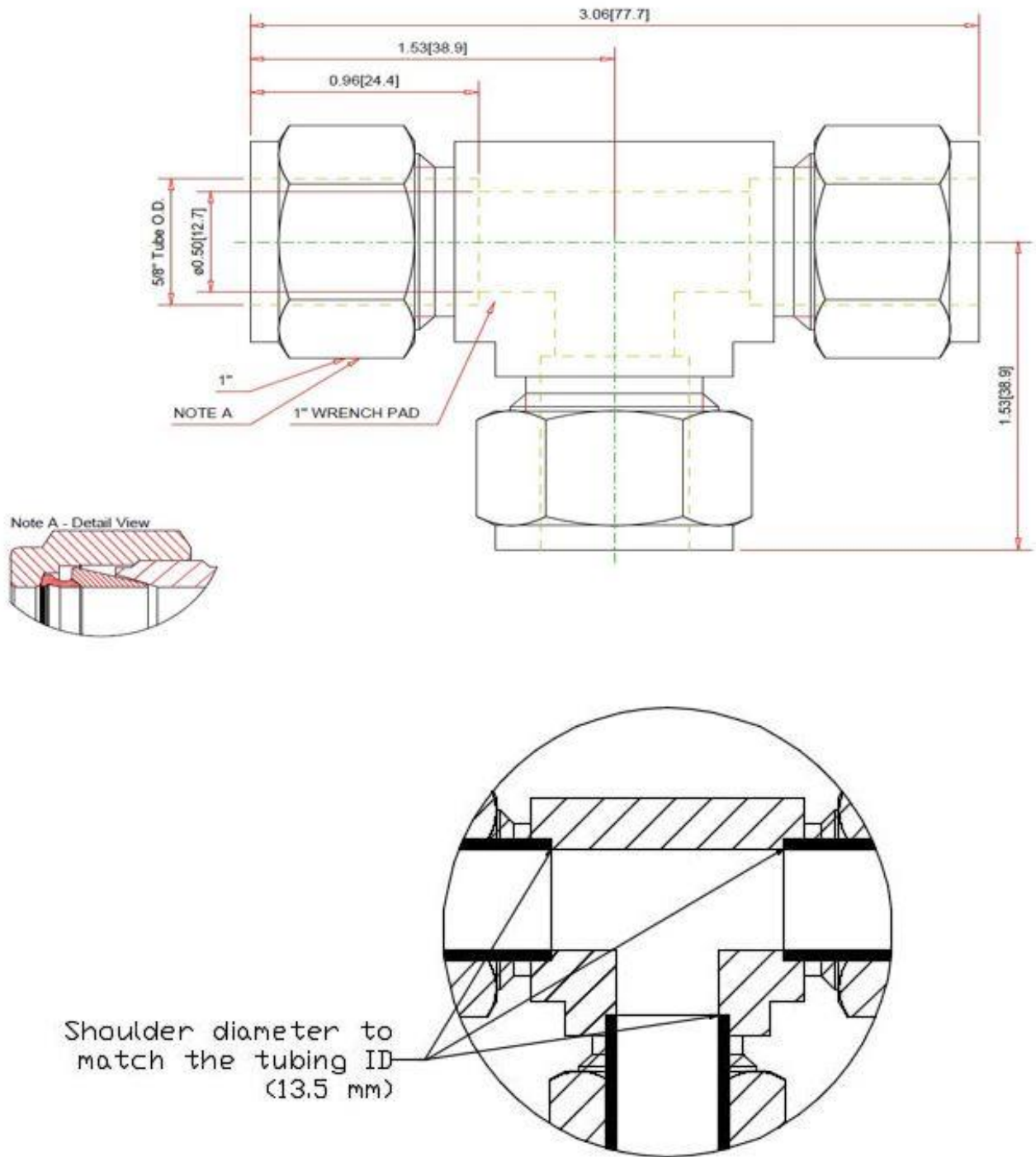
Figure 3.7   Diagram of the vertical tee junctions supplied by Swagelok
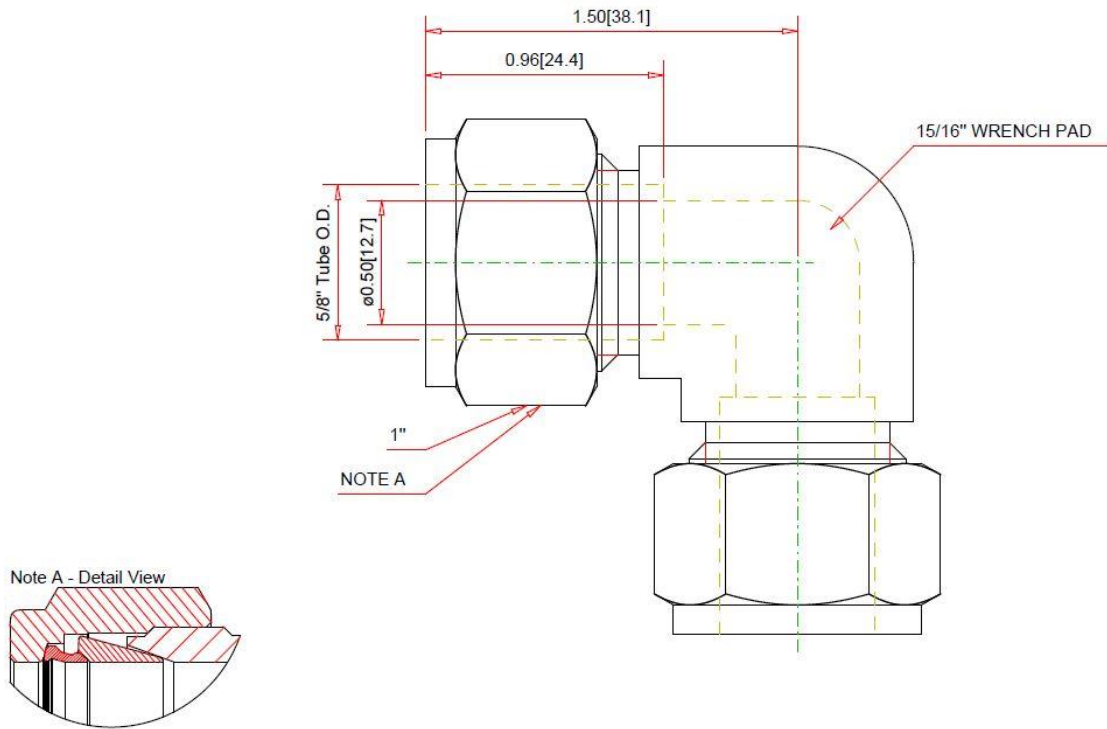
Figure 3.8   Diagram of the vertical tee junctions supplied by Swagelok
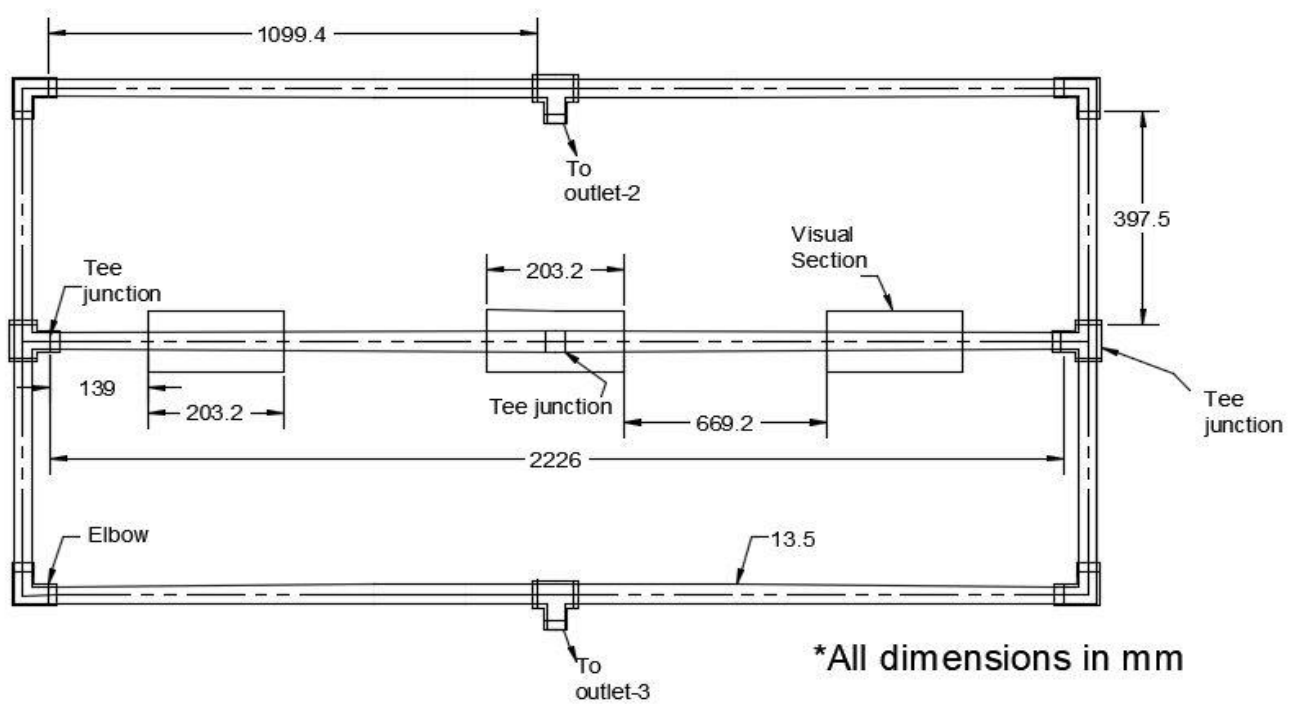
Figure 3.9   Tees and elbows in front view of the test section

3.2.2.3 Visual Sections

The test-rig had three visual sections; one in the inlet and two in the outlets of the horizontal impacting tee junction. They were machined from transparent acrylic resin blocks having dimensions of 203.2×90×76.2 mm. Bores having a diameter identical to the copper tubings (13.5 mm) were drilled through these acrylic resin blocks to pass the two-phase flow through them. Care was taken so that these bores were centrally aligned in the block and were co-axial with the copper tubings. Each visual section had two flanges on either side that connect them with the copper tubings and O-rings were used to seal them.

3.2.3 Mixer

Figure 3.10 contains a schematic diagram of the mixer used in the flow loop. Its main function was to develop a homogenous two-phase mixture of air and water. The mixer was made of copper and it had two co-axial pipes. The larger pipe had a diameter of 51 mm and inlet air entered it from a perpendicular pipe attached to it, also having 51 mm I.D. The smaller tube had an I.D. of 12.7 mm and it was perforated and capped at the end. The perforations were of 1.6 mm diameter and water was injected through them. The two-phase air-water homogenous mixture emerged from the mixture into the inlet of the horizontal impacting tee junction. Details of the mixer components can be found in the work of El-Shaboury (2005).

47
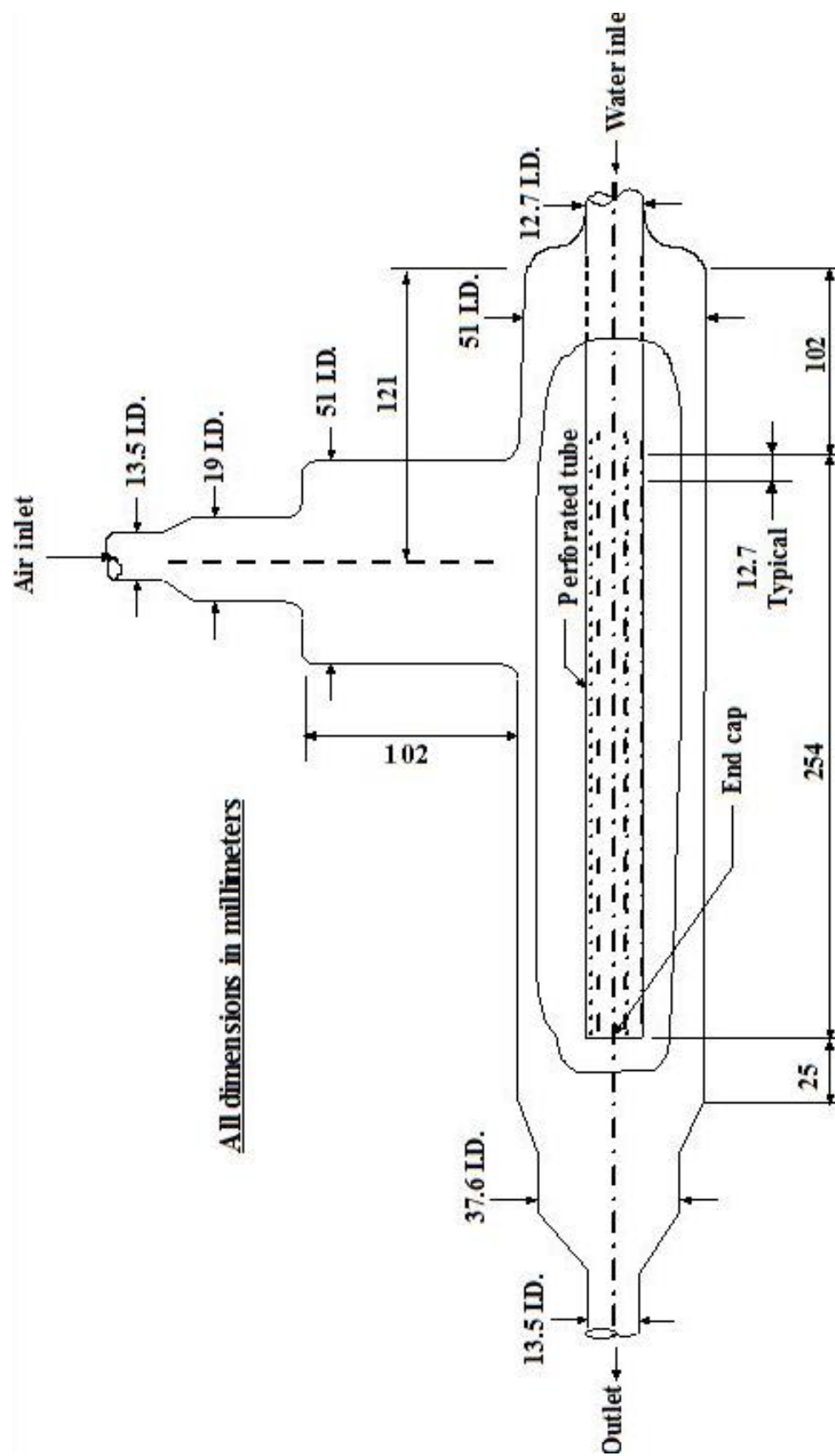
Figure 3.10   Schematic diagram of mixer, slightly modified from El-Shaboury (2005)

48

3.2.4 Separation Tanks

The test-rig had two identical separation tanks connected to each of the outlets, for separating air and water. Figure 3.11 shows a detailed diagram of one of the separation tanks along with its dimensions. The material used to construct these separation tanks was Type 304 stainless steel, schedule 40 pipe sections. Air-water two-phase flow entering the separation tanks were separated by means of gravitational force, where water exited downwards and air moved to the top. Perforated baffles made of stainless steel prevented droplets of water from entering the air stream in the top by means of centrifugal action. Safety valves set at 735 kPa were installed at the top blind flange of the separations tanks as a safety measure.

A transparent glass tube or sight glass was attached to the separation tank and placed parallel to it. This sight glass had two functions: one is to identify the water level in the separation tank and the other is to help measure the flowrate of water entering it. Any change in water level in the sight glass indicated that the amount of water entering the separation tank is not equal to the amount of water leaving it. In such a case, the water flowrate in the outlet rotameter needed to be adjusted in order to maintain steady liquid level in the sight glass. The separation tank had three different cross-sections at the bottom for exiting water through them, which accommodated measurement of water flowing at different rates. The smallest cross-section was sensitive to very low water flowrates and would cause change in water level in the separation tank and the sight glass even for a very small difference in flowrates. The larger cross-sections helped measuring higher flowrates of water. The connections of the separation tanks with other parts of the test rig were made by dielectric joints, to prevent any rusting or contamination of distilled water. Details of the separation tank components can be found in the work of El-Shaboury (2005).
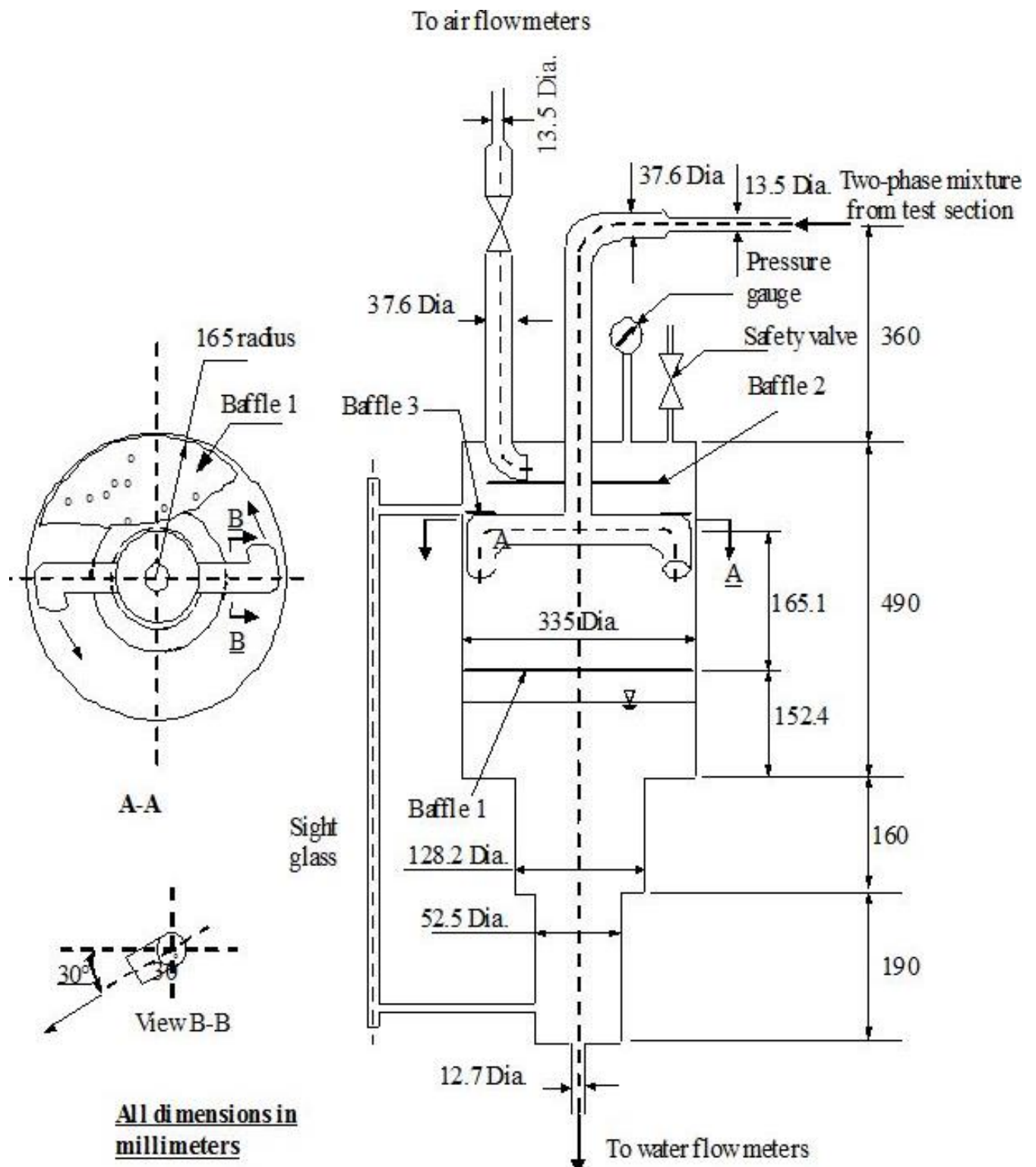
Figure 3.11   Detailed diagram of the separation tanks, slightly modified from

El-Shaboury (2005)

3.2.5 Measuring Devices

Three types of measuring devices were used in the test-rig:

i. Rotameters

ii. Pressure Gauges

iii. Thermocouples

There were 22 rotameters in the test rig, 11 of them were for measuring water flowrate and the other 11 for air. Inlet air and water each had banks of three rotameters. Each of the air and water outlets had banks of four rotameters. Rotameters in a bank had overlapping ranges chosen carefully so that a wide range of flow rates can be measured. Tables 3.1 and 3.2 contain specifications of the rotameters used in the test rig. Needle valves were placed before and after each rotameter to control the flowrate.

Spot checks (three points of each rotameter) were done for the calibration and results were compared with the calibration data reported by Mohamed (2012) for the same rotameters. Ninety-one percent of calibration data matched with Mohamed (2012) within ± 5.8% for air rotameters and ± 7.4% for water rotameters. The higher differences in calibration data were associated with very low flowrates. Due to close proximity of calibration data with Mohamed (2012), the data reported by him were used for calculation in this thesis. It should be mentioned that calibration data reported by the aforementioned author matched within ± 2% and ± 3% of manufacturer's values for air and water rotameters, respectively. Between any two consecutive points, linear interpolation was used to calculate flowrates for both air and water rotameters. Full calibration data are available in Mohamed (2012) and the spot checks for all rotameters are given in Tables A.4 and A.5 in Appendix A.

Table 3.1   Specifications and functions of air rotameters

Rotameter	Specification	Measured variable
IN-A-1	Brooks rotameter, Model: 1355EZ186 Range: 6.47-64.7 SLPM Float: Ball – Stainless Steel	Inlet air flowrate
IN-A-2	Brooks rotameter; Model: 1307EZ80 Range: 38.1-381 SLPM Float: Conventional – Stainless Steel	Inlet air flowrate
IN-A-3	Brooks rotameter, Model: 1307EZ84 Range: 200-2004 SLPM Float: Conventional – Stainless Steel	Inlet air flowrate
O-2-A-1	Brooks rotameter, Model: 1355EZ184 Range: 0.87-8.68 SLPM Float: Ball – Sapphire	Outlet-2 air flow-rate
O-2-A-2	Brooks rotameter, Model: 1355EZ186 Range: 6.47-64.7 SLPM Float: Ball – Stainless Steel	Outlet-2 air flowrate
O-2-A-3	Brooks rotameter, Model: 1307EZ80 Range: 38.1-381 SLPM Float: Conventional – Stainless Steel	Outlet-2 air flowrate
O-2-A-4	Brooks rotameter, Model: 1307EZ84 Range: 200-2004 SLPM Float: Conventional – Stainless Steel	Outlet-2 air flowrate
O-3-A-1	Brooks rotameter, Model: 1114DG41AEHAA Range: 0.86-8.6 SLPM Float: Ball– Glass	Outlet-3 air flowrate
O-3-A-2	Brooks rotameter, Model: 1307EZ186 Range: 4.64-46.4 SLPM Float: Ball – Sapphire	Outlet-3 air flowrate
O-3-A-3	Brooks rotameter, Model: 1307EZ80 Range: 38.1-381 SLPM Float: Conventional – Stainless Steel	Outlet-3 air flowrate
O-3-A-4	Brooks rotameter, Model: 1307EZ79 Range: 72.9-729 SLPM Float: Conventional – Stainless Steel	Outlet-3 air flowrate

Table 3.2   Specifications and functions of water rotameters

Rotameter	Specification	Measured variable
IN-W-1	Brooks rotameter, Model: 1355EZ183, Range: 8.54-85.4 cm³/min Float: Ball – Sapphire	Inlet water flowrate
IN-W-2	Brooks rotameter, Model: 1355EZ182, Range: 49.14-491.4 cm³/min Float: Ball – Stainless Steel	Inlet water flowrate
IN-W-3	Brooks rotameter, Model: 1307EZ81, Range: 250-2955 cm³/min Float: Conventional – Stainless Steel	Inlet water flowrate
O-2-W-1	Brooks rotameter Model: 1114DC91BDHAA Range: 1.0-10.0 cm³/min Float: Ball – Sapphire	Outlet-2 water flowrate
O-2-W-2	Brooks rotameter Model: 1114DC71BDHAA Range: 7.45-74.5 cm³/min Float: Ball – sapphire	Outlet-2 water flowrate
O-2-W-3	Brooks rotameter Model: 1114DG41BDHAA Range: 48.5-485 cm³/min Float: Ball – Stainless Steel	Outlet-2 water flowrate
O-2-W-4	Brooks rotameter Model: 1114DJ41BDHAA Range: 295-2950 cm³/min Float: Conventional – Stainless Steel	Outlet-2 water flowrate
O-3-W-1	Brooks rotameter Model: 1114DC91BDHAA Range: 1.0-10.0 cm³/min Float: Ball – Sapphire	Outlet-3 water flowrate
O-3-W-2	Brooks rotameter Model: 1114DC71BDHAA Range: 7.45-74.5 cm³/min Float: Ball – Sapphire	Outlet-3 water flowrate
O-3-W-3	Brooks rotameter Model: 1114DG41BDHAA Range: 48.5-485 cm³/min Float: Ball – Stainless Steel	Outlet-3 water flowrate
O-3-W-4	Brooks rotameter: Model: 1114DJ41BDHAA Range: 295-2950 cm³/min Float: Conventional – Stainless Steel	Outlet-3 water flowrate

The test rig had seven pressure gauges installed to measure pressures of inlet air, inlet water, test-section, air outlet 2, air outlet 3, separation tank 2 and separation tank 3. The calibration data for these pressure gauges can be found in the work by Mohamed (2012). To regulate pressure of air entering the test rig from the supply line, a feedback pressure controller (Fisher 4160K series) and a pressure regulator were used. Two additional pressure gauges were placed upstream and downstream of the pressure controller. Specifications of the pressure gauges used in the test rig are listed in Table 3.3. Six thermocouples (J-Type Omega) were installed in the test rig to measure temperatures of inlet and outlets of both air and water.

Table 3.3   Specifications and functions of pressure gauges

Instrument	Specification	Position in test rig
Pressure gauge 1	Marshall town Bourdon gauge Range: 0 - 689.8 kPa (0 - 100 psi)	Before pressure controller
Pressure gauge 2	USG Bourdon gauge Range: 0 - 1100 kPa (0 - 160 psi)	After pressure controller
Pressure gauge 3	USG Bourdon gauge Range: 0 - 689.8 kPa (0 - 100 psi)	Air inlet
Pressure gauge 4	Ashcroft gauge Range: 0 - 413.9 kPa (0 - 60 psi)	Water inlet
Pressure gauge 5	Wika Bourdon gauge Range: 0 - 413.9 kPa (0 - 60 psi)	Inlet of the combined tee junction
Pressure gauge 6	Marshall town Bourdon gauge Range: 0 - 413.9 kPa (0 - 60 psi)	Separation tank 2
Pressure gauge 7	Marshall town Bourdon gauge Range: 0 - 413.9 kPa (0 - 60 psi)	Separation tank 3
Pressure gauge 8	USG Bourdon gauge: Range: 0 - 689.8 kPa (0 - 100 psi)	Air outlet 2
Pressure gauge 9	USG Bourdon gauge Range: 0 - 689.8 kPa (0 - 100 psi)	Air outlet 3

3.3 Experimental Procedure

3.3.1 Partial-Phase-Separation Experiments

Partial-phase-separation experiments were performed to determine how phases were redistributed in the two outlets of the combined system for six sets of inlet conditions in the annular flow regime. For a fixed combination of J_{G1} and J_{L1}, the following procedure was followed for these experiments:

i. The atmospheric pressure, P_{atm} was recorded.

ii. The inlet and discharge valves of the separation tanks were kept fully opened.

iii. The outlet pressure of the pressure controller was fixed at 30 psig.

iv. The air supply line was fully opened.

v. The control valve downstream of the inlet air rotameters was kept fully open. The appropriate air rotameter was partially opened up to the desirable level (for a fixed J_{G1}), by adjusting the control valve upstream of it. Care was taken so that the float of the rotameter stayed in the same place throughout the experiment.

vi. Appropriate outlet air rotameters in sides 2 and 3 were opened up to the desired level, to the get required F_{G3} and F_{G2}. This was done by adjusting the control valves located upstream of the rotameters. The control valves downstream of the rotameters were kept opened to the atmosphere. These outlet air rotameters were adjusted in a way that the test-section pressure stayed at 15 psig.

vii. Cooling water supply for the water reservoir was turned on and the bypass valve was kept fully opened. The submersible pump was then turned on.

viii. Water flow rate (for a fixed J_{L1}) in the inlet was controlled by adjusting the control valves upstream of the appropriate water rotameter. The control valve downstream of the bank of inlet water rotameters was kept fully opened.

ix. Appropriate water rotameters were opened by adjusting the control valves located upstream and downstream of them in both outlets 2 and 3. Water level in the separation tanks were monitored for any change in level (in a cross-section that allowed proper monitoring) and the outlet water rotameters were adjusted accordingly.

x. A waiting time of 15 minutes was allowed to monitor the water level in the separation tanks. If the water levels remained steady for 15 minutes, the following readings were taken:

   a) Pressures of the inlet air and water, air outlets, separation tanks and test section.

   b) Temperatures of the inlet and outlet air and water.

   c) Inlet and outlet volume flowrates of air and water from rotameters (V_{G1}, V_{G2}, V_{G3}, V_{L1}, V_{L2}, V_{L3}, respectively).

Steps i-x were repeated for different values of F_{G3}, for a fixed set of J_{G1} and J_{L1}, until $F_{L3} = 1$ was reached for a particular inlet condition.

3.3.2 Full-Phase-Separation Experiments

Full-phase-separation experiments were performed to determine the limiting conditions of inlet liquid and gas superficial velocities for which full separation of phases can be achieved using the system of combined junctions. For $J_{G1} > 10$ m/s, these experiments were performed by fixing J_{L1} and increasing J_{G1}, until phases were not fully separated anymore. For $J_{G1} < 10$ m/s, J_{G1} was kept fixed and J_{L1} was decreased to find limiting conditions for full phase separation. Before

56

starting any full-phase-separation experiment, the system was dried properly by passing a large amount of air through the inlet and discharging them through the outlet air rotameters.

3.3.2.1 Full-Phase-Separation Experiments for $J_{G1} > 10$ m/s

The following procedure was followed for all full phase-separation experiments at $J_{G1} > 10$ m/s:

i. The atmospheric pressure, P_{atm} was recorded.

ii. The inlet and discharge valves of the separation tanks were kept fully opened.

iii. The outlet pressure of the pressure controller was fixed at 30 psig.

iv. The air supply line was fully opened.

v. The control valve downstream of the inlet air rotameters was kept fully open. Appropriate air rotameter was partially opened up to the desirable level (for a fixed J_{G1}), by adjusting the control valve upstream of it. Care was taken so that the float of the rotameter stayed in the same place throughout the experiment.

vi. The outlet air rotameters in side 3 were kept completely closed. This way, all of the inlet air was passed through the top outlet, i.e., outlet 2. The control valve downstream of the rotameters in side 2 was opened to the atmosphere. The appropriate air rotameter on side 2 was opened up to the desired level, by adjusting the control valve upstream of it, so that the test section pressure remained fixed at 15 psig or 200 kPa (abs).

vii. Cooling water supply for the water reservoir was turned on and the bypass valve was kept fully opened. The submersible pump was then turned on.

viii. Water flow rate in the inlet was controlled by adjusting the control valves upstream of the appropriate water rotameter. The control valve downstream of the bank of inlet water rotameters was kept fully opened.

ix. Appropriate water rotameter in outlet 3 was opened by adjusting the control valves located upstream and downstream of it. Water level in the separation tank in side 3 was monitored for any change in level (in a cross-section that allowed proper monitoring) and the outlet water rotameter was adjusted accordingly.

x. A waiting time of 10 minutes was allowed at this point to see if any liquid emerges from the top outlet (outlet-2). This was observed in the transparent tygon tube that connects this outlet with the separation tank.

xi. If no liquid appears in the top outlet within this waiting time, inlet gas flowrate was increased by adjusting the inlet air rotameter, while keeping the settings of the inlet and outlet water rotameters fixed. At the same time, outlet airflow on side 2 was also adjusted, so that the test-section pressure remained at 15 psig. Step x was then repeated for the new inlet air flowrate or J_{G1}.

xii. Step xi was repeated iteratively with increasing J_{G1} until a trace amount of liquid started appearing in the top outlet. The value of J_{G1} at this point was considered to be the limiting value for full phase-separation at the chosen J_{L1}.

The following data were recorded when limiting conditions for full phase separation were reached:

a) Pressures of the inlet air and water, air outlets, separation tanks and test section.

b) Temperatures of the inlet and outlets of air and water.

c) Inlet and outlet volume flowrates of air and water from rotameters (V_{G1}, V_{G2}, V_{G3}, V_{L1}, V_{L2}, V_{L3}, respectively).

3.3.2.2 Full-Phase-Separation Experiments for $J_{G1} < 10$ m/s

A special procedure was followed for full-phase-separation experiments at $J_{G1} < 10$ m/s. The reason for that is a special phenomenon, which was observed while working in the slug flow regime. Some liquid (very small in quantity) was observed coming from the top outlet (outlet-2) at random intervals, owing to the intermittent nature of this flow regime. These momentary appearances of liquid from the top outlet were not considered as limiting conditions for full phase-separation. Rather, in the slug flow regime, phases were considered to be fully (or largely) separated when at least 99% of the liquid passed through the bottom outlet, leaving only 1% or less of the inlet liquid through the top, i.e. $F_{L3} \geq 0.99$.

To identify these conditions of full phase separation at $F_{L3} \geq 0.99$, a procedure similar to the one described in section 3.3.2.1 was followed. The only difference was that, instead of changing J_{G1}, at fixed J_{L1}, J_{L1} was changed, at fixed J_{G1} until conditions of full phase-separation were reached. For these cases, water flowrate in the inlet or J_{L1} was set at a high value in the beginning, so that initially water appeared in both outlets of the combined system. The water flowrates in these outlets were recorded by monitoring the water level in the separation tanks and accordingly adjusting the outlet water rotameters. At this stage, calculations for split ratio of water in the two outlets (F_{L2} and F_{L3}) were done. If $F_{L3} \geq 0.99$ was reached, the value of J_{L1} at this point was considered to be the limiting value for full phase separation at the chosen J_{G1}. If that was not the case, the value of J_{L1} was decreased keeping J_{G1} fixed and calculations for F_{L3} were done for this new value of J_{L1}. The value of J_{L1} was decreased iteratively until $F_{L3} \geq 0.99$ was reached to determine the limiting conditions of full phase separation.

To demonstrate this procedure, a hypothetical situation is presented in Figure 3.12 in the flow-regime map of Mandhane et al. (1974). The value of J_{G1} is fixed at 2.5 m/s in this figure. A value of $J_{L1} = 2$ m/s, represented as Point A, is taken and F_{L3} for this point is determined as 0.6. Keeping J_{G1} fixed, J_{L1} is reduced to 1 m/s and F_{L3} for this point (Point B) is found to be 0.7. The value of J_{L1} was then reduced further in subsequent steps, until $F_{L3} \geq 0.99$ was reduced. In Figure 3.12, this condition was reached at Point E and the value of $J_{L1} = 0.2$ m/s at this point was considered to be the limiting value for full phase separation at $J_{G1} = 2.5$ m/s.
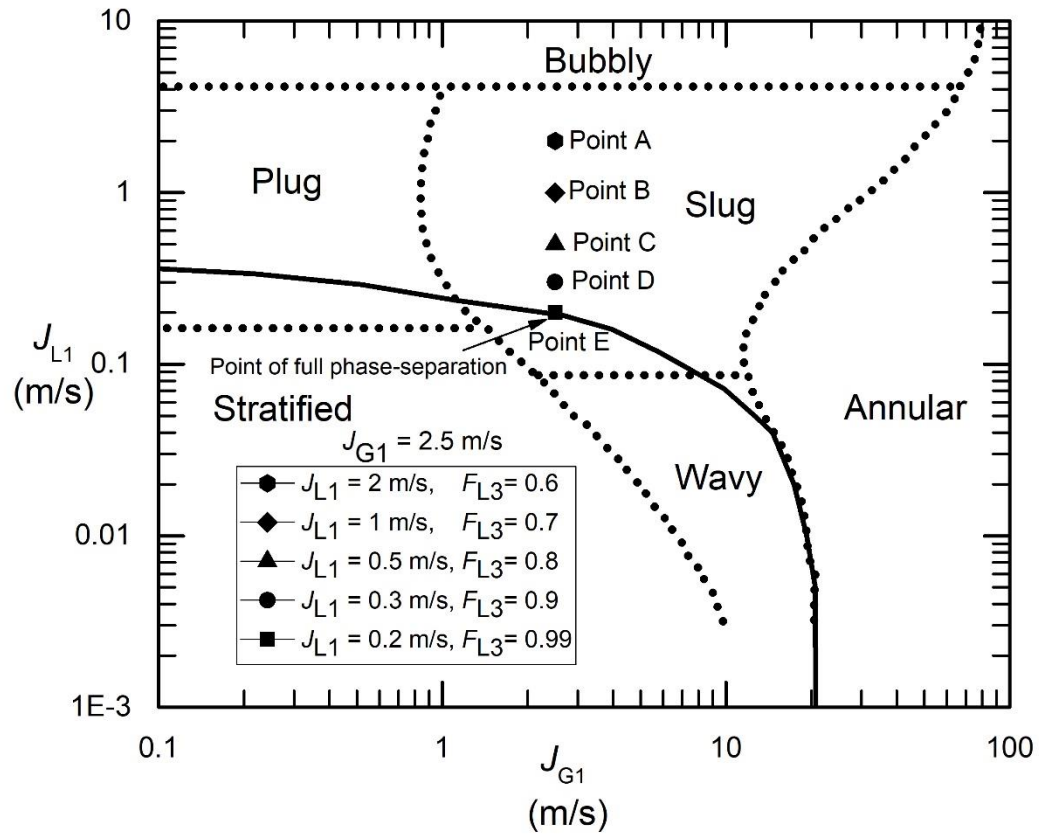
Figure 3.12   Demonstration of full-phase-separation experiments at $J_{G1} < 10$ m/s

Random appearance of trace amount of liquid in the top outlet was not observed in the plug flow regime. Nevertheless, the procedure described in this section was used to determine limiting values of J_{G1} and J_{L1} for full phase-separation in the plug flow regime also.

3.4 Data Reduction

The following steps contain the equations for calculating various parameters from the collected experimental data:

i. The gas density at any location in the loop was calculated from the equation of state as:

$$\rho_G = P / RT \tag{3.1}$$

The units of P and T in this equation are kPa and K, respectively, and the gas constant for air is $R = 0.287$ KJ/kg. The value of ρ_{STD} was calculated using Equation (3.1), with values of P and T at 101.3 kPa and 294.1 K, respectively.

ii. The liquid density at any location in the loop was calculated from the equation:

$$\rho_L = 1001.327 - (0.1708 \times T) \tag{3.2}$$

This equation was derived by linear interpolation of the values of water densities at various temperatures (K) collected from thermodynamic property tables of water.

iii. Air mass flowrate in the inlet and outlets, W_G were calculated using the equation:

$$W_G = V_G \times \rho_{STD} \times \text{SQRT}\ (\rho_G / \rho_{STD}) \tag{3.3}$$

The units of V_G and ρ in this equation are m³/s and kg/m³, respectively.

iv. Water mass flowrate in the inlet and outlets, W_L were calculated using the equation:

$$W_L = V_L \times \rho_L \tag{3.4}$$

The units of V_L and ρ_L in this equation are m³/s and kg/m³, respectively.

Equations to calculate other parameters like W_1, W_2, W_3, W_R, F_{G2}, F_{G3}, F_{L2}, F_{L3}, J_{L1} and J_{G1} has been included in section 1.3 in Chapter 1.

CHAPTER 4

RESULTS AND DISCUSSION

4.1 Data Range

Two groups of experiments were conducted in this thesis, aiming at finding partial- and full-phase-separation curves for air-water two-phase flows. All experiments were conducted at ambient temperature, with test-section pressure fixed nominally at 200 kPa (abs). Full-phase-separation data were collected within J_{G1} = 0.2 - 20 m/s and J_{L1} = 0.001 - 0.34 m/s, which fell in the annular, wavy, slug and plug flow regimes. Six sets of partial-phase-separation data were collected in the annular flow regime, with gas mass extraction ratio, F_{G3} ranging from 0 to 1. Three of these sets were collected at fixed J_{G1} of 40 m/s, with J_{L1} of 0.01, 0.04 and 0.18 m/s, while J_{L1} was fixed at 0.04 m/s for the other three sets, with J_{G1} of 20, 25 and 30 m/s.

Air and water mass balances were checked for every data point by calculating percentages of deviation of the sum of mass flow rates in the two outlets from the mass flow rate in the inlet. For all the test runs, the air and water mass balances were within ± 6.0% and ± 5.7%, respectively. Positive values of mass balance indicate higher value of inlet flow than the outlet flows, whereas negative values indicate higher value of outlet flows.

Tables 4.1 and 4.2 contain summaries of the ranges of various data related to the operating conditions of the test runs for full and partial phase separation, respectively. Tables B1 - B5 in Appendix B contain detailed results of these test runs.

The six data points for partial phase-separation are plotted on the flow-regime map of Mandhane et al. (1974) in Figure 4.1. The values of J_{G1} and J_{L1} were kept within ±3.5% and ±2.5%,

respectively, of the intended values for all test runs. Observed flow regimes in all cases were in close agreement with Mandhane et al. (1974).

Table 4.1   Range of operating conditions for full-phase-separation data

Number of data points	13
Inlet Flow regime	Annular, Wavy, Slug, Plug
Inlet gas superficial velocity, J_{G1} (m/s)	0.2 - 20
Inlet liquid superficial velocity, J_{L1} (m/s)	0.001 - 0.34
Temperature, T (°C)	21.5±1.8
Test-section pressure, P_s (kPa)	200±4
Air mass balance (%)	Within ±6.0
Water mass balance (%)	±4.5, for $J_{L1} > 0.001$ m/s

Table 4.2   Range of operating conditions for partial-phase-separation data

Number of data points	45
Inlet Flow regime	Annular
Inlet gas superficial velocity, J_{G1} (m/s)	20 - 40
Inlet liquid superficial velocity, J_{L1} (m/s)	0.01 - 0.18
Temperature, T (°C)	21.5±0.6
Test-section pressure, P_s (kPa)	200±5
Air mass balance (%)	±3.9
Water mass balance (%)	±5.7
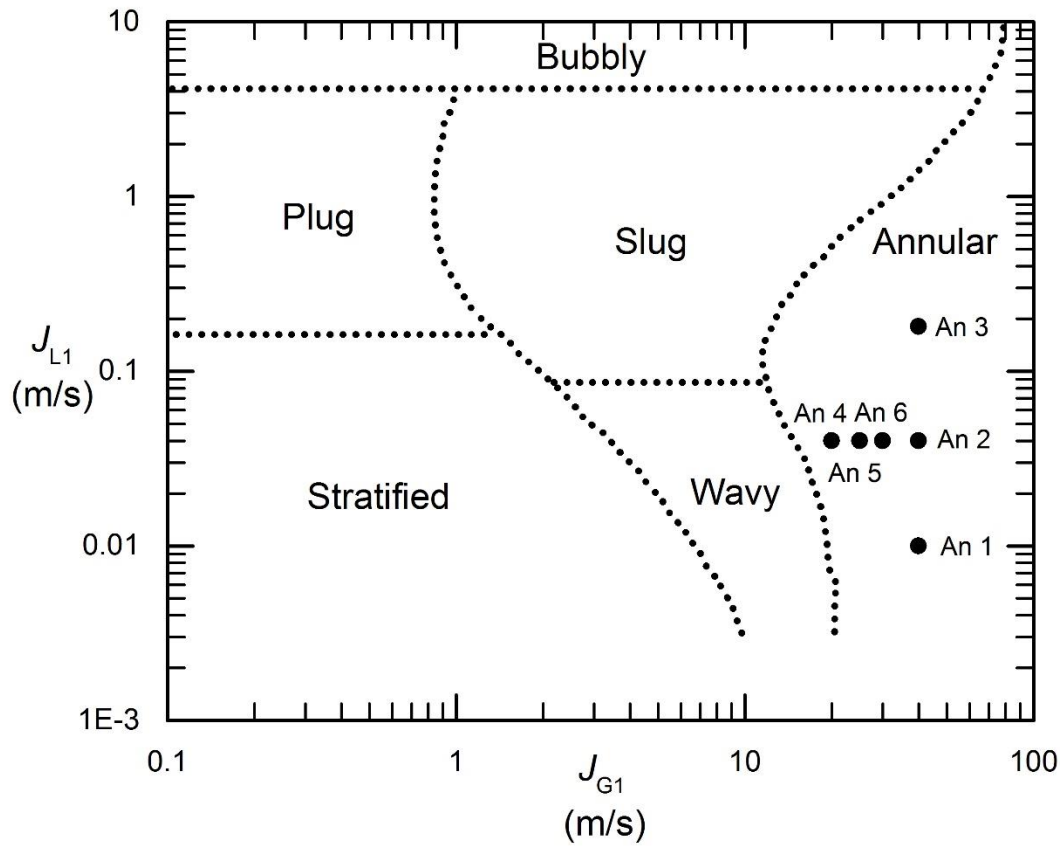
Figure 4.1   Inlet conditions for partial-phase-separation experiments
plotted on Mandhane et al. (1974) flow-regime map

4.2 Uncertainty Analysis

Uncertainties in results were calculated to accommodate the errors in calibration data and experimental procedures. Like all uncertainty analyses, uncertainty values were determined for various experimental parameters. Pre-determined fixed error bands for the various measuring devices used in the experiments are tabulated in Table 4.3. These fixed errors apply to both partial- and full-phase-separation experiments.

Table 4.3   Fixed uncertainties for partial and full-phase-separation experiments

Pressure Gauges	±1.8%
Thermocouples	±0.2°C
Air Rotameters	±2% of reading
Water Rotameters	±3% of reading
Diameter	±1.5%

A numerical method of sequential perturbation was used for the uncertainty analysis. Details of the procedure and results of this analysis is reported in Appendix C. Uncertainty analysis was performed for inlet parameters W_{G1}, W_{L1}, J_{G1}, J_{L1} and for outlet parameters W_{G2}, W_{G3}, W_{L2}, W_{L3}, F_{G3} and F_{L3} for both partial- and full-phase-separation data.

For full-phase-separation data, uncertainties in calculation of W_{G1} and W_{G2} were found to be within ±2.1%. Uncertainties were within ±3% for all values of W_{L1}, W_{L2} and W_{L3}. Values of J_{G1} and J_{L1} were uncertain within ±3.8% and ±4.2%, respectively. For F_{L3}, 92.5% of the data were within an uncertainty of ±7.5%; only one data which corresponds to $J_{L1} = 0.001$ m/s, had an uncertainty of +24.8%. This high value was due to the small inlet superficial liquid velocity, J_{L1}. The values of uncertainty for W_{G3} and F_{G3} were within ±0.4% and ±8.8%, respectively.

For partial-phase-separation data, uncertainties in calculation of W_{G1}, W_{G2} and W_{G3} were found to be within ±2.1%, ±2.1% and ±1.9%, respectively. Uncertainties were within ±3% for all values of W_{L1}, W_{L2} and W_{L3}. Values of J_{G1} and J_{L1} were uncertain within ±3.8% and ±4.2%, respectively. Eighty-two percent of the data were within an uncertainty of ±5% for F_{G3}; highest

value being +6.3%. For $F_{L3,}$ uncertainties were within ±8% for 88% of the data, with a highest value of +8.9%.

4.3 Symmetry and Reliability of the Test Loop

Symmetry of the test loop was tested by passing single-phase air through the system, at three different J_{G1} (2, 10 and 40 m/s), keeping the test-section pressure at 200 kPa (abs). The pressure of the two air outlets were set at exactly the same value for each run. The two separation tanks were also maintained at the same pressure (within 2% of each other). Under these identical conditions of the two outlets, the mass flow rate of air through each of them were measured and found to be equal (within 1.6% of each other). These results account for symmetry of the test loop. Table 4.4 contains the data of the tests for symmetry of the test loop.

Table 4.4   Data for symmetry of test loop

J_{G1} (m/s)	W_{G1} (kg/hr)	W_{G2} (kg/hr)	W_{G3} (kg/hr)	Percentage of Difference (%)
2	0.044	0.0239	0.0235	1.6
10	0.208	0.105	0.106	0.95
40	0.832	0.420	0.417	0.7

To validate the reliability of the test loop, some partial-phase-separation data reported by Mohamed et al. (2011) were regenerated in the wavy and annular flow regimes. Like the aforementioned authors, these tests were performed in a test loop having a single vertical impacting tee junction at a test-section pressure of 200 kPa. In all other aspects, their test loop is identical to the one used in these tests, thus making it logical to compare present data with theirs. Figure 4.2

67

shows partial phase-separation data at J_{L1} of 0.04 m/s. Closed symbols in the figure represent data collected in this investigation, whereas open symbols represent data reported by Mohamed et al. (2011).
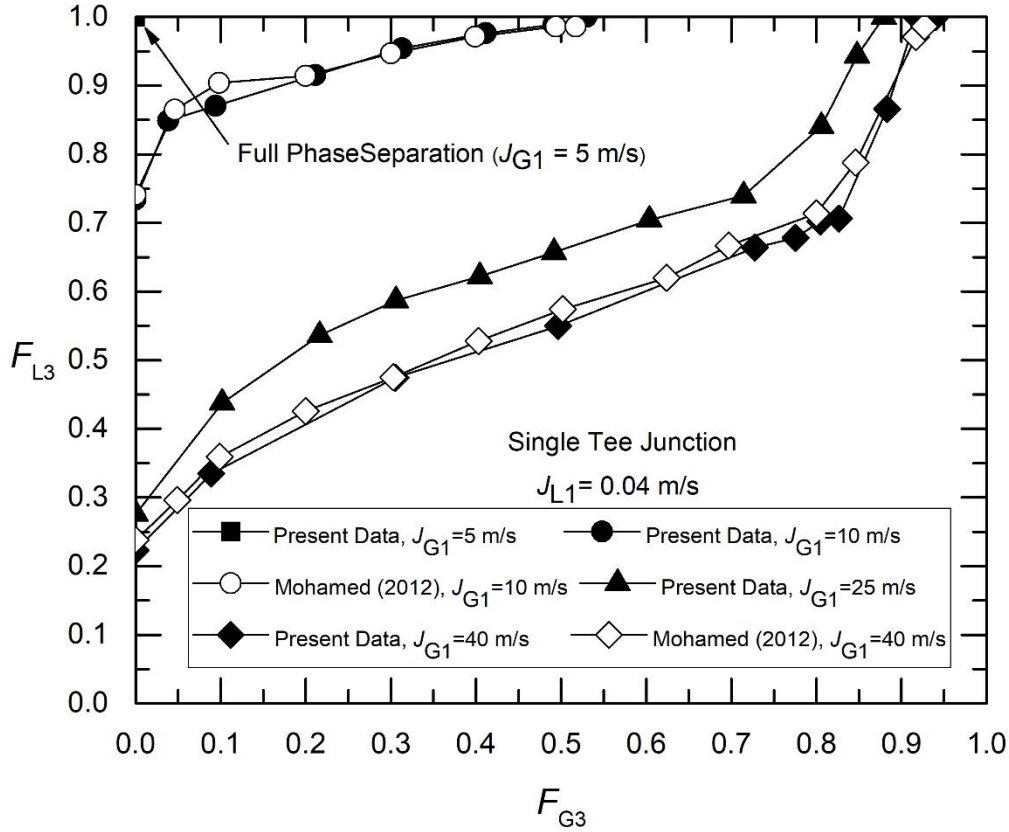
Figure 4.2   Comparison of data with Mohamed et al. (2011) at identical test conditions

At J_{G1} of 10 m/s (wavy flow) and 40 m/s (annular flow), partial-phase-separation data were compared. It can be observed that the partial phase-separation curves in both cases follow similar trend, with 94% of the present data repeatable within 4.2% of Mohamed et al. (2011). The percentage of deviation falls within the scope of procedural uncertainties and situational difference in input parameters.

In order to validate the system and test procedures further, partial-phase-separation curve was generated for J_{G1} of 25 m/s, also at J_{L1} of 0.04 m/s, which falls in the annular flow regime. In F_{G3} versus F_{L3} plot in Figure 4.2, this curve moved counter clockwise, towards the full-separation point, away from the partial-phase-separation curve of $J_{G1}= 40$ m/s, but not as much as the partial-phase-separation curve of $J_{G1}= 10$ m/s, at same J_{L1}. This indicated that reducing J_{G1} might lead to the point of full separation. This point of full separation was found to be at J_{G1} of 5 m/s, at $J_{L1}=$ 0.04 m/s, when a single vertical impacting tee junction was used. Thus, it was theorized that using a system of combined impacting tee junctions might further increase the values of both J_{G1} and J_{L1}, up to which full separation of phases can be achieved. Experiments in this thesis were designed with this aim in view.

4.4 Repeatability of Data

In order to ensure the quality of the collected data, some of the experiments were repeated to check if exact/almost identical results could be obtained. Some of these tests were done with the single vertical junction and others with the combined junction. Table 4.5 contains the results of some of the partial-phase-separation experiments that were repeated. It should be noted that minor difference in setting the inlet parameters for identical runs were due to minor changes in temperature and atmospheric pressure in the laboratory. The result of a full-phase-separation experiment presented in Table 4.5 shows that for the same J_{L1}, limiting value of J_{G1} for full-phase-separation could be repeated within 0.75%.

Table 4.5   Repeatability of partial-phase-separation data

Test section	J_{G1} (m/s)	J_{L1} (m/s)	F_{G3}	F_{L3}
Single Tee	10.17	0.04	0.09	0.89
	10.21	0.04	0.09	0.87
Single Tee	10.20	0.04	0.53	1
	10.21	0.04	0.53	1
Combined Tee	40.64	0.18	0	0.32
	41.09	0.18	0	0.32
Combined Tee	20.70	0.04	0.20	0.94
	20.52	0.04	0.20	0.94
Combined Tee	25.30	0.04	0.32	0.94
	25.47	0.04	0.30	0.94

Table 4.6   Repeatability of full-phase-separation data

Test section	F_{G3}	F_{L3}	J_{L1} (m/s)	J_{G1} (m/s)
Combined Tee	0	1	0.04	14.63
	0	1	0.04	14.52

4.5 Cases of Full Phase Separation

4.5.1 Shape of the Full-Phase-Separation Curve

Figure 4.3 contains an example of a full-phase-separation curve plotted on the flow regime map of Mandhane et al. (1974). Full-phase-separation curves can be identified as curves, which outline the limiting values of J_{G1} and J_{L1}, at which full separation of phases can be achieved. Any point under this curve, identified as 'Region of full phase separation' in Figure 4.3, will give full separation of phases, i.e., all the gas will flow through the top outlet (outlet-2) and all the liquid will flow through the bottom outlet (outlet-3). The region above this curve is identified as 'Region of partial phase separation', where there will be a mixture of air and water in at least one of the two outlets. Increasing either J_{G1} or J_{L1} from any point on the full-phase-separation curve will, thus, result in partial separation of phases.
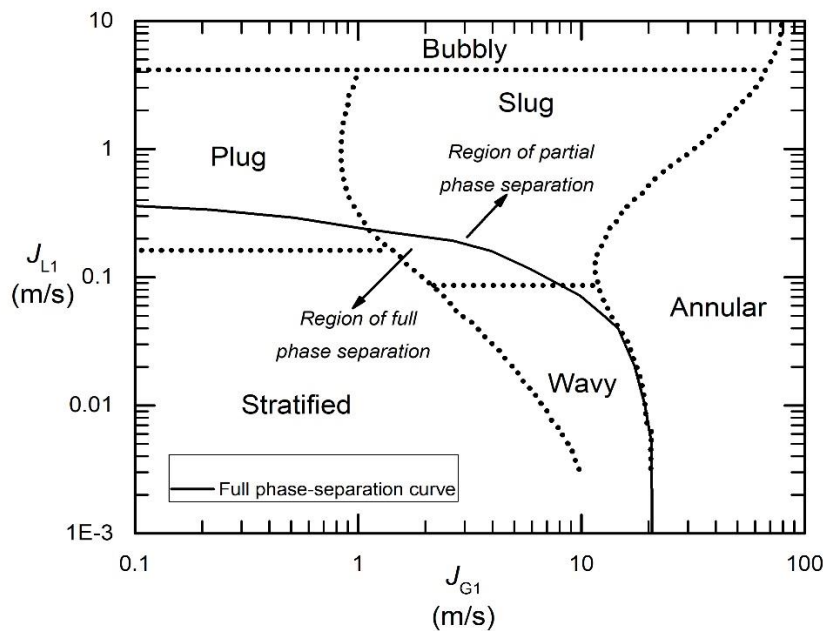
Figure 4.3   Full-phase-separation curve

4.5.2 Full-Phase-Separation Data

Figure 4.4 contains actual data for full separation of phases plotted on the flow-regime map of Mandhane et al. (1974). The curve drawn with closed symbols represents the limiting conditions of J_{G1} and J_{L1} for full phase separation when the present system of a combined tee junction is used. The observed flow regimes in the inlet, for all data points were in agreement with the predictions of Mandhane et al.'s map. The open rectangular symbols in the plot are the limiting values of J_{G1} and J_{L1}, reported by Mohamed et al. (2011) in a system with a single vertical impacting tee junction. It is evident from the figure that the present limiting values show considerable increase when the combined tee junction was used in place of a single one.
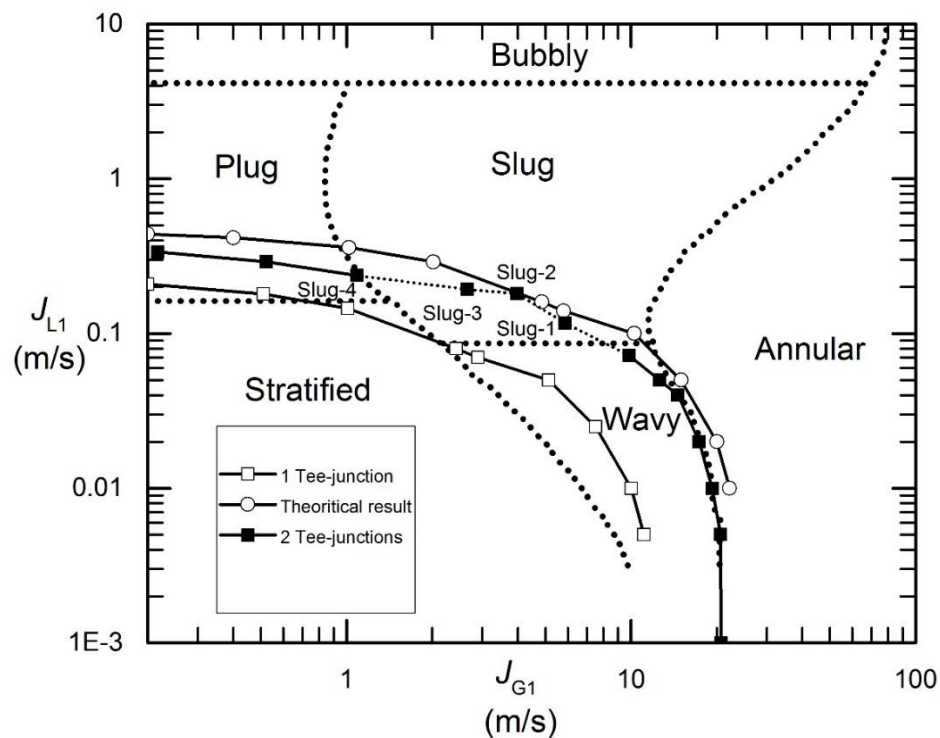
Figure 4.4   Limiting conditions of full phase separation plotted on Mandhane et al. (1974) flow-regime map

The third curve in Figure 4.4, put together with open circular symbols, is a theoretical curve drawn by doubling the limiting values of both J_{G1} and J_{L1} for full phase separation in a single vertical tee junction. It can be observed that the experimental results for the present system of a combined tee junction almost coincide with this theoretical line in the wavy-annular flow regime, which implies that limiting values of J_{G1} and J_{L1} for full phase separation is almost twice for the present system compared to an otherwise identical system with a single tee. However, in the slug and plug flow regimes, these values do not coincide with the theoretical curve and are not doubled.

The reason for this might lie in the nature of the flow regimes. While the wavy and annular flow regimes are quasi-steady in nature, the slug and plug flow regimes are intermittent and non-steady. In the experimental set-up of this thesis, there is a horizontal impacting tee junction, which directs the inlet flow to the two vertical impacting tee junctions (refer to Figure 3.5). Theoretically, owing to the symmetry of the system, this horizontal impacting junction should divide the inlet flow equally, in terms of quality and quantity in its two outlets, which act as inlets to the two vertical impacting tee junctions. Thus, each of the two vertical tees should get half of the inlet flow, i.e., J_{G1} and J_{L1} should be half of the inlet values in their inlets in theory. When the output of these two vertical junctions are combined, the limiting values of J_{G1} and J_{L1} for full phase separation should be an addition of the two. Thus, doubling the limiting inlet J_{G1} and J_{L1} for full separation in a single tee should give the condition for full phase separation in the present system. Due to uniformity of nature of wavy and annular flow regime, this theory was approximately valid in those flow regimes. However, in the slug and plug flow regimes, the instantaneous values of J_{G1} or J_{L1} at the junction might be higher than the average values. This might have resulted in gas or liquid flow rate (or J_{G1} and J_{L1}) intermittently higher than the limiting values for full phase separation in a single junction at the inlet of one or both of the vertical junctions. Consequently,

73

this would have led to earlier onset of liquid from the top outlet than expected, resulting in lower values of the limiting J_{G1} and J_{L1} for full phase-separation for the present combined junction.

4.5.3 Anomaly in Slug Flow Regime

Full-phase-separation data in the slug flow regime are represented with dotted lines in Figure 4.4. The reason for this is a phenomenon observed during the experiments. At the onset of slug flow ($J_{L1} > 0.11$ m/s and $J_{G1} > 2$ m/s), some liquid (very small in quantity) was observed coming from the top outlet at random intervals. Depending on the inlet conditions, small streaks of liquid seem to come from the top outlet intermittently or continuously in this flow regime. After repeated observation of this phenomenon, the author concluded that, due to the intermittent nature of slug flow, it was not possible to get 100% phase separation in this flow regime at the expected (double) values of J_{G1} or J_{L1}. Rather, a criterion of full phase separation was decided for this flow regime: the phases will be considered fully (or largely) separated when 99% of the liquid phase passes through the bottom outlet, with 1% of the liquid coming from the top. The random nature of liquid coming from the top in the slug flow regime was taken into consideration and the time-averaged mass flow rate from this outlet was recorded. The reason behind selecting such a criterion is illustrated in Figure 4.5.

Figure 4.5 illustrates how F_{L3}, which is the fraction of liquid passing from the bottom outlet, changes with J_{L1}, for the point slug-3 (in Figure 4.4). Keeping J_{G1} constant at 2.65 m/s and $F_{G3}= 0$ (passing all the gas from the top outlet), F_{L3} initially increases rapidly as J_{L1} is lowered. On further decreasing J_{L1}, the change in F_{L3} becomes very small. The value of J_{L1} was lowered until a value of 0.193 m/s for this point, when $F_{L3} \geq 0.99$, i.e., at least 99% of the liquid was passing through the bottom outlet and this point was considered as the point of full separation of phases.

Between $J_{L1} = 0.193$ m/s and $J_{L1} = 0.11$ m/s (where the flow regime changes from slug to wavy), F_{L3} varies very slowly from 0.993 to 1. Therefore, it is probably acceptable to consider this criterion of 99% F_{L3} as an estimate of J_{L1}, at a fixed J_{G1}, for full separation of phases.

The points of full separation of phases for plug flow regime was also estimated using the criterion of 99% F_{L3}, consistent with the slug flow points. However, in the plug flow regime, random appearance of liquid in the top outlet was not observed. Figure 4.6 shows how F_{L3} increases with a decrease in J_{L1} for fixed J_{G1} in the slug and plug flow regimes. For all six points in these flow regimes, J_{L1} was lowered until F_{L3} crosses the line of 0.99 at which the point of full separation of phases was estimated.
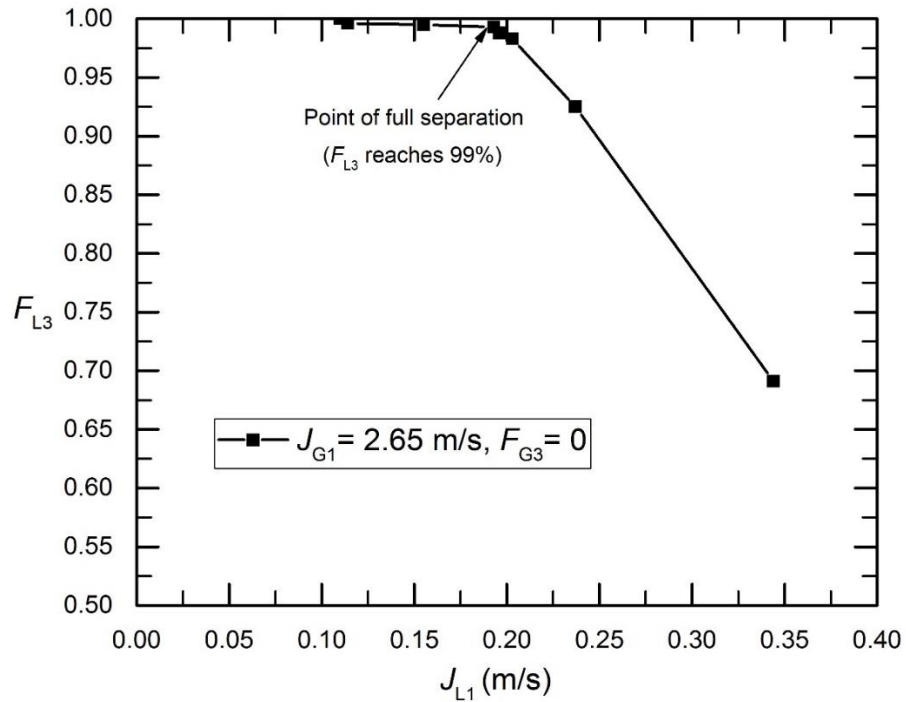
Figure 4.5   Estimation of J_{L1} for full separation of phases for the point slug-3
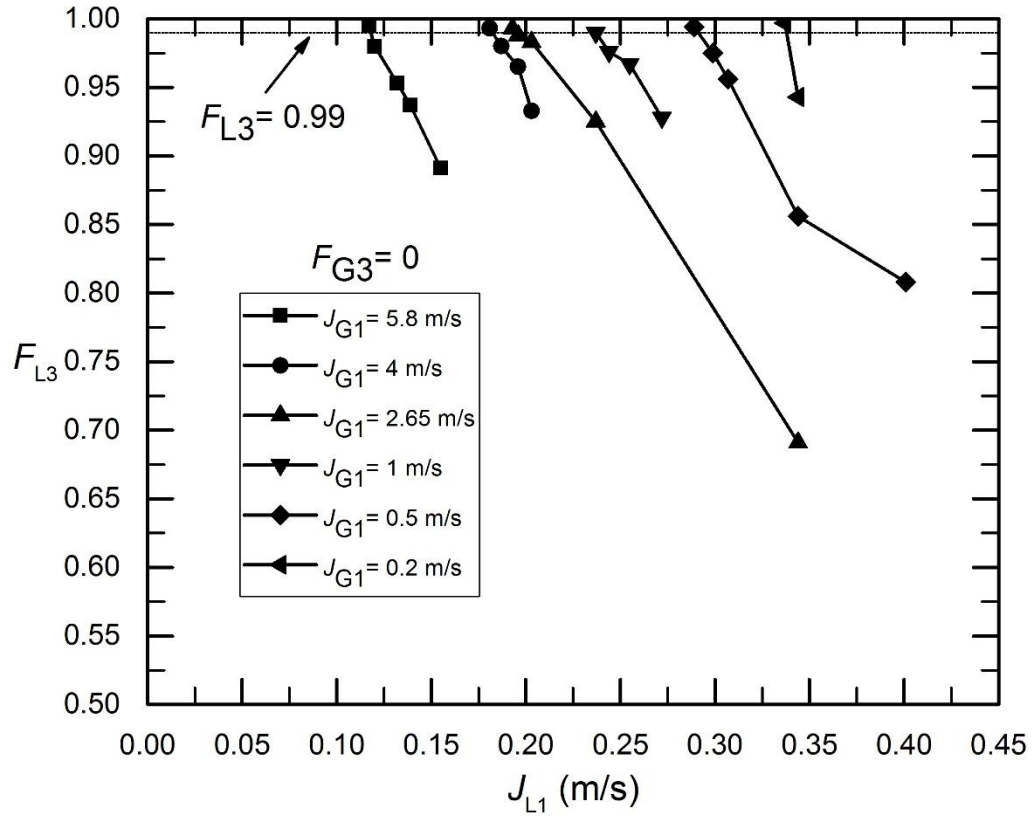
Figure 4.6   Estimation of J_{L1} for full separation of phases in the slug and plug flow regimes

Figures 4.7 and 4.8 show in detail how phases are redistributed, until full separation of phases was achieved for the points slug-1 and slug-3, respectively. It can be observed from these figures that with decreasing J_{L1}, the phase-redistribution or partial-phase-separation curves move towards point of full separation corresponding to F_{L3} of 0.99.
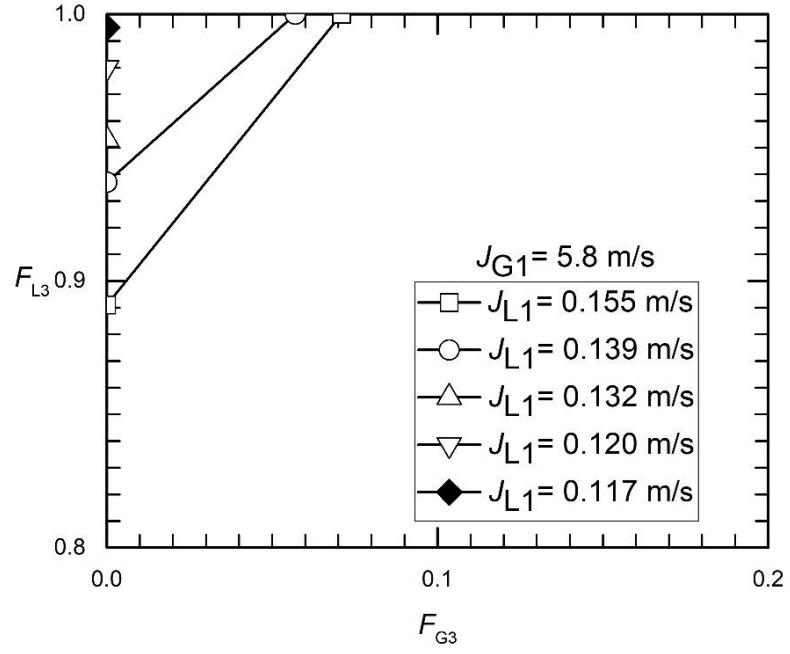
Figure 4.7   Phase redistribution for the point slug-1
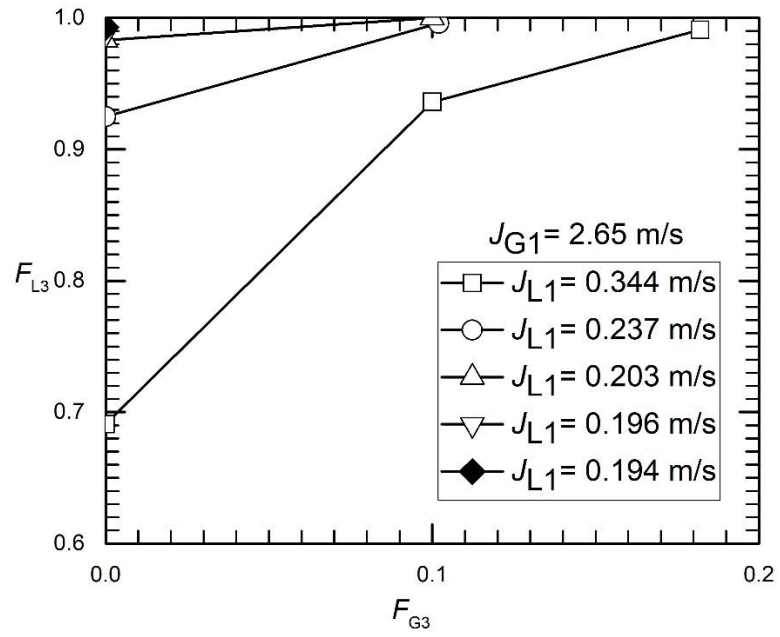
Figure 4.8   Phase redistribution for the point slug-3

77

4.6 Cases of Partial Phase Separation

4.6.1 Overview

As illustrated in Figure 4.3, beyond the curve of full phase separation, partial separation of phases takes place. Six annular points (shown in Figure 4.1) have been chosen in the region of partial phase separation and phase-redistribution data have been generated for them. The data are presented in F_{G3} versus F_{L3} plots. Thus, these curves show how the phases are redistributed in the two outlets, when they cannot be separated completely. For each of the curves, mass flow rate of gas in the bottom outlet, W_{G3}, has been increased gradually from 0, up to a point where $F_{L3} = 1$, i.e., all of the liquid enters the bottom outlet.

4.6.2 Partial-Phase-Separation Data at Fixed J_{L1}

Figure 4.9 shows the effect of changing the inlet superficial gas velocity, J_{G1}, on partial-phase-separation data. Keeping J_{L1} fixed at 0.04 m/s, four values of J_{G1} (20, 25, 30 and 40 m/s) have been used, which correspond to the points An 4, An 5, An 6 and An 2, respectively. It can be observed from the figure that as J_{G1} is decreased at fixed J_{L1}, the partial-phase-separation curves move in counter clockwise direction towards the point (0, 1) in the F_{G3} versus F_{L3} plot. Thus, reducing J_{G1} affects phase redistribution in a way that higher fraction of liquid enters the bottom outlet with lower fraction of gas. On reducing J_{G1} to a value of 14.6 m/s (Point An 0 in Figure 4.9), it was observed that all of the liquid enters the bottom outlet with no gas entering that outlet, i.e., the phases were separated completely.

The reason for such a trend is two-fold: liquid's natural tendency to enter the bottom outlet owing to the effect of gravity and gas inertia force or the capacity of gas to drag liquid with it to the top outlet, represented by $\rho_G J_G^2$. At higher J_{G1}, higher gas inertia force drags more liquid with

it to the top, thus, increasing F_{L2} and consequently, reducing F_{L3}. As F_{G3} is increased, the amount of gas entering the top outlet is reduced, which reduces the gas inertia force and the amount of liquid being dragged to the top. As a result, F_{L3} is increased. When F_{G3} is sufficiently increased, gas inertia force is lowered to a level that liquid cannot be dragged to the top anymore and all of the liquid will pass through the bottom outlet, giving $F_{L3} = 1$. This point of $F_{L3} = 1$ comes earlier for smaller J_{G1} because of the lower value of gas inertia force. On further reducing J_{G1}, a point is reached where the effect of gravity is higher than the gas inertia force and all liquid enters the bottom outlet with no gas giving full separation of phases, which happens in this case at $J_{G1} = 14.6$ m/s.
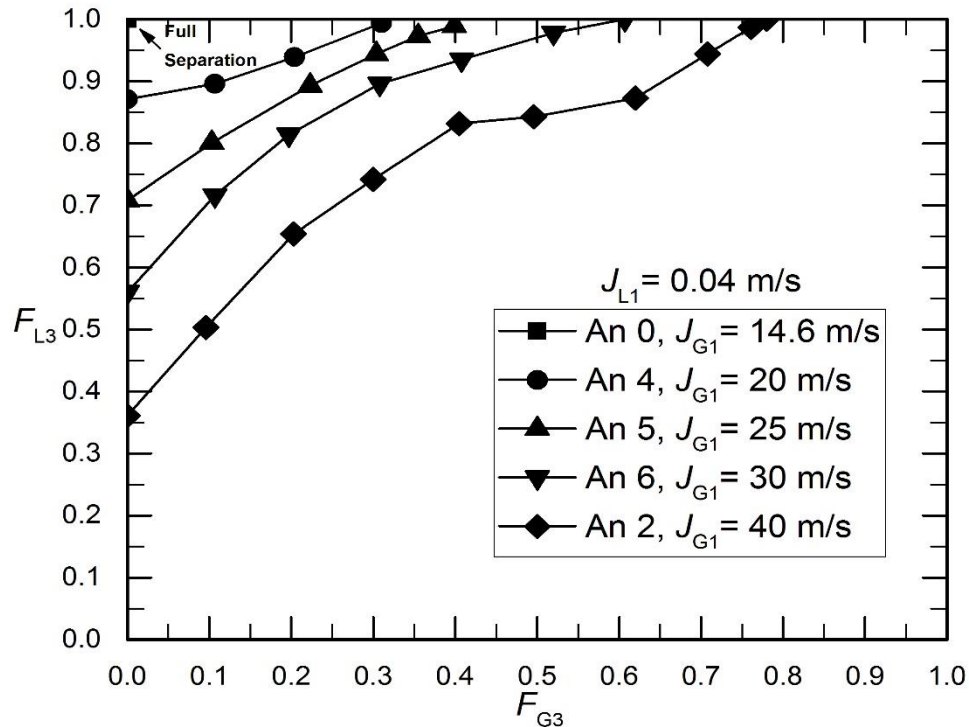
Figure 4.9   Partial-phase-separation data at fixed $J_{L1} = 0.04$ m/s (refer to Figure 4.1 for the inlet conditions in the annular flow regime)

79

4.6.3 Partial-Phase-Separation Data at Fixed J_{G1}

Figure 4.10 shows the effect of changing inlet superficial liquid velocity, J_{L1}, on partial-phase-separation data. Keeping J_{G1} fixed at 40 m/s, three values of J_{L1} (0.01, 0.04 and 0.18 m/s) have been tested, which correspond to the points An 1, An 2 and An 3, respectively. It can be observed from the figure that with changing J_{L1}, the partial-phase-separation curves show no fixed trend. A prominent change in trend seem to take place near $F_{G3} = 0.15$, after which the partial-phase-separation curves move in counter-clockwise direction with decreasing J_{L1}. It can be said that for these cases, after $F_{G3} = 0.15$, with decreasing J_{L1}, higher amounts of liquid enter the bottom outlet and the curves move towards the point of full phase-separation (0, 1). The change in trend around $F_{G3} = 0.15$ is hard to solidly explain on physical grounds, but it may be due to the balance
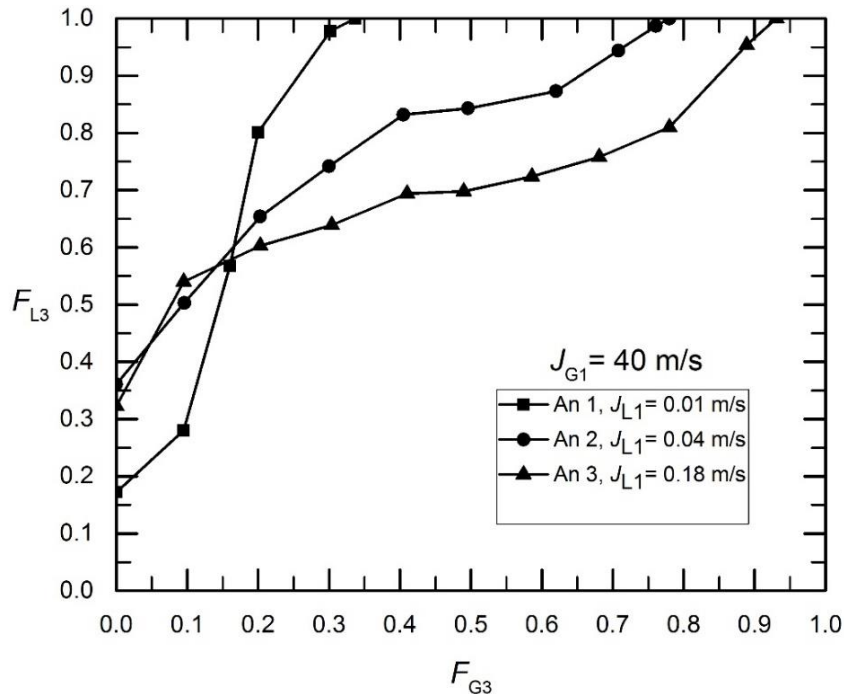
Figure 4.10   Partial phase-separation data at fixed $J_{G1} = 40$ m/s

between gas inertia and liquid gravity forces. The inconsistency in trend of partial-phase-separation curves with changing J_{L1} was also observed by Mohamed et al. (2011).

4.7 Phase-Separation Parameter

4.7.1 Definition

It is evident from partial- and full-phase-separation data presented in sections 4.5 and 4.6 that changing J_{G1} or J_{L1} affects the manner, in which phases are redistributed in the two outlets, which leads to changes in phase-separation effectiveness of the present system. In order to quantify this effect, a 'phase-separation parameter' was defined, considering the fractions of both inlet gas and liquid entering the same outlet. In this thesis, the phase-separation parameter is defined as:

$$\eta = (F_{G2} - F_{L2}) \times 100\% \qquad (4.1)$$

In Figure 4.11, a typical plot of phase-separation parameter, η, as a function of F_{G3} is presented. The significance of the four limiting points, (0, 0), (0, 100), (1, 0) and (1, -100), of this plot are as follows:

Point 1: The point (1, 0) in Figure 4.11 corresponds to the point (1, 1) in the partial-phase-separation (F_{G3} vs. F_{L3}) plot, where all the gas and liquid enter outlet-3 (the bottom outlet). This is a point of zero phase separation, yielding, $\eta = 0\%$.

Point 2: The point (0, 100) in Figure 4.11 corresponds to the point (0, 1) in the partial-phase-separation (F_{G3} vs. F_{L3}) plot, where all the gas enter outlet-2 (top outlet) and all liquid enter outlet 3 (bottom outlet). This is a point of full phase separation yielding, $\eta = 100\%$.

Point 3: The point (0, 0) in Figure 4.11 corresponds to the point (0, 0) in the partial-phase-separation (F_{G3} vs. F_{L3}) plot, where all the gas and liquid enter the top outlet. This is a point of zero phase separation, yielding, $\eta = 0\%$.

Point 4: The point (1, -100) in Figure 4.11 corresponds to the point (1, 0) in the partial-phase-separation (F_{G3} vs. F_{L3}) plot, where all the gas enter outlet 3 (bottom outlet) all liquid enter outlet-2 (top outlet). This limiting point is highly unlikely to be achieved in practice.
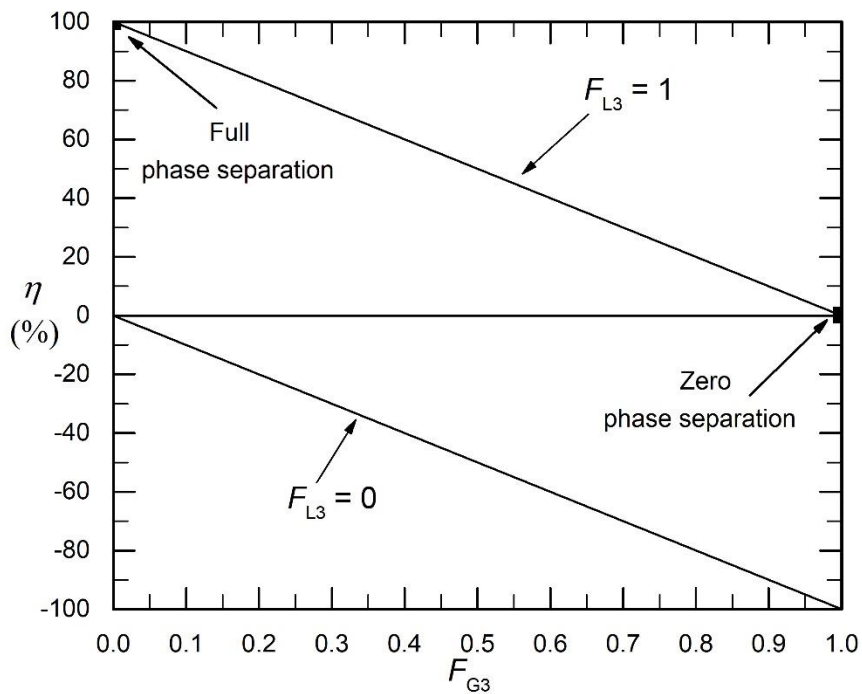
Figure 4.11   Plot of phase-separation parameter, η, as a function of F_{G3}

4.7.2 Phase-Separation Parameter at Fixed J_{L1}

Figure 4.12 contains the curves of phase-separation parameter, η, as a function of F_{G3} for the four points An 4, An 5, An 6 and An 2, all of which have $J_{L1}= 0.04$ m/s. Inlet superficial gas

velocity, J_{G1} is different for each of these points and it can be observed from the figure that with decreasing J_{G1}, η has a higher value for every corresponding F_{G3}.
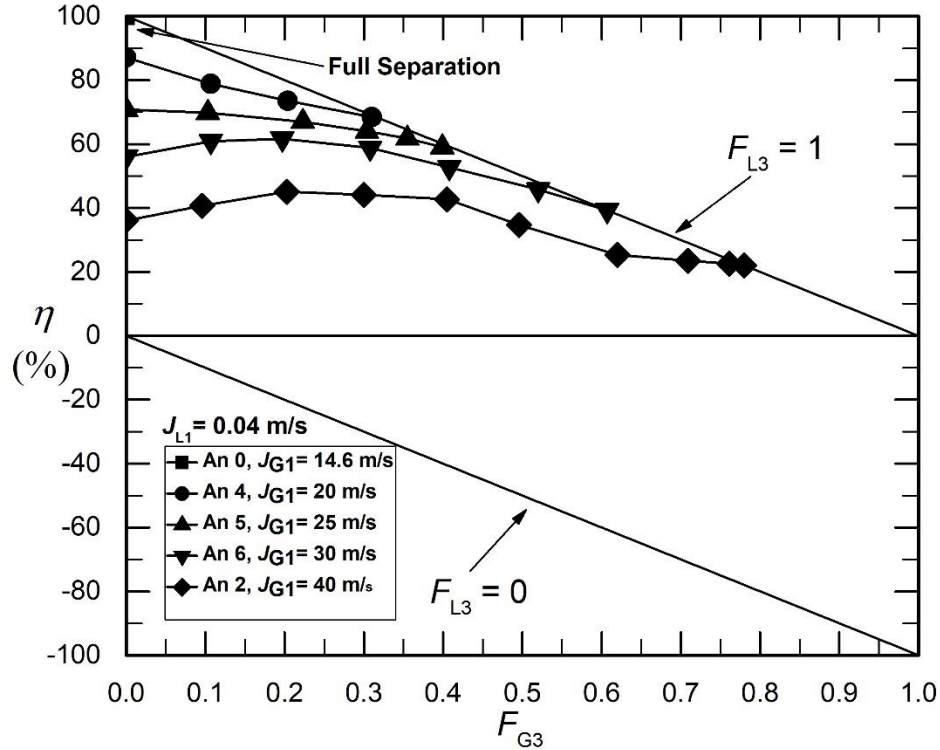
Figure 4.12   Phase-separation parameter, η, at fixed $J_{L1}= 0.04$ m/s

At $F_{G3} = 0$, η increases from less than 40% to more than 80% as J_{G1} is decreased from 40 m/s (An 2) to 20 m/s (An 4). Again, with decreasing J_{G1}, the last point in each curve ($F_{L3} = 1$, where all liquid enters the bottom outlet), climbs up the line joining the points of zero and full phase separation. It is evident from these observations that decreasing J_{G1} affects phase redistribution in a way that the effectiveness of phase separation is increased, which is the reason for higher value of η for all F_{G3}. It can also be noticed from Figure 4.11 that as J_{G1} is decreased further to 14.6 m/s, $\eta = 100\%$ is achieved, indicating that full separation of phases took place.

4.7.3 Phase-Separation Parameter at Fixed J_{G1}

The effect of J_{L1}, on phase-separation parameter, η, at fixed $J_{G1}= 40$ m/s is illustrated in Figure 4.13 for three annular points: An 1, An 2 and An 3. It can be observed from the figure that the comparative trend of change of η with F_{G3} for these three annular points is reversed pivoting at $F_{G3} = 0.15$. For $F_{G3} > 0.15$, η is higher for all F_{G3}, as J_{L1} is decreased. Under these conditions with decreasing J_{L1}, the last point in each curve ($F_{L3} = 1$) climbs up the line joining the points of zero and full phase separation, which is a clear indication of increased effectiveness of phase separation. From $0 < F_{G3} < 0.15$, with decreasing J_{L1}, η decreases at a given F_{G3} indicating lower phase-separation effectiveness. This decrease in values of η for $F_{G3} < 0.15$ may be attributed to the balance between gas inertia and liquid gravity forces. Undoubtedly, there is much scope for future work, both empirical and theoretical, to analyze this inconsistency in trend of η with F_{G3}, as J_{L1} is changed.
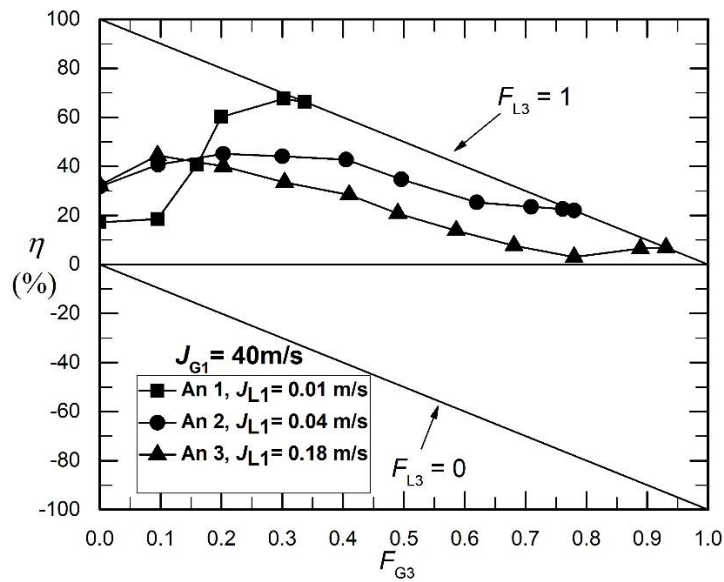
Figure 4.13   Phase-separation parameter, η, at fixed $J_{G1}= 40$ m/s

4.8 Comparison with a Single Vertical Tee Junction

4.8.1 Overview

In this section, partial-phase-separation data and separation parameter, η, collected with the present combined tee have been compared to similar data collected with a system of a single tee. The aim of this comparison is to illustrate the improvement in phase-separation effectiveness when a combined tee is used. Data have been compared for the points An 1, An 2, An 3 and An 5. Mohamed et al. (2011) have reported partial-phase-separation data for a system of single tee, for the first three points under test conditions identical to the present work. Similar data for An 5 point for a single tee have been collected by the author of this thesis. Phase-separation parameter, η, for all these annular points have also been calculated and compared in this section.

4.8.2 Comparison of Partial-Phase-Separation Data

Figure 4.14 shows two sets of partial-phase-separation data for An 1 data point: generated with the present system of a combined tee and with a system of a single tee junction of the same kind. Figures 4.15 - 4.17 contain similar data for An 2, An 3 and An 5 data points. In all of these figures, closed and open symbols represent the data for the combined tee and the single tee, respectively.

It can be observed from Figures 4.14 - 4.17 that, for every F_{G3}, the corresponding value of F_{L3} is higher for the present system. This causes the partial-phase-separation curves for the present system to move in counter clockwise direction from the partial-phase-separation curves for the system with single tee towards the point of full phase-separation (0, 1) in the F_{G3} versus F_{L3} plot. Thus, it can be concluded that, compared to the system of single tee, the present system redistributes phases in the two outlets in a way that is closer to the point of full phase separation.
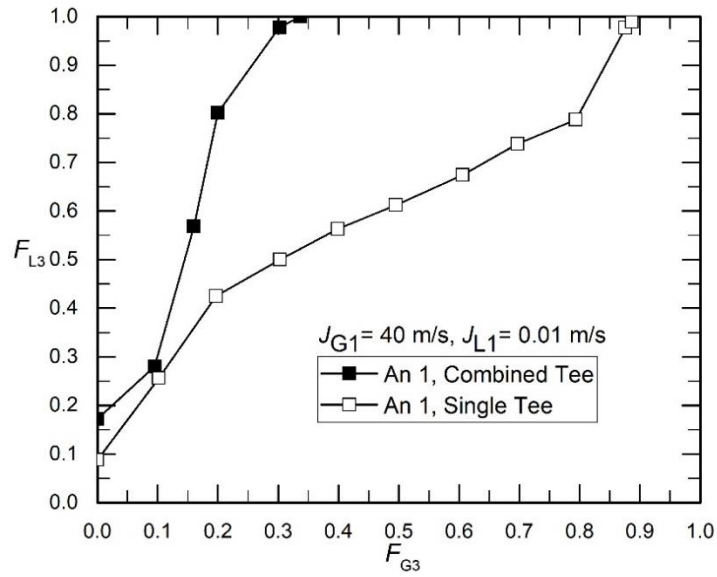
Figure 4.14   Comparison of partial-phase-separation data of the present system with a system of a single vertical impacting tee junction for An 1 data point
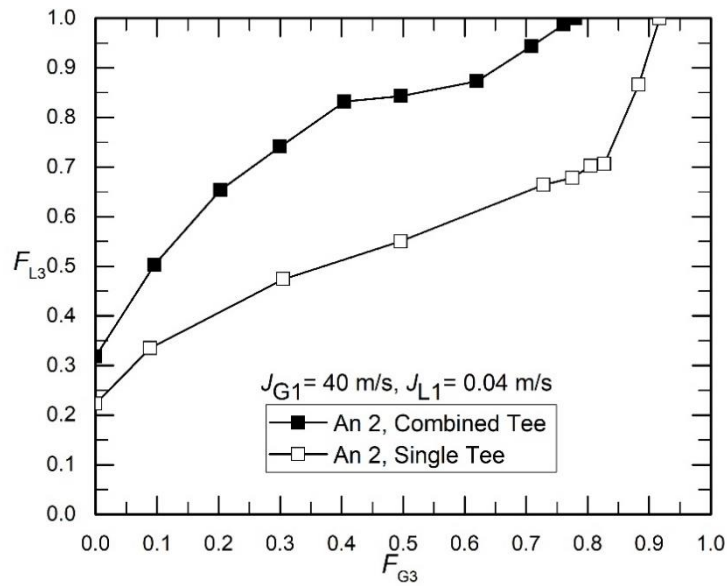
Figure 4.15   Comparison of partial-phase-separation data of the present system with a system of a single vertical impacting tee junction for An 2 data point
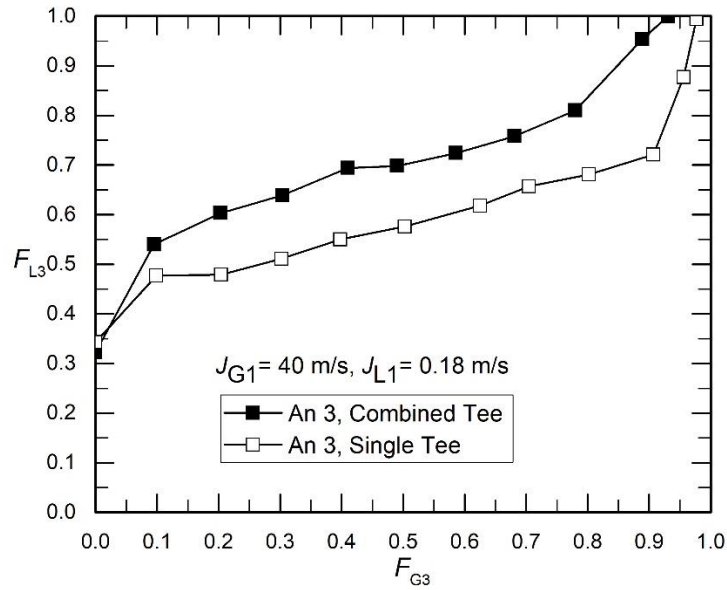
Figure 4.16   Comparison of partial-phase-separation data of the present system with a system of a single vertical impacting tee junction for An 3 data point
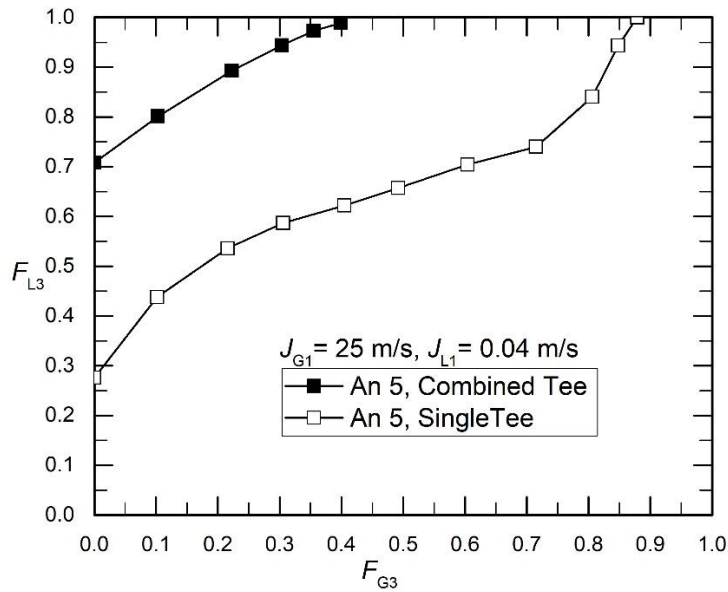
Figure 4.17   Comparison of partial-phase-separation data of the present system with a system of a single vertical impacting tee junction for An 5 data point

It is therefore safe to conclude that increasing the number of tee junctions in a system increases its effectiveness as a phase separator.

It is also apparent from the figures that, the shift of the partial-phase-separation curves in anti-clockwise direction for the present system, is more prominent when J_{G1} is decreased (evident from comparing Figures 4.15 and 4.17), compared to when J_{L1} is decreased (evident from comparing Figures 4.14 -4.16). Thus, it can be said that partial-phase-separation data are more affected by a change in J_{G1} rather than a change in J_{L1}.

4.8.3 Comparison of Phase-Separation Parameter

Figures 4.18-4.21 show the phase-separation parameter, η as a function of F_{G3}, for the present system and the system with a single tee, generated for An 1, An 2, An 3and An 5 points, respectively. In all of these figures, closed symbols represent the data for the combined tee and the open symbols represent the same for the system of single tee.
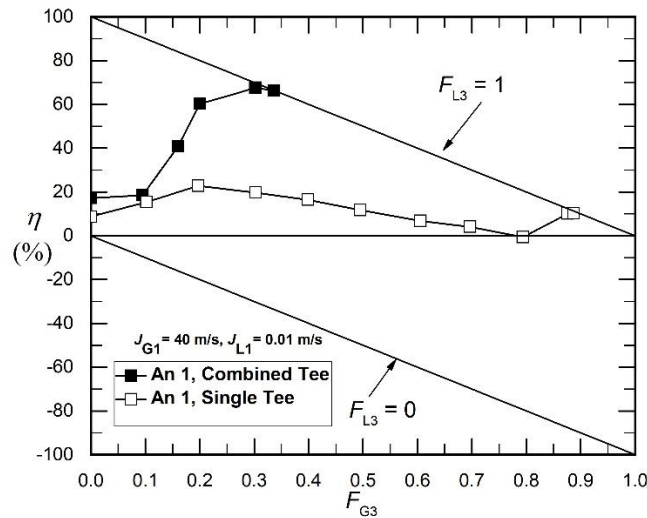
Figure 4.18   Comparison of phase-separation parameter, η, of the present system with a system of a single vertical impacting tee junction for An 1 data point
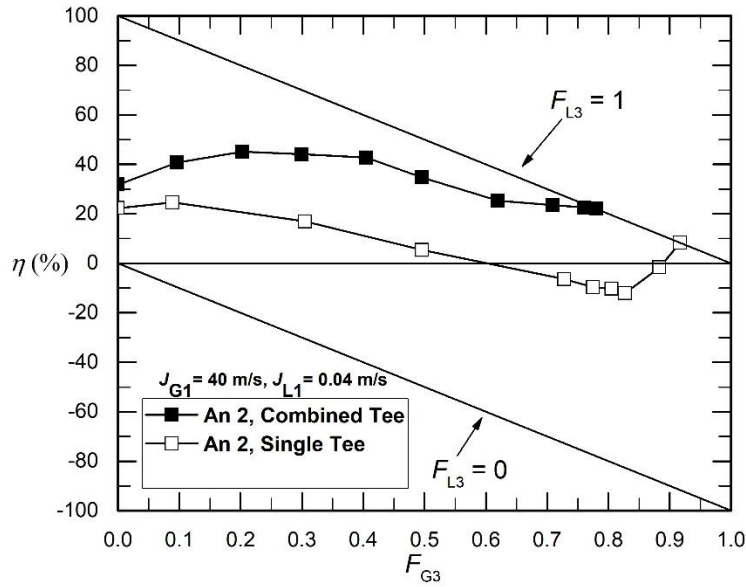
Figure 4.19   Comparison of phase-separation parameter, η, of the present system with a system of a single vertical impacting tee junction for An 2 data point
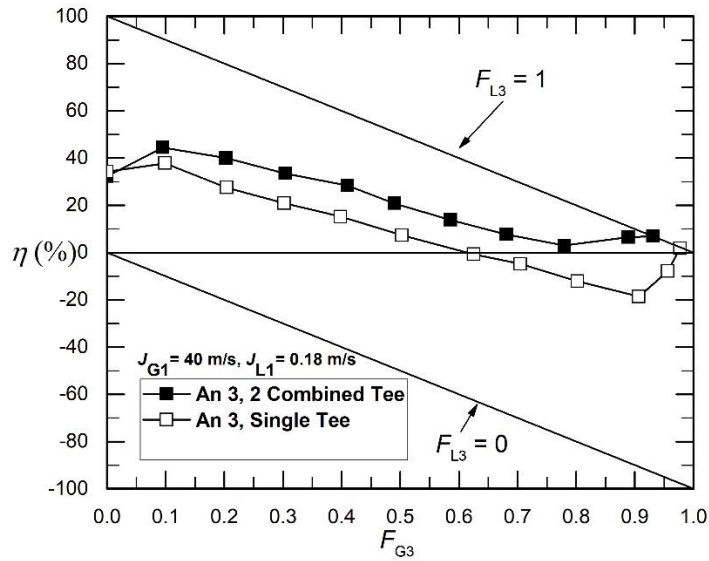
Figure 4.20   Comparison of phase-separation parameter, η, of the present system with a system of a single vertical impacting tee junction for An 3 data point
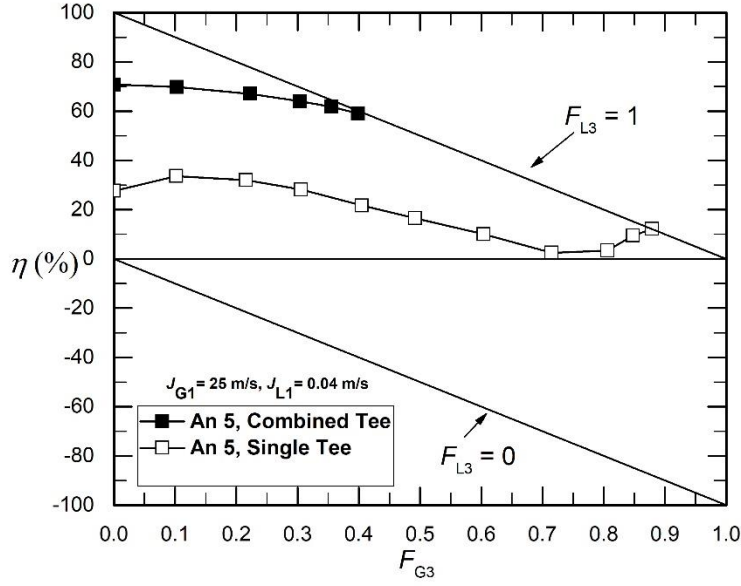
Figure 4.21   Comparison of phase-separation parameter, η, of the present system with a system of a single vertical impacting tee junction for An 5 data point

It can be observed from the figures that for every F_{G3}, the corresponding η is higher when the combined junction is used. In all four figures, the last point in each curve ($F_{L3}= 1$, where all liquid enters the bottom outlet), climbs up the line joining the points of zero and full phase separation. However, this increase in η is higher when J_{G1} is decreased (evident from comparing Figures 4.19 and 4.21) compared to when J_{L1} is decreased (evident from comparing Figures 4.18 -4.20). Thus, it can be concluded that, increasing the number of tee junctions in the system increases its phase-separation effectiveness; this increase in η is more affected by a change in J_{G1} compared to J_{L1}.

4.9 Comparison with Other Combined Tees

The phase-separation data obtained for the present system of combined impacting tee were compared with phase-separation data of other systems of combined tees available in the literature. Comparisons were only possible when the working fluids and data ranges matched with the present study. Analyses revealed that, for the same number of dividing tees in the system, the present system is capable of fully separating phases of air-water two-phase flows having higher values of J_{G1} and J_{L1}, i.e. the present system shows better phase-separation effectiveness.

The phase-separation data from the present system were compared with data from a two-layer system of combined branching tees consisting of 3, 5 or 7 connecting tubes or dividing tees used by Yang et al. (2010). Schematic diagram of this system is included in Figure 2.2 in Chapter 2. The same group of authors, Yang et al. (2017), published another work in which phase-separation data for two- and three-layer systems of combined branching tees were reported. The two-layer system in this paper is same as the one used in Yang et al. (2010) and the three-layer system had four upwards and three downwards connecting tubes or 7 branching tees in total. Schematic diagram of the three-layer set-up is included in Figure 2.5 in Chapter 2.

Figure 4.22 shows the points in the stratified and plug flow regimes that were tested by Yang et al. (2010, 2017). The solid line in this figure is the full-phase-separation curve obtained with the present system. The data for the annular flow regime in this figure were collected in the present study.
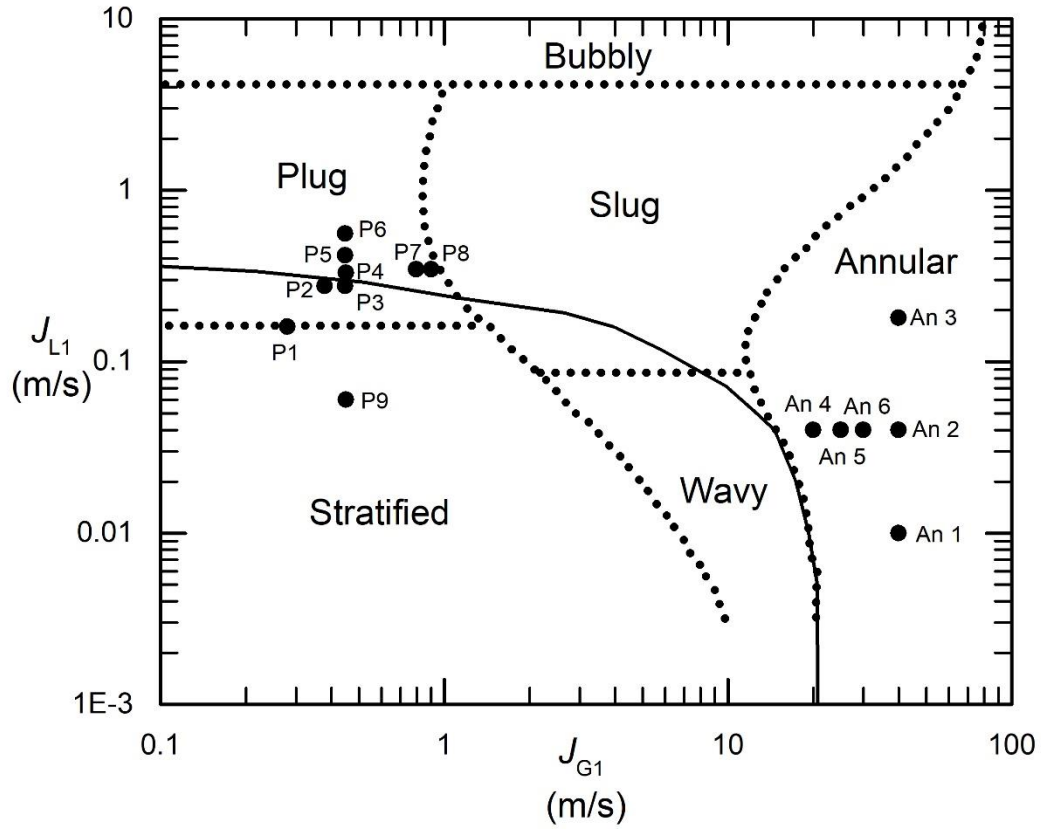
Figure 4.22   Inlet conditions for the data reported by Yang et al. (2010, 2017)

The point P9 in the stratified flow regime in Figure 4.22 lies below the full-phase-separation curve generated in this study with a combined junction of three impacting tees. Yang et al. (2010) reported maximum phase-separation efficiency (η_{max}) of 95% when three connecting tubes or branching tees were used in their system. The authors have reported full separation of phases when 5 or 7 connecting tubes were used for this point. The point P4 in the figure lies just above the full-phase-separation curve, which means η for this point should be very close to 100% with the present system. However, Yang et al. (2010) reported $\eta_{max} = 81\%$ for this point when three branching tees were used. The authors reported $\eta_{max} = 98\%$ and 100% when 5 and 7

branching tees were used, respectively. Full phase separation was obtained for these two points when the three-layer system was used (Yang et al., 2017). Yang et al. (2010) reported full phase separation or $\eta_{max} = 100\%$ for the point P1 when at least 5 branching tees were used. With the present system, full separation of phases can be achieved for this point with three impacting tees.

The points P2 and P3 lie below the full-phase-separation curve, which means full separation of phases can be reached for these two points with the present system. Yang et al. (2017) reported the use of at least five branching tees to achieve $\eta_{max} = 100\%$ for these two points. The points P5 – P8 lie very close to the full-phase-separation curve, indicating that the values of η for these points should be close to 100% with the present system having three dividing tees. The values of η_{max} for these points were reported in Yang et al. (2017) and full phase separation could not be achieved for any of these points with three branching tees in their system. For the point P5, full phase separation was obtained when 7 branching tees in the two-layer system or the three-layer system were used. The values of η_{max} were reported to be 88%, 96% and 90% with the three-layer system for the points P6, P7 and P8, respectively.

The present study is in agreement with Yang et al. (2010, 2017) on the fact that increasing J_{G1} or J_{L1} is detrimental to phase-separation effectiveness of the system and that increased number of tee junctions can improve phase-separation effectiveness. With the present system, $\eta_{max} = 67.6\%, 45.1\%, 44.5\%, 87.1\%, 70.8\%$ and 61.7% were obtained for the points An 1, An 2, An 3, An 4, An 5 and An 6, respectively. It is expected that future studies with increased number of impacting tees in the system would improve phase-separation effectiveness for these points and it might even be possible to achieve full phase separation.

CHAPTER 5

CONCLUSIONS AND RECOMMENDATIONS

FOR FUTURE STUDIES

5.1 Conclusions

This study aims at finding the limiting conditions (liquid and gas superficial velocities, J_{G1} and J_{L1}) for full separation of phases for air-water two-phase flows when passed through a system of combined junctions having a diameter of 13.5 mm at a nominal pressure of 200 kPa (abs). Beyond these limiting conditions, six points have been chosen in the annular flow regime and partial-phase-separation data have been generated for those points with the aim of studying the effectiveness of the combined system as phase separators. A 'phase-separation parameter' has also been defined in this thesis in order to quantify this effect. The following conclusions can be drawn from the results of the full- and partial-phase-separation experiments:

Full-Phase-Separation Experiments:

1. The system of combined junctions extends the range of J_{G1} and J_{L1} for which full separation of phases of air-water two-phase flows can be achieved, in comparison to a system of a single vertical tee junction of the same diameter.

2. In annular and wavy flow regimes, limiting J_{L1} at a fixed J_{G1} and limiting J_{G1} at a fixed J_{L1}, for total phase separation with the combined junction is almost double that of a single vertical tee junction.

3. Due to the intermittent nature of slug flow, it was not possible to get 100% separation of phases. However, it can be postulated that early appearances of liquid in the top outlet in this flow regime may be due to the formation of slugs, which may lead to higher instantaneous values of J_{G1} or J_{L1}.

94

4. In the slug flow regime, phases were considered to be fully or largely separated when a criterion of 99% F_{L3} (at least 99% of the inlet liquid passing through the bottom outlet, leaving 1% or less of the inlet liquid through the top outlet) was met. In order to maintain uniformity with slug flow regime, same criterion was adopted for plug flow regime even though sudden appearances of liquid in the top outlet was not observed in this flow regime.

5. Based on the criterion of 99% F_{L3}, limiting conditions of J_{G1} and J_{L1} for full phase separation has increased when the combined system is used in comparison with a single tee junction.

<u>Partial-Phase-Separation Experiments:</u>

1. For a fixed J_{L1}, as J_{G1} is decreased, the partial-phase-separation curves move in anti-clockwise direction towards the point of full phase-separation (0, 1) in the F_{G3} versus F_{L3} plot. On decreasing J_{G1}, for all F_{G3}, corresponding value of F_{L3} is higher, which means decreasing J_{G1} allows higher proportion of inlet liquid to pass through the bottom outlet with same proportion of gas. On sufficiently decreasing J_{G1}, full separation of phases can be achieved.

2. For a fixed J_{G1}, decreasing J_{L1} did not seem to have a consistent effect on partial-phase-separation curves. For the tested conditions, the trend of these curves reversed after a particular F_{G3}. Before this particular F_{G3}, decreasing J_{L1} yielded lower proportion of liquid to pass through the bottom outlet with same proportion of gas. After that, as J_{L1} was decreased, the partial-phase-separation curves started to move in anti-clockwise direction towards the point of full phase separation.

3. On decreasing J_{G1}, at a fixed J_{L1}, phase-separation parameter, η, increases for every corresponding value of F_{G3}. On sufficiently decreasing J_{G1}, 100% phase-separation effectiveness can be achieved with the combined system of impacting tee junctions.

4. On decreasing J_{L1}, at a fixed J_{G1}, phase-separation parameter, η, increases for corresponding F_{G3}, for $F_{G3} > 0.15$, for the tested conditions. For $F_{G3} < 0.15$, η decreases with decreasing J_{L1}.

5. Comparison of partial-phase-separation curves generated with the system of combined junctions with those generated with a system of a single vertical junction show that, for every F_{G3}, corresponding F_{L3} is higher for the present system of combined junctions. The partial-phase-separation curves move in anti-clockwise direction towards the point of full phase separation when the combined system is used.

6. For the same number of dividing tees in the system, the present system is capable of fully separating phases of air-water two-phase flows having higher values of J_{G1} and J_{L1}, in comparison to other combined tees reported in the literature, i.e., the present system shows better phase-separation effectiveness.

5.2 Recommendations for Future Studies

The present experimental investigation explored the idea of developing phase separators with just impacting type tee junctions. The results obtained shows that this is a viable idea and there is much scope of future research in this area. The author of this thesis proposes the following recommendations for future research in this field:

1. Increasing the number of vertical impacting tee junctions in the test section.

2. Generating partial phase-separation data in other flow regimes, with higher inlet liquid and gas superficial velocities.

3. More in-depth numerical and experimental analysis of the nature of slug flow and its effect on limiting conditions of full phase separation.

4. Experiments with more industrially relevant diameters and flowrates of liquid and gas, in order to develop commercial phase separators out of tee junctions.

5. To study the effects of different test-section pressures or working fluids on partial and full-phase-separation data.

REFERENCES

Azzopardi, B.J., Whalley, P.B., 1982. The effect of flow patterns on two-phase flow in a T junction. International Journal of Multiphase Flow 8, 491-507.

Azzopardi, B.J., Colman, D.A., Nicholson, D., 2002. Plant application of a T-junction as a partial phase separator. Chemical Engineering Research and Design 80, 87-96.

Azzopardi, B.J., Purvis, A., Govan, A.H., 1986a. Two Phase Flow Split at an Impacting T. UKAEA Atomic Energy Research Establishment.

Azzopardi, B.J., Purvis, A., Govan, A. H, 1986b. Flow split of churn flow at a vertical impacting T. Atomic Energy Research Establishment Harwell (England), AERE-R-12440.

Baker, G., Clark, W.W., Azzopardi, B.J., Wilson, J. A, 2007. Controlling the phase separation of gas–liquid flows at horizontal T-junctions. AIChE journal 53 (8), 1908-1915.

Chien, S., Rubel, M.T., 1992. Phase splitting of wet steam in annular flow through a horizontal impacting tee junction. SPE production engineering 7 (04), 368-374.

Chen, J., He, L., Luo, X., Bai, H., Wei, Y., 2012. Simulation of oil-water two phase flow and separation behaviors in combined T junctions. Journal of Hydrodynamics 24 (6), 848-857.

Chen, J., Wang, S., Ke, H., Zhou, M., Li, X., 2014. Experimental investigation of annular two-phase flow splitting at a microimpacting T-junction. Chemical Engineering Science 118, 154-163.

Chen, J, Wang, S., Zhang, X., Ke, H., Li, X., 2015. Experimental investigation of two-phase slug flow splitting at a micro impacting T-junction. International Journal of Heat and Mass Transfer 81, 939-948.

Elazhary, A.M., Soliman, H. M., 2012. Two-phase flow in a horizontal mini-size impacting T-junction with a rectangular cross-section. International journal of multiphase flow 42, 104-114.

El-Shaboury, A.M. F., Soliman, H.M., Sims, G. E., 2007. Two-phase flow in a horizontal equal-sided impacting tee junction. International journal of multiphase flow 33 (4), 411-431.

Fujii, T., Takenaka, N., Nakazawa, T., Asano, H., 1995. The phase separation characteristics of a gas–liquid two-phase flow in the impacting T-junction. Proc. 2nd Int. Conf. on Multiphase Flow, Kyoto, Japan, 627-632.

Hong, K.C., 1978. Two-phase flow splitting at a pipe tee. Journal of Petroleum Technology 30 (02), 290-296.

Hong, K.C., Griston, S., 1995. Two-phase flow splitting at an impacting tee. SPE Production & Facilities 10 (03), 184-190.

Hwang, S.T., Soliman, H.M., Lahey Jr., R.T., 1989. Phase separation in impacting wyes and tees. International Journal of Multiphase Flow 15 (6), 965-975.

Mandhane, J.M., Gregory, G.A., Aziz, K., 1974. A flow pattern map for gas—liquid flow in horizontal pipes. International Journal of Multiphase Flow 1 (4), 537-553.

Mohamed, M.A., Soliman, H.M., Sims, G.E., 2011. Experimental investigation of two-phase flow splitting in an equal-sided impacting tee junction with inclined outlets. Experimental Thermal and Fluid Science 35 (6), 1193-1201.

Mohamed, M.A., Soliman, H.M., Sims, G.E., 2012. Conditions for complete phase separation in an impacting tee junction at various inclinations of the outlet arms. International Journal of Multiphase Flow 47, 66-72.

Mohamed, M.A., 2012. Phase redistribution and separation of gas-liquid flows in an equal-sided impacting tee junction with a horizontal inlet and inclined outlets.

Mohamed, M.A., Soliman, H.M., Sims, G.E., 2014. Effects of pipe size and system pressure on the phase redistribution in horizontal impacting tee junctions. Experimental Thermal and Fluid Science 54, 219-224.

Sun, W., Liu, Y., He, K., Wang, S., 2018. The phase distribution of gas-liquid two-phase flow in microimpacting T-junctions with different branch channel diameters. Chemical Engineering Journal 333, 34-42.

Tuo, H., Hrnjak, P., 2012. Experimental Study of Refrigerant Two Phase Separation in a Compact Vertical T-junction. ASHRAE Transactions 118 (1).

Tuo, H., Hrnjak, P., 2014a. Vapor–liquid separation in a vertical impact T-junction for vapor compression systems with flash gas bypass. International Journal of Refrigeration 40, 189-200.

Tuo, H., Hrnjak, P., 2014b. Enhancement of vapor–liquid separation in vertical impact T-junctions for vapor compression systems with flash gas bypass. International Journal of Refrigeration 40, 43-50.

Wren, E., Azzopardi, B.J., 2004. The phase separation capabilities of two T-junctions placed in series. Chemical Engineering Research and Design 82 (3), 364-371.

Yang, L., Azzopardi, B.J., Belghazi, A., Nakanishi, S., 2006. Phase separation of liquid-liquid two-phase flow at a T-junction. AIChE Journal 52 (1), 141-149.

Yang, L., Zhao, Z., Qi, P., Zhao, L., Azzopardi, B.J., 2010. Phase Separation of Gas-Liquid Two-Phase Flows in Multi-tube T-Junction Separators. Second China Energy Scientist Forum.

Yang, L, Wang, J., Zhao, Z., Xu, S., Azzopardi, B.J., Wang, H., 2017. Phase separation of gas–liquid two-phase stratified and plug flows in multitube T-junction separators. AIChE Journal 63 (6), 2285-2292.

Zheng, N., Hwang, Y., Zhao, L., Deng, S., 2016a. Experimental study on the distribution of constituents of binary zeotropic mixtures in vertical impacting T-junction. International Journal of Heat and Mass Transfer 97, 242-252.

Zheng, N., Zhao, L., Hwang, Y., Zhang, J., Yang, X., 2016b. Experimental study on two-phase separation performance of impacting T-junction. International Journal of Multiphase Flow 83, 172-182.

APPENDIX A

CALIBRATION OF ROTAMETERS

Spot checks for three points of each rotameter used in the test facility (listed in Tables 3.1 and 3.2) were done and results were compared with the calibration data reported by Mohamed (2012) for the same rotameters. The results of these spot checks matched closely with that reported by Mohamed (2012). Thus, in-house calibration data for both air and water rotameters reported by the aforementioned author were used for most calculations in this thesis. The calibration data for the rotameters IN-A-1 and O-3-A-4 were collected by the author of this thesis and they were used in calculations. Between any two consecutive points, linear interpolation was used to calculate flowrates for both air and water rotameters.

A.1 Calibration of Air Rotameters

The 11 air rotameters used in the experiments were calibrated using either wet test meters or venturis, depending on their capacity. The two wet test meters used were Elster-Handel GmbH with calibration ranges of (1 - 10 SLPM) and (2.5 - 250 SLPM). Calibration using wet test meters included the following steps:

1. The rotameter to be tested was connected to the selected wet test meter after ensuring that the wet test meter was levelled and there was no leak.

2. Standard air density (ρ_{STD}), actual air density at the rotameter ($\rho_{ACTUALi}$) and air density in the wet test meter (ρ_{WTM}) were calculated using the equation of state:

$$\rho = P / RT \tag{A.1}$$

3. Actual air mass flow rate through the rotameter was calculated by taking the volume reading (V) from the wet test meter in a given time (t) and substituting in the formula:

$$W_{ACTUAL} = (V / t) \times \rho_{WTM} \tag{A.2}$$

where, the units of V, t, ρ_{WTM} and W_{ACTUAL} are in m^3, seconds, kg/m^3 and kg/s, respectively.

4. Measured air mass flow rate was calculated as:

$$W_{MEASURED} = W_{ACTUAL} \times SQRT (\rho_{STD} / \rho_{ACTUAL}) \qquad (A.3)$$

where, the units of $W_{MEASURED}$, W_{ACTUAL}, ρ_{STD} and ρ_{ACTUAL} are in kg/s, kg/s, kg/m^3 and kg/m^3, respectively.

The value of $W_{MEASURED}$ was converted to $V_{MEASURED}$ in units of SLPM using the formula:

$$V_{MEASURED} = W_{MEASURED} \times 1000 \times 60 / \rho_{STD} \qquad (A.4)$$

where, the units of $V_{MEASURED}$, $W_{MEASURED}$ and ρ_{STD} are in SLPM, kg/s and kg/m^3, respectively.

The two venturis used in calibrations were from FOX Valve Development Corp. Some important factors about them are listed in the Table A.1.

Table A.1 Specifications of the venturis

Venturi model	Maximum flow rate (SLPM)	Minimum flow rate (SLPM)	Inlet area $A_{VENTURI,INLET}$ (m^2)	Throat area $A_{VENTURI, THROAT}$ (m^2)
¾"	931.4	132.77	2.79E-04	7.13E-05
1- ¼"	2544.78	376.75	8.276E-04	1.979E-04

Calibration of air rotameters using venturis included the following steps:

1. The outlet of the rotameter to be calibrated was connected to a specific venturi, depending on the flow rate to be measured.

2. Inlet pressure (P_1) and throat pressure (P_2) of the venturi were measured using a water manometer (The Meriam Instrument Co., range: 204 cm).

3. Air density in the rotameter (ρ_{ROT}) and at the inlet of the venturi (ρ_{INLET}) were calculated using the equation of state (Equation A.1).

4. The actual mass flow rate was calculated using the formula:

$$W_{ACTUAL} = YC_dMA_{VENTURI,\ THROAT} \times SQRT\ (2\ (P_1\text{-}P_2) \times \rho_{INLET}) \qquad (A.5)$$

where, $\quad Y$ = expansion factor

$$Y = [(P_2/P_1)^{2/\kappa} \times (\kappa/\kappa\text{-}1) \times \{(1\text{-}(P_2/P_1)^{(\kappa\text{-}1)/\kappa})\ /\ (1\text{-}(P_2/P_1))\} \times \{(1\text{-}(D_2/D_1)^4)\ /\ (1\text{-}((D_2/D_1)^4 \times (P_2/P_1)^{2/\kappa}))\}]^{1/2}$$

κ = ratio of specific heats = 1.4

D_2 = diameter of venture throat (m)

D_1 = diameter of venture inlet (m)

C_d = coefficient of discharge (supplied by the manufacturer)

$M = 1\ /\ SQRT\ (1 - (D_2\ /\ D_1)^4)$

5. Measured air mass flow rate was calculated as:

$$W_{MEASURED} = W_{ACTUAL} \times SQRT\ (\rho_{STD}\ /\ \rho_{ROT}) \qquad (A.6)$$

where, the units of $W_{MEASURED}$, W_{ACTUAL}, ρ_{STD} and ρ_{ACTUAL} are in kg/s, kg/s, kg/m^3 and kg/m^3, respectively.

The value of $W_{MEASURED}$ was converted to $V_{MEASURED}$ in units of SLPM using the formula:

$$V_{MEASURED} = W_{MEASURED} \times 1000 \times 60\ /\ \rho_{STD} \qquad (A.7)$$

where, the units of $V_{MEASURED}$, $W_{MEASURED}$ and ρ_{STD} are in SLPM, kg/s and kg/m^3, respectively.

The calibration data for the rotameters IN-A-1 and O-3-A-4 collected by the author of this thesis are listed in Tables A.2 and A.3, respectively. Calibration results of spot checks for air rotameters are listed in Table A.4. Manufacturer flow rates and measured flow rates by Mohamed (2012) for the tested points are also listed in this table.

A.2 Calibration of Water Rotameters

The 11 water rotameters used in the test facility were calibrated using weight and time method. The weight machine used was "Signum 1" series of Sartorius AG Germany and had a maximum capacity of 35 kg, with an accuracy of 1/10000 kg. The timer used was Lab-chron 1402 with accuracy of one-tenth of a second.

Calibration results of spot checks for water rotameters are listed in Table A.5. Manufacturer flow rates and measured flow rates by Mohamed (2012) for the tested points are also listed in this table.

Table A.2 Calibration data of air inlet rotameter, IN-A-1

Reading (%)	Manufacturer Flowrate (SLPM)	Measured Flowrate (SLPM)
10	5	5.98
20	10.5	11.62
30	16.2	17.59
40	22.2	24.23
50	28.5	30.68
60	36	37.83
70	42.2	45.74
80	49.2	53.53
90	56.5	62.31
100	64	71.61

Table A.3 Calibration data of air outlet rotameter, O-3-A-4

Reading (%)	Manufacturer Flowrate (SLPM)	Measured Flowrate (SLPM)
10	210	210
20	375	390.5
30	560	589.3
40	740	747.6
50	930	945
60	1120	-
70	1320	-
80	1540	-
90	1755	-
100	-	-

Table A.4   Spot checks for calibration of air rotameters

Rotameter	Reading (%)	Manufacturer Flow Rate (SLPM)	Measured Flow Rate (SLPM)	Flow Rate from Mohamed (2012) (SLPM)
IN-A-1	20	10.5	11.1	10.25
	50	28.5	29.5	28.3
	80	49.2	53.3	49.3
IN-A-2	20	82	85.8	83
	50	192	190.5	192
	80	297	290	293
IN-A-3	20	375	363	375
	30	560	567.2	560
	40	740	760.3	745
O-2-A-1	20	1.72	1.8	1.66
	50	4.3	4.4	4.18
	80	6.88	7.4	6.82
O-2-A-2	20	12.3	11.2	12.9
	50	26.6	24	25.5
	80	39.5	38.2	39.5
O-2-A-3	20	87	86.9	88
	50	195	195.1	195
	80	305	315.8	306
O-2-A-4	20	146	149.2	143
	50	365	345.5	346
	80	584	565.6	580
O-3-A-1	20	1.55	1.7	1.52
	50	4.2	4.7	4.2
	80	6.9	7.2	7.1
O-3-A-2	20	10.5	11.6	10.75
	50	29	32.4	30.4
	80	49.5	53	51
O-3-A-3	20	87	89.4	89
	50	195	195.7	195
	80	305	300.5	306
O-3-A-4	20	375	390.5	378
	50	560	589.3	565
	80	740	747.6	755

Table A.5   Spot checks for calibration of water rotameters

Rotameter	Reading (%)	Measured Flow Rate (cc/min)	Manufacturer Flow Rate (cc/min)	Flow Rate from Mohamed (2012) (cc/min)
IN-W-1	20	11.77	10.5	11
	50	41.49	38.75	39.6
	80	66.89	66	65.5
IN-W-2	20	96.35	87	89
	50	229.71	240	246
	80	387.99	393	388
IN-W-3	20	626.4	660	675
	50	1437.2	1455	1470
	80	2344.1	2320	2340
O-2-W-1	20	1.3	2	1.5
	50	4.61	5	4.5
	80	7.41	8	7.2
O-2-W-2	20	14.13	15	14.5
	50	37.53	37.5	36.75
	80	60.53	60	60
O-2-W-3	20	91.03	96	95
	50	230.11	240	240
	80	372.53	384	392
O-2-W-4	20	565.96	583	573
	50	1450.8	1457	1433
	80	2303.5	2332	2312
O-3-W-1	20	1.3	2	1.5
	50	4.3	5	4.1
	80	7.21	8	7.2
O-3-W-2	20	13.43	15	14.5
	50	35.27	37.5	37.2
	80	57.62	60	59.5
O-3-W-3	20	92.95	96	92.5
	50	236.92	240	240
	80	375.33	384	377
O-3-W-4	20	545.41	583	548
	50	1466.7	1457	1456
	80	2317.1	2332	2312

APPENDIX B

EXPERIMENTAL DATA

The data for both full-phase-separation and partial-phase-separation experiments are tabulated in this section. Tables B.1 and B.2 list the relevant inlet parameters and results of full-phase-separation experiments in the wavy and annular; and slug and plug flow regimes, respectively. The mass flow rates of all full-phase-separation experiments are tabulated in Table B.3. The operating conditions and results of partial-phase-separation experiments are listed in Table B.4. Table B.5 contains the mass flow rates for partial-phase-separation experiments.

The nomenclature and units of various parameters used in these tables are listed below:

J_{G1} Inlet gas (air) superficial velocity, m/s

J_{L1} Inlet liquid (water) superficial velocity, m/s

P_{TS} Test-section pressure or pressure at the center of the combined junction, kPa

T_{G1} Inlet air temperature, K

F_{G3} Fraction of inlet gas entering outlet-3 (bottom outlet)

F_{L3} Fraction of inlet liquid entering outlet-3 (bottom outlet)

MB_{G} Mass balance error of gas flow, %

MB_{L} Mass balance error of liquid flow, %

W_{G} Mass flow rate of gas (air), kg/s

W_{L} Mass flow rate of liquid (water), kg/s

Table B.1   Full-phase-separation experiments (wavy and annular flow regimes)

Data Point	P_{TS} kPa	T_{G1} K	J_{G1} m/s	J_{L1} m/s	F_{G3}	F_{L3}	MB_G %	MB_L %
FS-1	200.0	294.5	20.7	0.001	0	1	1.74	-
FS-2	200.2	294.5	20.6	0.005	0	1	0.92	-3.54
FS-3	200.8	294.5	19.2	0.01	0	1	-0.21	4.28
FS-4	199.9	294.6	17.3	0.02	0	1	2.59	3.29
FS-5	198.8	294.5	14.6	0.04	0	1	1.64	4.26
FS-6	202.4	295.5	12.6	0.05	0	1	1.09	0.95
FS-7	199.3	294.5	9.85	0.072	0	1	1.88	4.49

Table B.2   Data for the slug and plug flow regimes (related to Figures 4.7 and 4.8 for Slug-1 and Slug-3, respectively)

Data Point	P_{TS} kPa	T_{G1} K	J_{G1} m/s	J_{L1} m/s	F_{G3}	F_{L3}	MB_G %	MB_L %
Slug-1								
Sl -1-1	199.4	295.2	5.80	0.155	0	0.891	-3.22	1.31
	198.1	295.2	5.78	0.155	0.07	1	-0.70	-0.58
Sl -1-2	197.3	295.2	5.83	0.139	0	0.937	-3.71	2.68
	200.9	293.9	5.72	0.139	0.06	1	-3.35	1.71
Sl -1-3	198.3	293.8	5.79	0.133	0	0.953	-4.13	1.66
Sl -1-4	198.3	295.3	5.87	0.121	0	0.980	-4.17	1.17
Sl -1-5	197.3	294.2	**5.86**	**0.117**	0	**0.995**	-3.25	1.45
Slug-2								
Sl -2-1	199.6	294.1	3.98	0.203	0	0.933	-4.80	-2.21
	197.5	293.8	4.01	0.204	0.09	1	-5.51	-1.21
Sl -2-2	199.5	294.0	3.98	0.196	0	0.965	-4.29	-1.14
	199.5	294.2	3.98	0.196	0.05	1	-4.86	-1.04
Sl -2-3	200.3	294.2	3.97	0.187	0	0.980	-4.89	-1.81
Sl -2-4	200.3	294.1	**3.97**	**0.181**	0	**0.993**	-4.91	-2.06

Data Point	P_{TS} kPa	T_{G1} K	J_{G1} m/s	J_{L1} m/s	F_{G3}	F_{L3}	MB_G %	MB_L %
Slug-3								
Sl -3-1	198.2	296.6	2.65	0.344	0	0.691	-1.30	1.10
	198.0	296.6	2.71	0.344	0.1	0.936	-4.15	-0.97
	199.4	296.5	2.71	0.344	0.18	0.991	0.80	0.77
Sl -3-2	199.9	296.1	2.63	0.237	0	0.925	-2.00	-0.05
	198.6	295.8	2.73	0.237	0.1	0.996	-3.90	-0.30
Sl -3-3	202.1	296.2	2.61	0.203	0	0.984	-1.80	-0.37
	197.1	295.0	2.71	0.203	0.1	1	-3.76	-0.41
Sl -3-4	200.1	295.8	2.69	0.196	0	0.988	1.29	-1.71
Sl -3-5	200.0	296.3	**2.65**	**0.193**	0	**0.993**	0.03	-0.72
Slug-4								
Sl -4-1	198.7	294.2	1.06	0.272	0	0.928	-4.38	0.31
	200.0	295.7	1.09	0.272	0.10	0.997	-3.76	-0.35
Sl -4-2	198.6	294.6	1.09	0.255	0	0.967	-5.98	1.75
	198.0	296.1	1.09	0.255	0.07	0.998	-5.81	-0.52
Sl -4-3	198.6	295.0	1.09	0.244	0	0.976	-6.01	-0.19
Sl -4-4	198.7	295.1	**1.09**	**0.237**	0	**0.99**	-5.19	-0.64
Plug-1								
Pl-1-1	197.8	293.4	0.52	0.401	0	0.808	0	0.75
Pl-1-2	198.1	293.4	0.52	0.344	0	0.856	0	0.06
Pl-1-3	204.0	294.0	0.53	0.307	0	0.956	0	-1.58
Pl-1-4	198.4	293.9	0.52	0.300	0	0.975	0	0.01
Pl-1-5	197.8	294.1	**0.52**	**0.290**	0	**0.994**	0	-0.32
Plug-2								
Pl-2-1	200.5	293.7	0.21	0.344	0	0.943	0	-0.16
Pl-2-2	196.8	294.4	**0.22**	0.337	0	**0.997**	-0.03	1.16

Table B.3   Mass flow rates for full-phase-separation experiments

Data Point	W_{G1} kg/s	W_{G2} kg/s	W_{G3} kg/s	W_{L1} kg/s	W_{L2} kg/s	W_{L3} kg/s
FS-1	0.007	0.007	0	0.0001	0	0.0001
FS-2	0.0069	0.007	0	0.001	0	0.0007
FS-3	0.0065	0.007	0	0.001	0	0.001
FS-4	0.006	0.006	0	0.003	0	0.003
FS-5	0.005	0.005	0	0.006	0	0.005
FS-6	0.004	0.004	0	0.007	0	0.007
FS-7	0.003	0.003	0	0.01	0	0.01
Slug-1						
Sl -1-1	0.002	0.002	0	0.022	0.002	0.019
	0.002	0.002	0.0001	0.022	0	0.022
Sl -1-2	0.002	0.002	0	0.02	0.001	0.018
	0.002	0.002	0.0001	0.02	0	0.019
Sl -1-3	0.002	0.002	0	0.019	0.001	0.018
Sl -1-4	0.002	0.002	0	0.017	0.0003	0.017
Sl -1-5	0.002	0.002	0	0.017	0.00007	0.016
Slug-2						
Sl -2-1	0.001	0.001	0	0.029	0.002	0.028
	0.001	0.001	0.0001	0.029	0	0.029
Sl -2-2	0.001	0.001	0	0.028	0.001	0.027
	0.001	0.001	0.00006	0.028	0	0.028
Sl -2-3	0.001	0.001	0	0.027	0.0005	0.027
Sl -2-4	0.001	0.001	0	0.026	0.0002	0.026
Slug-3						
Sl -3-1	0.001	0.001	0	0.05	0.015	0.034
	0.001	0.001	0.00009	0.05	0.003	0.047
	0.001	0.001	0.0002	0.05	0.0004	0.048
Sl -3-2	0.001	0.001	0	0.034	0.003	0.031
	0.001	0.001	0.0001	0.034	0.0001	0.034
Sl -3-3	0.001	0.001	0	0.029	0.0004	0.029
	0.001	0.001	0.00009	0.029	0	0.029

Data Point	W_{G1} kg/s	W_{G2} kg/s	W_{G3} kg/s	W_{L1} kg/s	W_{L2} kg/s	W_{L3} kg/s
Sl -3-4	0.001	0.001	0	0.028	0.0003	0.028
Sl -3-5	0.001	0.001	0	0.028	0.0002	0.028

Slug-4

Data Point	W_{G1} kg/s	W_{G2} kg/s	W_{G3} kg/s	W_{L1} kg/s	W_{L2} kg/s	W_{L3} kg/s
Sl -4-1	0.0004	0.0004	0	0.039	0.003	0.036
	0.0004	0.0003	0.00004	0.039	0.0001	0.039
Sl -4-2	0.0004	0.0004	0	0.036	0.001	0.035
	0.0004	0.0004	0.00003	0.036	0.00007	0.037
Sl -4-3	0.0004	0.0004	0	0.035	0.0009	0.034
Sl -4-4	0.0004	0.0004	0	0.034	0.0003	0.034

Plug-1

Data Point	W_{G1} kg/s	W_{G2} kg/s	W_{G3} kg/s	W_{L1} kg/s	W_{L2} kg/s	W_{L3} kg/s
Pl-1-1	0.0002	0.0002	0	0.058	0.011	0.046
Pl-1-2	0.0002	0.0002	0	0.049	0.007	0.042
Pl-1-3	0.0002	0.0002	0	0.044	0.002	0.043
Pl-1-4	0.0002	0.0002	0	0.043	0.001	0.042
Pl-1-5	0.0002	0.0002	0	0.042	0.0002	0.041

Plug-2

Data Point	W_{G1} kg/s	W_{G2} kg/s	W_{G3} kg/s	W_{L1} kg/s	W_{L2} kg/s	W_{L3} kg/s
Pl-2-1	0.00007	0.00007	0	0.049	0.003	0.046
Pl-2-2	0.00007	0.00007	0	0.048	0.0001	0.047

Table B.4   Partial-phase-separation experiments

Data Point	J_{G1} m/s	J_{L1} m/s	P_{TS} kPa	T_{G1} K	F_{G3}	F_{L3}	MB_G %	MB_L %
An 1								
An-1-1	40.1	0.01	200.5	294.4	0	0.172	-2.19	0.97
An-1-2	40.4	0.01	201.2	294.5	0.095	0.280	-3.75	2.07
An-1-3	41.4	0.01	200.3	294.5	0.160	0.568	-1.67	4.81
An-1-4	41.1	0.01	196.1	294.6	0.201	0.802	-1.97	2.97
An-1-5	40.3	0.01	199.2	294.5	0.302	0.978	-1.84	1.83
An-1-6	40.4	0.01	201.4	294.5	0.337	1	-2.98	1.19
An 2								
An-2-1	40.2	0.04	199.0	294.5	0	0.318	-3.23	1.34
An-2-2	40.8	0.04	202.3	294.5	0.096	0.503	-1.93	1.65
An-2-3	40.7	0.04	196.5	294.5	0.203	0.654	-1.36	2.18
An-2-4	40.6	0.04	196.7	294.4	0.300	0.742	-1.21	2.43
An-2-5	40.7	0.04	196.3	294.4	0.405	0.832	0.21	3.42
An-2-6	40.6	0.04	195.5	294.4	0.496	0.843	-1.59	3.07
An-2-7	40.4	0.04	198.3	294.5	0.620	0.873	-1.73	1.77
An-2-8	40.7	0.04	198.2	294.4	0.709	0.944	-3.50	5.68
An-2-9	40.2	0.04	197.6	294.4	0.761	0.987	-1.83	3.08
An-2-10	40.6	0.04	197.6	294.4	0.780	1	-1.01	3.66
An 3								
An-3-1	40.6	0.18	199.1	294.4	0	0.323	-0.48	4.52
An-3-2	40.7	0.18	200.7	294.6	0.095	0.541	-3.66	0.38
An-3-3	40.6	0.18	201.2	294.5	0.203	0.603	0.03	1.58
An-3-4	40.9	0.18	199.2	294.5	0.304	0.639	-2.32	0.71
An-3-5	40.6	0.18	201.1	294.5	0.410	0.694	-2.84	3.52
An-3-6	40.9	0.18	198.5	294.6	0.490	0.698	-3.91	1.11
An-3-7	40.9	0.18	199.0	294.5	0.586	0.724	-0.30	0.48
An-3-8	40.5	0.18	200.1	294.5	0.681	0.758	-1.15	-0.66
An-3-9	39.9	0.18	202.0	294.5	0.780	0.810	-1.15	-1.55
An-3-10	41.0	0.18	196.8	294.4	0.889	0.954	-3.68	-2.11
An-3-11	40.5	0.18	197.2	294.4	0.931	1	-2.62	-0.29

Data Point	J_{G1} m/s	J_{L1} m/s	P_{TS} kPa	T_{G1} K	F_{G3}	F_{L3}	MB_G %	MB_L %
An 4								
An-4-1	20.3	0.04	199.0	294.5	0	0.871	0.81	4.76
An-4-2	20.7	0.04	198.7	294.5	0.107	0.896	0.52	4.44
An-4-3	20.5	0.04	199.3	294.4	0.204	0.939	0.36	5.26
An-4-4	20.8	0.04	201.4	294.4	0.310	0.994	0.05	5.07
An 5								
An-5-1	25.3	0.04	200.4	294.5	0	0.708	-2.39	3.69
An-5-2	25.2	0.04	200.9	294.3	0.103	0.801	-2.09	4.76
An-5-3	25.4	0.04	198.8	294.3	0.223	0.893	-2.26	4.85
An-5-4	25.5	0.04	197.7	294.1	0.304	0.944	-1.03	5.02
An-5-5	25.5	0.04	197.9	294.3	0.355	0.973	-0.70	5.07
An-5-6	25.3	0.04	198.5	294.3	0.399	0.989	-0.85	4.63
An 6								
An-6-1	30.3	0.04	200.6	294.2	0	0.561	-0.99	3.73
An-6-2	30.6	0.04	197.9	294.3	0.107	0.716	-0.54	3.72
An-6-3	30.8	0.04	198.6	294.2	0.197	0.814	-1.04	4.60
An-6-4	30.7	0.04	199.2	294.3	0.308	0.896	-0.55	4.44
An-6-5	30.8	0.04	198.8	294.3	0.408	0.935	-0.08	4.85
An-6-6	30.6	0.04	197.5	294.2	0.520	0.978	0.04	4.88
An-6-7	30.4	0.04	198.3	294.4	0.607	1	-0.62	4.96

Table B.5   Mass flow rates for partial-phase-separation experiments

Data Point	W_{G1} kg/s	W_{G2} kg/s	W_{G3} kg/s	W_{L1} kg/s	W_{L2} kg/s	W_{L3} kg/s
An 1						
An-1-1	0.014	0.014	0	0.001	0.0012	0.0003
An-1-2	0.014	0.013	0.001	0.001	0.001	0.0004
An-1-3	0.014	0.012	0.002	0.001	0.006	0.0008
An-1-4	0.014	0.011	0.003	0.001	0.0003	0.0011
An-1-5	0.014	0.010	0.004	0.001	0.00003	0.00137
An-1-6	0.014	0.009	0.005	0.001	0	0.0014
An 2						
An-2-1	0.014	0.014	0	0.006	0.004	0.0018
An-2-2	0.014	0.013	0.001	0.006	0.003	0.003
An-2-3	0.014	0.011	0.003	0.006	0.002	0.004
An-2-4	0.014	0.01	0.004	0.006	0.001	0.004
An-2-5	0.014	0.008	0.005	0.006	0.0009	0.0045
An-2-6	0.013	0.007	0.007	0.006	0.00086	0.00459
An-2-7	0.014	0.005	0.009	0.006	0.0007	0.0048
An-2-8	0.014	0.004	0.01	0.006	0.0003	0.005
An-2-9	0.013	0.003	0.0104	0.006	0.00007	0.00537
An-2-10	0.014	0.0029	0.0106	0.006	0	0.0054
An 3						
An-3-1	0.014	0.014	0	0.025	0.016	0.008
An-3-2	0.014	0.013	0.001	0.025	0.012	0.014
An-3-3	0.014	0.011	0.003	0.025	0.01	0.015
An-3-4	0.014	0.01	0.004	0.025	0.009	0.016
An-3-5	0.014	0.008	0.006	0.025	0.007	0.017
An-3-6	0.014	0.007	0.007	0.025	0.008	0.018
An-3-7	0.014	0.006	0.008	0.025	0.007	0.0183
An-3-8	0.014	0.004	0.009	0.025	0.006	0.019
An-3-9	0.014	0.003	0.011	0.025	0.005	0.021
An-3-10	0.014	0.0016	0.013	0.025	0.001	0.025
An-3-11	0.014	0.001	0.013	0.025	0	0.025

Data Point	W_{G1} kg/s	W_{G2} kg/s	W_{G3} kg/s	W_{L1} kg/s	W_{L2} kg/s	W_{L3} kg/s
An 4						
An-4-1	0.007	0.007	0	0.006	0.0007	0.0046
An-4-2	0.007	0.006	0.0007	0.006	0.0006	0.0048
An-4-3	0.007	0.005	0.001	0.006	0.0003	0.005
An-4-4	0.007	0.0047	0.002	0.006	0.00003	0.0053
An 5						
An-5-1	0.009	0.009	0	0.006	0.002	0.0038
An-5-2	0.009	0.008	0.0009	0.006	0.001	0.004
An-5-3	0.009	0.007	0.002	0.006	0.0006	0.0047
An-5-4	0.009	0.006	0.003	0.006	0.0003	0.005
An-5-5	0.009	0.0055	0.0031	0.006	0.0001	0.0052
An-5-6	0.009	0.0051	0.0034	0.006	0.00006	0.0053
An 6						
An-6-1	0.01	0.01	0	0.006	0.002	0.003
An-6-2	0.01	0.009	0.001	0.006	0.002	0.0039
An-6-3	0.01	0.008	0.002	0.006	0.001	0.004
An-6-4	0.01	0.007	0.003	0.006	0.0006	0.0048
An-6-5	0.01	0.006	0.004	0.006	0.0003	0.005
An-6-6	0.01	0.005	0.005	0.006	0.0001	0.0052
An-6-7	0.01	0.004	0.006	0.006	0	0.0053

APPENDIX C

UNCERTAINTY ANALYSIS

In order to estimate errors in calibration data and experimental procedures, uncertainty analyses were done for relevant calculated inlet and outlet terms of both full and partial phase-separation experiments. A numerical method of sequential perturbation was applied to perform these uncertainty analyses. In this method, uncertainties based on fixed errors of all the measured parameters (listed in Table 4.3) that were used in calculating a term were considered. The method required repeated calculation of a particular term, each time changing one parameter to its highest or lowest value based on the fixed uncertainties of that parameter. Root-sum-method was used to calculate positive and negative perturbations of a term, considering all the measured parameters that consist in calculating that term. Averaging of the negative and positive perturbations gave total uncertainty for that term.

Uncertainty analysis was performed for inlet parameters W_{G1}, W_{L1}, J_{G1}, J_{L1} and for outlet parameters W_{G2}, W_{G3}, W_{L2}, W_{L3}, F_{G3} and F_{L3}. The method of sequential perturbation to calculate uncertainty of a term (in this case, W_{L1}) is described below:

i. Calculate W_{L1} using all nominal values.

$$W_{L1} = f(V_{L1}, \rho_{L1}) = f(V_{L1}, f(T_{L1})) = f(V_{L1}, T_{L1}) \qquad (C.1)$$

ii. Recalculate W_{L1}, using nominal values of all parameters, except one, which will be replaced by its positive perturbed value based on fixed uncertainty. For example, for positive perturbed value of T_{L1}:

$$W_{L1}{}^{+\delta\,T_{L1}} = f(V_{L1}, T_{L1} + \delta\,T_{L1}) \qquad (C.2)$$

iii. Recalculate W_{L1}, using nominal values of all parameters, except one, which will be replaced by its negative perturbed value based on fixed uncertainty. For example, for negative perturbed value of T_{L1}:

$$W_{L1}^{-\delta\,TL1} = f(V_{L1}, T_{L1} - \delta\,T_{L1}) \qquad\qquad (C.3)$$

iv. Repeat step ii and iii for all parameters used in calculating W_{L1}.

v. Calculate the combined effect of all positive perturbations by using the root-sum method.

$$\delta\,W_{L1}^{+\delta} = (\,\Sigma\,(W_{L1} - W_{L1}^{+\delta i})^2\,)^{1/2} \qquad\qquad (C.4)$$

vi. Calculate the combined effect of all negative perturbations by using the root-sum method.

$$\delta\,W_{L1}^{-\delta} = (\,\Sigma\,(W_{L1} - W_{L1}^{-\delta i})^2\,)^{1/2} \qquad\qquad (C.5)$$

vii. Take average of the effect of both positive and negative perturbations to calculate overall uncertainty.

$$\delta\,W_{L1} = (\delta\,W_{L1}^{+\delta} + \delta\,W_{L1}^{-\delta}) / 2 \qquad\qquad (C.6)$$

Table C.1 and C.2 contain the results of uncertainty analysis for different parameters of full- and partial-phase-separation experiments, respectively.

Table C.1   Uncertainty analysis for full-phase-separation experiments

Data Point	J_{G1} %	J_{L1} %	W_{G1} %	W_{G2} %	W_{G3} %	W_{L1} %	W_{L2} %	W_{L3} %	F_{G3} %	F_{L3} %
FS-1	3.8	4.2	2.1	2.0	-	3.0	-	3.0	-	24.8
FS-2	3.8	4.2	2.1	2.0	-	3.0	-	3.0	-	6.7
FS-3	3.8	4.2	2.1	2.0	-	3.0	-	3.0	-	7.2
FS-4	3.8	4.2	2.1	1.9	-	3.0	-	3.0	-	6.2
FS-5	3.8	4.2	2.1	2.0	-	3.0	-	3.0	-	7.2
FS-6	3.8	4.2	2.1	2.0	-	3.0	-	3.0	-	4.4
FS-7	3.7	4.2	2.1	2.0	-	3.0	-	3.0	-	7.5

Slug-1

Data Point	J_{G1} %	J_{L1} %	W_{G1} %	W_{G2} %	W_{G3} %	W_{L1} %	W_{L2} %	W_{L3} %	F_{G3} %	F_{L3} %
Sl -1-1	3.7	4.2	2.1	2.1	-	3.0	3.0	3.0	-	4.6
	3.7	4.2	2.1	1.9	0.1	3.0	-	3.0	3.1	4.4
Sl -1-2	3.7	4.2	2.1	2.1	-	3.0	3.0	3.0	-	5.6
	3.8	4.2	2.1	2.0	0.1	3.0	-	3.0	5.6	4.8
Sl -1-3	3.7	4.2	2.1	2.1	-	3.0	3.0	3.0	-	4.8
Sl -1-4	3.7	4.2	2.1	2.1	-	3.0	3.0	3.0	-	4.5
Sl -1-5	3.7	4.2	2.1	2.1	-	3.0	3.0	3.0	-	4.6

Slug-2

Data Point	J_{G1} %	J_{L1} %	W_{G1} %	W_{G2} %	W_{G3} %	W_{L1} %	W_{L2} %	W_{L3} %	F_{G3} %	F_{L3} %
Sl -2-1	3.8	4.2	2.1	2.1	-	3.0	3.0	3.0	-	5.4
	3.7	4.2	2.1	1.9	0.2	3.0	-	3.0	8.4	4.6
Sl -2-2	3.8	4.2	2.1	2.1	-	3.0	3.0	3.0	-	4.6
	3.8	4.2	2.1	2.0	0.1	3.0	-	3.0	7.5	4.6
Sl -2-3	3.8	4.2	2.1	2.1	-	3.0	3.0	3.0	-	5.1
Sl -2-4	3.8	4.2	2.1	2.1	-	3.0	3.0	3.0	-	5.3

Slug-3

Data Point	J_{G1} %	J_{L1} %	W_{G1} %	W_{G2} %	W_{G3} %	W_{L1} %	W_{L2} %	W_{L3} %	F_{G3} %	F_{L3} %
Sl -3-1	3.7	4.2	2.1	2.0	-	3.0	3.0	3.0	-	4.5
	3.7	4.2	2.1	1.9	0.2	3.0	3.0	3.0	6.6	4.5
	3.7	4.2	2.1	1.6	0.4	3.0	3.0	3.0	3.1	4.3

Data Point	J_{G1} %	J_{L1} %	W_{G1} %	W_{G2} %	W_{G3} %	W_{L1} %	W_{L2} %	W_{L3} %	F_{G3} %	F_{L3} %
Sl -3-2	3.7	4.2	2.1	2.0	-	3.0	3.0	3.0	-	4.2
	3.7	4.2	2.1	1.9	0.2	3.0	3.0	3.0	6.3	4.3
Sl -3-3	3.7	4.2	2.1	2.0	-	3.0	3.0	3.0	-	4.3
	3.7	4.2	2.1	1.9	0.2	3.0	-	3.0	6.1	4.3
Sl -3-4	3.8	4.2	2.1	2.0	-	3.0	3.0	3.0	-	5.0
Sl -3-5	3.8	4.2	2.1	2.0	-	3.0	3.0	3.0	-	4.4

Slug-4

Data Point	J_{G1} %	J_{L1} %	W_{G1} %	W_{G2} %	W_{G3} %	W_{L1} %	W_{L2} %	W_{L3} %	F_{G3} %	F_{L3} %
Sl -4-1	3.8	4.2	2.1	2.1	-	3.0	3.0	3.0	-	4.2
	3.8	4.2	2.1	1.9	0.2	3.0	3.0	3.0	6.1	4.3
Sl -4-2	3.8	4.2	2.1	2.1	-	3.0	3.0	3.0	-	4.8
	3.8	4.2	2.1	2.0	0.1	3.0	3.0	3.0	8.8	4.3
Sl -4-3	3.8	4.2	2.1	2.1	-	3.0	3.0	3.0	-	4.3
Sl -4-4	3.8	4.2	2.1	2.1	-	3.0	3.0	3.0	-	4.4

Plug-1

Data Point	J_{G1} %	J_{L1} %	W_{G1} %	W_{G2} %	W_{G3} %	W_{L1} %	W_{L2} %	W_{L3} %	F_{G3} %	F_{L3} %
Pl-1-1	3.7	4.2	2.0	2.0	-	3.0	3.0	3.0	-	4.3
Pl-1-2	3.7	4.2	2.0	2.0	-	3.0	3.0	3.0	-	4.2
Pl-1-3	3.7	4.2	2.0	2.0	-	3.0	3.0	3.0	-	4.9
Pl-1-4	3.7	4.2	2.0	2.0	-	3.0	3.0	3.0	-	4.2
Pl-1-5	3.7	4.2	2.0	2.0	-	3.0	3.0	3.0	-	4.3

Plug-2

Data Point	J_{G1} %	J_{L1} %	W_{G1} %	W_{G2} %	W_{G3} %	W_{L1} %	W_{L2} %	W_{L3} %	F_{G3} %	F_{L3} %
Pl-2-1	3.7	4.2	2.0	2.0	-	3.0	3.0	3.0	-	4.3
Pl-2-2	3.7	4.2	2.0	2.0	-	3.0	3.0	3.0	-	4.5

Table C.2   Uncertainty analysis for-partial phase-separation experiments

Data Point	J_{G1} %	J_{L1} %	W_{G1} %	W_{G2} %	W_{G3} %	W_{L1} %	W_{L2} %	W_{L3} %	F_{G3} %	F_{L3} %
An 1										
An-1-1	3.8	4.2	2.1	2.1	-	3.0	3.0	3.0	-	4.4
An-1-2	3.8	4.2	2.1	1.9	0.2	3.0	3.0	3.0	6.1	5.0
An-1-3	3.8	4.2	2.1	1.7	0.3	3.0	3.0	3.0	1.0	7.9
An-1-4	3.8	4.2	2.1	1.6	0.4	3.0	3.0	3.0	4.1	5.8
An-1-5	3.8	4.2	2.1	1.4	0.6	3.0	3.0	3.0	3.9	4.9
An-1-6	3.8	4.2	2.1	1.4	0.7	3.0	-	3.0	5.2	4.5
An 2										
An-2-1	3.8	4.2	2.1	2.1	-	3.0	3.0	3.0	-	4.6
An-2-2	3.8	4.2	2.1	1.8	0.2	3.0	3.0	3.0	4.0	4.8
An-2-3	3.8	4.2	2.1	1.6	0.4	3.0	3.0	3.0	3.5	5.1
An-2-4	3.8	4.2	2.1	1.4	0.6	3.0	3.0	3.0	3.4	5.3
An-2-5	3.8	4.2	2.1	1.2	0.8	3.0	3.0	3.0	2.9	6.3
An-2-6	3.8	4.2	2.1	1.0	1.0	3.0	3.0	3.0	3.7	5.9
An-2-7	3.8	4.2	2.1	0.8	1.3	3.0	3.0	3.0	3.8	4.8
An-2-8	3.8	4.2	2.1	0.6	1.5	3.0	3.0	3.0	5.8	8.9
An-2-9	3.8	4.2	2.1	0.5	1.6	3.0	3.0	3.0	3.9	5.9
An-2-10	3.8	4.2	2.1	0.4	1.6	3.0	-	3.0	3.3	6.5
An 3										
An-3-1	3.8	4.2	2.1	2.0	-	3.0	3.0	3.0	-	7.5
An-3-2	3.8	4.2	2.1	1.9	0.2	3.0	3.0	3.0	6.0	4.3
An-3-3	3.8	4.2	2.1	1.6	0.4	3.0	3.0	3.0	2.9	4.7
An-3-4	3.8	4.2	2.1	1.4	0.6	3.0	3.0	3.0	4.4	4.3
An-3-5	3.8	4.2	2.1	1.2	0.8	3.0	3.0	3.0	5.0	6.4
An-3-6	3.8	4.2	2.1	1.1	1.0	3.0	3.0	3.0	6.3	4.5
An-3-7	3.8	4.2	2.1	0.8	1.2	3.0	3.0	3.0	2.9	4.3
An-3-8	3.8	4.2	2.1	0.6	1.4	3.0	3.0	3.0	3.4	4.4
An-3-9	3.8	4.2	2.1	0.4	1.6	3.0	3.0	3.0	3.4	4.9
An-3-10	3.8	4.2	2.1	0.2	1.8	3.0	3.0	3.0	6.0	5.3
An-3-11	3.8	4.2	2.1	0.1	1.9	3.0	-	3.0	4.8	4.3

Data Point	J_{G1} %	J_{L1} %	W_{G1} %	W_{G2} %	W_{G3} %	W_{L1} %	W_{L2} %	W_{L3} %	F_{G3} %	F_{L3} %
An 4										
An-4-1	3.8	4.2	2.1	2.0	-	3.0	3.0	3.0	-	7.8
An-4-2	3.8	4.2	2.1	1.8	0.2	3.0	3.0	3.0	2.9	7.4
An-4-3	3.7	4.2	2.1	1.6	0.4	3.0	3.0	3.0	2.9	8.4
An-4-4	3.8	4.2	2.1	1.4	0.6	3.0	3.0	3.0	2.9	8.2
An 5										
An-5-1	3.8	4.2	2.1	2.1	-	3.0	3.0	3.0	-	6.6
An-5-2	3.8	4.2	2.1	1.8	0.21	3.0	3.0	3.0	4.2	7.8
An-5-3	3.8	4.2	2.1	1.6	0.5	3.0	3.0	3.0	4.4	7.9
An-5-4	3.8	4.2	2.1	1.4	0.6	3.0	3.0	3.0	3.3	8.1
An-5-5	3.8	4.2	2.1	1.3	0.7	3.0	3.0	3.0	3.1	8.2
An-5-6	3.8	4.2	2.1	1.2	0.8	3.0	3.0	3.0	3.1	7.6
An 6										
An-6-1	3.8	4.2	2.1	2.0	-	3.0	3.0	3.0	-	6.6
An-6-2	3.8	4.2	2.1	1.8	0.2	3.0	3.0	3.0	3.0	6.6
An-6-3	3.8	4.2	2.1	1.6	0.4	3.0	3.0	3.0	3.3	7.6
An-6-4	3.8	4.2	2.1	1.4	0.6	3.0	3.0	3.0	3.0	7.4
An-6-5	3.8	4.2	2.1	1.2	0.8	3.0	3.0	3.0	2.9	7.9
An-6-6	3.8	4.2	2.1	1.0	1.0	3.0	3.0	3.0	2.9	7.9
An-6-7	3.8	4.2	2.1	0.8	1.2	3.0	-	3.0	3.0	8.0